Master's thesis

NTNU
Norwegian University of Science and Technology
Faculty of Natural Sciences
Department of Chemical Engineering

Ingeborg Helga Hus Nesse

Researching the behaviour of aerosol emissions in an amine scrubbing system

Master's thesis in Chemical Engineering and Biotechnology
Supervisor: Hanna Knuutila
Co-supervisor: Lucas Braakhuis, Hallvard F. Svendsen
June 2021

NTNU
Kunnskap for en bedre verden

Ingeborg Helga Hus Nesse

Researching the behaviour of aerosol emissions in an amine scrubbing system

Master's thesis in Chemical Engineering and Biotechnology
Supervisor: Hanna Knuutila
Co-supervisor: Lucas Braakhuis, Hallvard F. Svendsen
June 2021

Norwegian University of Science and Technology
Faculty of Natural Sciences
Department of Chemical Engineering

NTNU
Norwegian University of
Science and Technology

Preface

This Master Thesis was written during the spring semester of 2021 at the Norwegian University of Science and Technology (NTNU) as a part of the five-year Master's Degree program of Chemical Engineering and Biotechnology. The final report is the result of TKP4900 - Chemical Engineering Master Thesis, in the research area of Environmental Engineering and Reactor Technology.

I would like to express my greatest gratitude towards my supervisor and co-supervisors Hanna Knuutila, Lucas Braakhuis and Hallvard F. Svendsen. Their insight and experience has been invaluable and their kind willingness to help has improved the quality of this thesis. I would also like to express gratitude towards my fellow students for the experiences we have shared and the motivation they have provided me with.

Abstract

In the work of this thesis, the behaviour of aerosol phase amine emissions from an amine scrubbing system is investigated. Aerosol emissions has in the last few years been reported as significant and causes increased operating costs to the system as well has having an undesirable effect on the environment.

The aim of this thesis is to contribute to the research on the behaviour of aerosol based amine emissions to gain necessary insight on how to design an amine scrubbing system with reduced emissions. This is done by performing several case studies where the effect of operating variables and modifications to amine scrubbing is investigated in regards to aerosol amine emissions.

The case studies are performed using the simulation tool CO2SIM. To ensure reliable results, the equilibrium model used is validated for ranges where the amine concentration is low. A Base Case with an absorber and two water washes was set up and validated against experimental data. The Base Case is used to compare the effect of the different variables and modifications.

The effect of water wash height, the effect of the intercooling modification with and without a height reduction in the absorber, the effect of operating the absorber isothermally and the effect of CO_2 content in the flue gas as well as the effect of not cooling the gas before entering the absorber was investigated in the case studies. The aerosol phase is predicted using a separate model by Majeed et. Al (2017).

The research in this thesis contributes to gaining better knowledge of the behaviour of aerosol emissions and identifies the temperature profile in the absorber column as an important parameter in regards to aerosol emissions. The results from the case studies shows that the variables and modifications that has the effect of reducing the magnitude of the bulge temperature in the absorber column also had the effect of reducing the aerosol emissions by reducing the transfer of MEA into the aerosol phase. A reduced temperature bulge also reduces the growth of the droplets both in the absorber and in the wash sections. It was also found that increasing the height of the water wash contributed to an increased residence time in the wash sections, which reduced the overall emissions.

Sammendrag

Denne mastergradsavhandlingen undersøker oppførselen til aerosol amin utslipp fra karbonfangstanlegg som anvender kjemisk absorbsjon med aminløsemiddel for å fange CO_2. Aerosol utslipp har i de siste årene fått økt oppmerksomhet ettersom utslippene kan være svært høye. Utslippene fører til økte kostnader forbundet med operasjon av systemet og har en uønsket påvirkning på miljøet.

Målet med denne forskningen er å bidra til økt forståelse av aerosolfasen i karbonfangstsystem for å få avgjørende kunnskap om hvordan et slikt system kan utformes med reduserte utslipp. Dette ble gjennomført ved å gjennomføre flere studier som undersøkte effekten av systemvariabler og ulike modifikasjoner på systemet.

Studiene ble utført ved å sette opp en base simulering som ble sammenlignet med simuleringer hvor forandringer av systemet var implementert. Base simuleringen bestod av en absorber og to vannvask seksjoner, og simuleringene ble gjennomført i simuleringsprogrammet CO2SIM. En ekstern aerosol modell av Majeed m.fl (2017) ble brukt til å prediktere aerosolfasen. For å sikre pålitelige resultater ble likevektsmodellen i simuleringsprogrammet validert mot eksperimentelle data. Base simuleringen ble også validert mot eksperimentelle data.

Systemvariablene som ble undersøkt var høyden til vannvask seksjonen, og CO_2 innhold i røykgassen som ble behandlet. Effekten av å ikke kjøle ned røykgassen med lavt CO_2 innhold ble også undersøkt. Videre ble modifikasjonen intern nedkjøling, med og uten redusert absorber høyde undersøkt. Den siste modifikasjonen som ble undersøkt var effekten av å operere absorberen isotermt.

Denne avhandlingen har bidratt til bedre forståelse av aerosol utslippene til karbonfangstanlegg ved kjemisk absorpsjon i aminbaserte løsemidler. Oppgaven identifiserer temperaturprofilen i absorber kolonnen som en viktig parameter i forhold til aerosol utslipp, og oppdaget at modifikasjoner og systemvariabler som reduserte temperaturtoppen også reduserte utslippene ved å redusere mengden MEA som ble overført til aerosol fasen. Redusert temperaturtopp førte også til redusert vekst av aerosolpartiklene i absorberen og i vannvask seksjonen. Økt vekst av aerosolpartiklene i vannvaskseksjonen kan derimot oppnås ved å øke høyden på vannvask kolonnene.

Contents

List of Figures

List of Tables

1 Introduction

1.1 Carbon Capture and Storage (CCS)

In a world with an increasing population, the demand for energy gets higher every day. At the same time the concern for environmental change limits the use of fossil fuels, due to its contribution to carbon dioxide (CO_2) emissions. CO_2 is considered to be a greenhouse gas, which is defined as a gas that absorbs and radiates heat, and thus contributes to raising the global temperature of the earth [1]. To avoid further increase in the global temperature there is a need to stabilize the concentration of CO_2 in the atmosphere. This can be done by either avoiding the use of fossil fuels as a energy source, or by reducing the amount of CO_2 emitted to the atmosphere. Carbon capture and storage (CCS) technologies are considered to be promising methods for reducing the CO_2 emissions from processes using fossil fuels by capturing CO_2 before it is emitted and storing it permanently.

These carbon capture processes are currently under extensive research. Several different technologies have been developed, but the main strategies are post-combustion, pre-combustion and oxy-combustion technologies. The type of technology used for a system is dependent on the gas to be cleaned and if implementation to existing systems are to be considered. The aim for CCS technologies is to produce a relatively pure stream of CO_2 that are to be compressed for transportation and stored in a geological formation. Pre-combustion technologies aims at separating CO_2 from gas prior to burning, while post-combustion technologies absorbs the CO_2 produced after combustion processes.[2] As an alternative to post-combustion, oxy-fuel technologies has been developed. These technologies burns fuel using pure oxygen instead of air. This renders a flue gas with high concentration of CO_2, which can then be easily separated and sent directly to storage [3].

Of the mentioned methods, post-combustion technologies is the most researched technology and industrial applications are being demonstrated at the TMC Mongstad, Norway and BD3 SaskPower in Canada. There are several different methods, but CCS by chemical absorption is considered to be the most mature option among the post-combustion technologies [2]. This is reasoned with the method allowing for easy retrofitting because the system is similar to other environmental control units used at power plants. The method is also effective for dilute CO_2 streams, like flue gases

from power plants where the pressure is low. [4], [5]

The technology is based on chemical absorption of CO_2 using an aqueous solvent. When the solvent is based on an amine solution, the method is referred to as Amine scrubbing. The amine solution used is often a 30 wt % Monoethanolamine (MEA) solution and can be considered as a base solvent because of its relatively cheap price and proven efficiency [6]. Absorption in this solvent is extensively referred to in literature and most studies done on emissions from amine scrubbing system uses this solvent.

Amine scrubbing consists of two stages, an absorber stage and a stripping stage. A typical flowsheet for the process is presented in Figure 1.

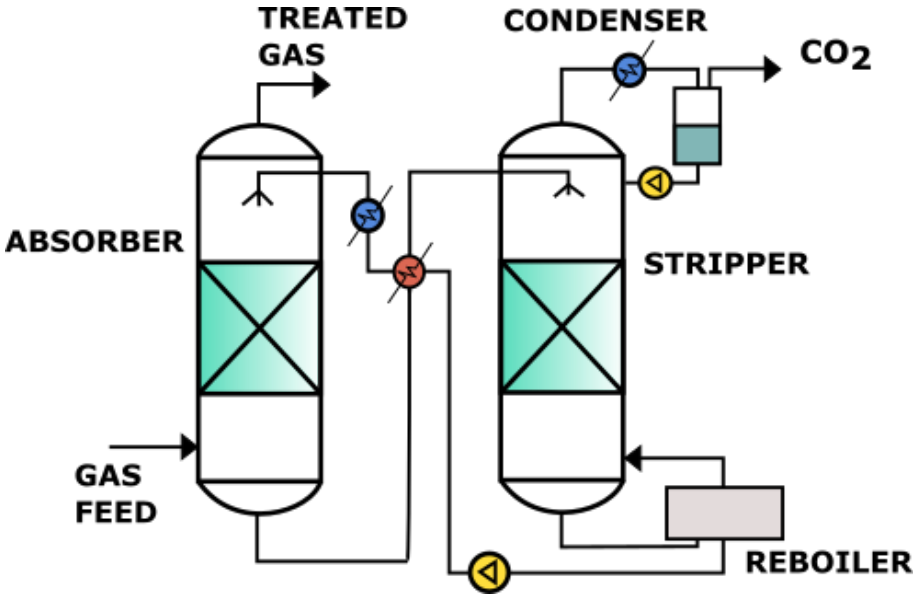

Figure (1) A simple flowsheet of CO_2 capture by amine scrubbing.

In the absorber column, flue gas rich in CO_2 is inserted into the bottom. Counter-current to the gas flows a liquid amine solvent stream which is inserted at the top of the column. The column is typically packed and liquid flows along the packing, where it comes into contact with the gas. When there is contact between the gas and liquid, gas phase CO_2 is absorbed by a series of chemical reactions and heat is being released. The gas then flows towards the top, lean in CO_2 and is released to the environment. At the bottom of the column the solvent is rich in CO_2 and is inserted

into a heat exchanger. Here the solvent is further heated and inserted into a stripper column, where water steam is flowing upwards the column. The steam is hot, usually around 100-120 °C [7] and heats the liquid rich in CO_2. By heating the solvent, the reactions in the absorber is reversed and the solvent loses affinity for CO_2, making it dissolve. The CO_2 is picked up by the steam. The steam with the CO_2 is led out of the column and sent to a condenser. Here the water is being recirculated back into the stripper. The gas stream is relatively pure in CO_2 and ready to be sent to compression. In the stripper, the solvent flowing towards the bottom is now lean in CO_2 and is sent back to the absorber. Before being recirculated into the absorber, the solvent releases heat to the rich solvent stream in the heat exchanger. [2], [3], [8]

As mentioned, steam picks up the CO_2 dissolved in the solvent. The steam has the effect of lowering the CO_2 partial pressure in the gas phase, which drives more CO_2 to be dissolved. An equilibrium between the CO_2 dissolved in the gas and liquid also arise in the absorber column. As the CO_2 is dissolved in the amine solvent, it reacts with MEA and forms insoluble compounds. When this happens, the equilibrium shifts and more CO_2 can dissolve in the solvent. This is what is driving the absorption. As there is a equilibrium for CO_2, there is also a equilibrium for MEA. Most of the amines used in amine scrubbing is volatile, and MEA is one of the most volatile amines [9]. This means that the compound has the ability to vaporize into the gas phase and be carried out of the absorber column with the treated gas, creating amine emissions.

1.2 Amine emissions from post-combustion absorption

Amine emissions is one of the challenges still to be solved before CCS post-combustion technologies are commercially available. Over the last few years there has been a larger focus on the amine based emissions from carbon capture plants. This is because loss of solvent to the environment can lead to an increase in operating costs as well as being harmful to the environment [10],[11]. When amines are released into the environment they can participate in atmospheric reactions to produce ozone and other toxic compounds [12]. There is also an issue with degradation productions like Nitrosamines and Nitramines being formed, which are known to be carcinogenic. [13], [14], [15] Because of these effects, it is desirable to keep the amine emissions

low. There are no official regulations for the emissions, but when setting up a carbon capture system a permit needs to be given where the amine emissions from the plant is assessed. In Norway, the longterm Environmental Assesments Levels for MEA has been proposed as 10 $\mu g/m^3$ based on a long-term occupational exposure limit of 0.3 mg/m^3 [16].

Also, when emissions are increasing, the countermeasures used to reduce them gets less effective and thus more costly [17]. Therefore, knowing how to operate these countermeasures as efficiently as possible without increasing the costs to much is crucial for making carbon capture commercially available and to avoid human and ecological threats.

Amine emissions are commonly detected as amine vapor emissions, amine droplet emissions or as amine aerosol emissions. Both vapor based and droplet based emissions are well known and effective counter measures exists for these emissions. For vapor emissions a water wash is used to control the emissions, while a demister unit controls the droplet emissions. Aerosol emissions are however in such a size range that these countermeasures are normally ineffective at removing them.

An important part of the issue is that recently published studies researching amine emissions from carbon capture systems indicate that the amine aerosols emissions can be significant. Mertens et. Al reported that with the presence of sulphuric acid aerosols in the gas phase the concentration of MEA was much higher than expected from the volatility of MEA, indicating high amounts of MEA in the aerosol phase [18]. While Khakharia and co-authors identified aerosol based emissions in the order of g/m^3 compared to vapor emissions in order of mg/m^3 [19]. Also Da Silva et. Al reported that aerosol based emissions dominated the total amine emissions [20]. These findings indicates that the amounts of solvent emitted with the aerosols are much more significant than what was first assumed. As these emissions are more difficult to control with normal countermeasures, understanding the behaviour of the aerosol phase and parameters effecting their formation and growth is thus crucial insight. Classifying the effect of these parameters is thus required to design carbon capture plants with efficient aerosol control units. As mentioned, countermeasures exists for controlling the droplet and vapor based emissions. It is thus thought to be possible to effect the aerosol emissions so that these countermeasures are effective in reducing the emissions.

Some research has been devoted to investigating what is effecting the aerosol emissions, but far less than the work devoted to detecting and characterising the aerosol emissions. There is still a knowledge gap regarding this issue and the aim of this report is to contribute to filling this gap.

1.3 Scope of Work

This thesis investigates the effect of various operating conditions and modifications of an amine scrubbing system on aerosol based amine emissions from the system. This is done to get a better understanding on how the aerosols behave and how to operate such a system in order to reduce the overall amine emissions.

To investigate the effects of varying operating conditions and implementing modifications to the system a base case is set up as to have a comparison for the studies performed. This was done by simulating a typical amine scrubbing process based on and validated against experimental data. The Base Case consist of an absorber column, and two identical water wash sections placed on top. The simulation tool used was CO2SIM, an in-house simulator especially developed for carbon capture by chemical absorption. Liquid side profiles were obtained as results from the simulation. These results were used in an external model, developed to predict aerosol emissions. Professor Emeritus Hallvard Fjøsne Svendsen performed all simulations done with the external model. From the aerosol model internal profiles for the gas, liquid and aerosol phase was obtained.

In former work, a validation of the simulation tool against an experimental campaign was performed. The results from this work is further used in this thesis. However, this work only included the absorber section of an amine scrubbing system. Thus, to ensure reliable data from the water wash section a validation of the equilibrium model used in CO2SIM was performed in this work. The validation validates the model for the areas where the amine concentration is in the lower ranges, as this is the case for water wash sections.

To gain insight in how aerosol emissions behaves and changes with operating conditions and modifications in an amine scrubbing system, four case studies were performed. At the beginning of the work the focus was on the water wash, and the first case study performed was on the height of the water wash section.

The report then moves on to focus on modifications to the system, mainly in the absorber section. The second case study investigates the effect of intercooling in the absorber column. In this study the placement of the intercooling unit is varied, and the height of the absorber column is also varied with different placements of the intercooling unit.

As the intercooling showed a substantial effect on the aerosol emissions, the effect of operating the absorber column isothermally was investigated in the third case study.

Lastly, a fourth case study was performed on a case with flue gas from a natural gas source. In this study the effect of the CO_2 content was investigated, as this is lower for natural gas based gases than coal based gases. More extensively was the effect of not letting the flue gas be pre-treated with a direct contact cooler before entering the absorber researched. This causes the gas to enter unsaturated with water and with a high temperature.

The case studies performed contributes to gaining a better insight on how to operate an amine scrubbing system in regards to minimizing overall amine emissions from amine scrubbing based carbon capture systems.

1.4 Outline of this project

An introduction to carbon capture and the challenges concerning amine emissions from carbon capture by chemical absorption systems has already been introduced in this thesis. Proceeding, theory on the chemical equilibrium in the system, aerosol formation and aerosol growth will be given, followed by a literature review of studies addressing the issue.

In the next section the model used to predict the aerosol phase in the system is described. Then the work done with validating the equilibrium model in CO2SIM is given. Next is the set up of the Base Case described, and a description of the case studies performed follows.

Finally, the results and discussions are presented. This section first presents results from the Base Case, going thoroughly through how the aerosol phase is behaving through out the columns. The rest of the section presents the results for each case

in the case studies performed, comparing them to the Base Case results. Lastly, recommendations for further work and conclusions are given.

2 Theory

2.1 Chemical equilibrium in Amine Scrubbing

When CO_2 in the gas phase is contacted with the solvent in an amine scrubbing system as described in the introduction, a concentration gradient appears and CO_2 diffuses into the solvent until equilibrium is reached. It is the solubility of CO_2 that determines how much of the compound will be absorbed by the liquid phase before the solution becomes saturated. When CO_2 has diffused into the liquid, it reacts with the amine in the solution. This causes CO_2 to undergo a chemical change, and the liquid phase is no longer saturated with CO_2. Thus, more CO_2 can dissolve in the liquid.

The major chemical species identified in the liquid stream after CO_2 is absorbed is molecular MEA, protonated MEA ($MEAH^+$), carbamate ($MEACOO^-$), bicarbonate ($HCO_3{}^-$), carbonate ($CO_3{}^{2-}$) and molecular CO_2. These species are formed through the following reactions. [12]

Water dissociation:

$$H_2O \longleftrightarrow H^+ + OH^-$$

Amine protonation:

$$MEA + H^+ \longleftrightarrow MEAH^+$$

Carbon dioxide first ionization:

$$CO_2 + H_2O \longleftrightarrow HCO_3{}^- + H^+$$

Carbamate formation:

$$MEAH^+ + HCO_3{}^- \longleftrightarrow MEACOO^- + H_2O$$

Carbon dioxide second ionization:

$$HCO_3{}^- \longleftrightarrow CO_3{}^{2-} + H^+$$

The amount of CO_2 absorbed in the solvent is commonly defined by the loading α. In

terms of the CO_2 and MEA balance we can write the following equations [21]

$$[CO_2]_{total} = [{CO_3}^{2-}] + [HCO_3^-] + [CO_2] + [MEACOO^-] \tag{1}$$

$$[MEA]_{total} = [MEA] + [MEAH^+] + [MEACOO^-] \tag{2}$$

From these equations, loading α can be defined as

$$\alpha = \frac{[{CO_3}^{2-}] + [HCO_3^-] + [CO_2] + [MEACOO^-]}{[MEA] + [MEAH^+] + [MEACOO^-]} \tag{3}$$

As MEA is a primary amine, the stoichiometry requires two molecules of MEA per molecule of absorbed CO_2. Hence, the maximal theoretical loading from chemical absorption is $\alpha = 0.5$. The loading in the solution is an important measure of how much of the CO_2 is absorbed and gives information about the cyclic capacity of the process. Likewise, it is also a measure of how much of the MEA has reacted. The main species formed from the reaction between CO_2 and MEA is the compound carbamate, which is non-volatile. Thus, when MEA is transformed into carbamate it no longer has the ability to vaporize. As the stoichiometry of the carbamate formation suggests, the volatility of MEA should approach zero at loading α equal to 0.5.[17]. Maintaining a high loading is thus desirable for both the CO_2 absorption capacity and for minimizing volatile MEA emissions.

2.2 Amine Emissions Mechanisms

MEA being a volatile compound does not only create vapor based emissions. Droplet emissions and aerosol emissions are two other mechanisms that releases amine emissions to the atmosphere.

Vapor based solvent emissions obey Henry's law and is highly dependent on temperature [22]. Volatility is a measure of how readily a substance vaporizes. This form of emissions is thus based on the amine evaporating from the liquid phase to the gas phase which carries the amine out to the atmosphere. The volatility of the given amine is dependent on the structure of the substance itself, the temperature and the

CO_2 loading. Increasing temperature increases the vapour pressure and thus increases the volatility, while the formation of carbamate and bicarbonate reduces the vapour pressure [17], [23]. Water wash units are usually used to reduce these vapor based amine emissions in industrial processes. A water wash section is a packed column on top of the absorber, placed over the lean amine inlet. The treated gas from the absorber section flows into the bottom of the water wash while water is led into the top of the column and flows counter-current to the gas. The water flow into the wash section is usually relatively cold and contains low amine concentrations. This condensates the amine components as well as the low concentrations shifts the amine equilibrium to make amine dissolve in the liquid phase. [24]

Liquid emissions is when droplets of the solvent is being carried out of the system with the gas phase [23]. In amine scrubbing systems, packed bed absorber columns are usually used. In these columns liquid is flowing on the packing, counter current to the gas phase. In columns like these the easiest way for the liquid to flow within packing sections is sometimes through free falling. This results in drops being formed which are picked up by the gas phase and carried out of the column. A demister unit is commonly used to reduce these emissions and the collection mechanism is based on either inertial impaction, direct interception, brownian movement or electrostatic attraction. The unit is normally placed before a water wash section as droplets entering the water wash can contain high amine concentrations, which may reduce the efficiency of the water wash. [24]

The last mechanism for amine emissons is aerosol based emissions. Aerosols are classified as systems of particles or droplets suspended in gas phase [25] and these emissions are often referred to as mist emissions. Aerosol particles are in the size range of 0.01 to 10 μm [26]. This size range makes normal countermeasures like demisters and water wash units ineffective at removing them.

2.3 Aerosol formation

As introduced in the introduction, aerosol emissions have been reported to dominate the total amine emissions. Four key elements has been identified as important when it comes to the formation of aerosols. These elements include particle number concentration, particle size distribution, supersaturation and reactivity of the solvent [18].

Aerosol formation is commonly initiated by SO_3 present in the flue gas, especially in flue gases from coal fired power plants. As coal inhibits a small fraction of sulphur (S), it gets converted to SO_3 under combustion processes [27]. When SO_3 is present in gas it will react with water vapor to form H_2SO_4. As the gas is cooled H_2SO_4 condenses and can form aerosols through two main mechanisms, homogeneous and heterogeneous nucleation [28]. Heterogeneous nucleation is initiated when there is a foreign particle in the gas that serves as a nucleation point, in which the sulphuric acid condenses on. In amine scrubbing processes, particles like soot and flyaway ashes can be present in the gas stream and serve as the nucleation point. The higher the inlet particle number concentration of the soot and H_2SO_4 particles, the higher the aerosol based amine emissions [19].

Homogeneous nucleation is when the nuclei is generated only of condensable components and be engaged when there is a supersaturated environment in the column [29],[26]. The degree of saturation (S), given in Equation 4, is defined as the actual vapour pressure of the component divided by its equilibrium vapor pressure [30], [29].

$$S = \frac{P(T, y_1^G, ..., y_k^G)}{Ps(T, y_1^G, ..., y_k^G)} \tag{4}$$

where P is the total partial pressure of all the condensing components at the actual temperature T and mole fraction y_i of the components. P_s is the total partial pressure of all the condensing components corresponding to the phase equilibrium. Supersaturation is defined as S>1 and can occur in the absorption column either by chemical reactions in the gas phase and then desublimation of the product substances, or by simultaneous heat and mass transfer, which causes an intersection of the phase equilibrium [31], [26]. Brachert et. Al reported that supersaturation in the absorber column initiated gas-phase H_2SO_4 to cross its dew point and form aerosols through homogeneous nucleation [28].

The temperature profile in chemical absorption columns has shown to be important in regards to supersaturation. In a typical CO_2 absorption column there is a small difference between the inlet liquid and gas temperatures, but due to the CO_2 being absorbed by chemical reactions heat is released and used to heat up the gas. Towards the end of the column, heated gas meets cold liquid which creates the characteristic

temperature bulge often seen in amine scrubbing systems. Among the studies investigating aerosol amine emissions, Khakharia et. Al worked on predicting supersaturation profiles in an amine scrubbing column [32]. Their predicted supersaturation profile and the corresponding temperature profile in their column is included in Figure 2. As their findings suggests the environment in the column gets supersaturated when there is a large difference between the gas and liquid temperatures.

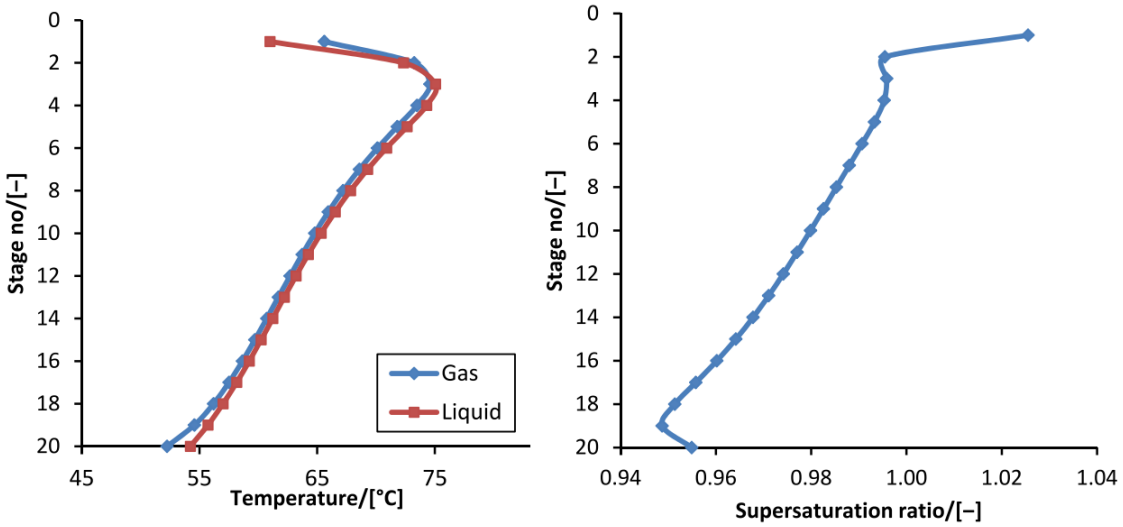

Figure (2) Temperature profile and supersaturation profile along an absorber column by Khakharia et. Al [32].

The reactivity of the amine and the structure of the component is also important in regards to aerosol emissions. This is due to amines with little hindering, like primary amines, has higher volatility and is more likely to be found in the gas phase, where it is available to condense on the aerosols. MEA is a primary amine and is amongst the most volatile amines [9]. Also, as mentioned, the formation of insoluble components like carbamate reduces the volatility of the amine. However, in this work only one solvent is investigated and this parameter is thus not considered to be relevant.

2.4 Aerosol growth

In the column the gas and liquid phases can be considered to be in a thermodynamic equilibrium. When there is a aerosol nuclei present, a third phase exists in form of a aerosol droplet [33]. As the hot gas containing aerosol particles meets the cold

liquid, the environment can be supersaturated. When this is the case, the condensable components in the gas phase can condense on the aerosol nuclei, causing it to grow [32].

In a paper by Fulk and Rochelle the droplet aerosol growth was modelled in both an absorber and a water wash. Their results indicated that aerosols grew in the absorber column by continual uptake of CO_2 and amine solution which creates a driving force for water uptake in the aerosols. They also found that the growth was faster in the water wash section due to elevated partial pressure of water relative to the absorber column [34].

Kang et. Al also modelled aerosol growth and their work showed some of the same conclusions. Aerosol growth is controlled by amine uptake in the absorber and by water uptake in the water wash. The authors also suggests that more volatile amines accelerates growth in the absorber. In addition, it was reported that the growth of the aerosols is closely associated with the temperature difference between gas and solvent liquid. Their modelled aerosols seemed to grow quickly when the liquid temperature was higher than the gas temperature. The growth was slower but stable when the temperatures were in equilibrium and the size decrease when gas temperature was higher than liquid temperature. Also in this work does the aerosols grow rapidly at the beginning of the wash section, before the growth stabilizes and is expected to grow stably with increased residence times [35].

2.5 Literature Review

The rest of this section focuses on findings in previous work addressing the effect of different parameters on the aerosol emissions. From the theory it is clear that the temperature profile in both the absorber and water wash has a effect on both the growth and the formation of aerosols. A similarity between the studies reviewed is that the effects found to impact the aerosol emissions also has an effect on the temperature profiles in the column.

The temperature profile, specifically the temperature bulge in the absorber section is repeatedly reported as important in regards to amine emissions from the system. The bulge temperature is quantified by its magnitude and the location of the bulge in the column. Kvamsdal and Rochelle researched the behaviour of the temperature

bulge and found that it is dependent on the heat of absorption, L/G ratios, height of packing and flue gas CO_2 concentration. They also found that the magnitude of the bulge is mainly affected by heat of absorption and increased with increasing CO_2 content in the gas. [36]

Khakharia et Al. performed a study were the effect of the lean solvent temperature in an MEA based amine scrubbing process was investigated. This was done by changing the temperature of the lean solvent from 40 °C to 80 °C while keeping the flue gas temperature constant at 45 °C. Their results showed that the when the lean solvent temperature was increased the aerosol based emissions decreased [37].

A similar study was performed by Yi. et Al where lean solvent temperature was increased from 30 °C to 50 °C. In this work the increased lean solvent temperature resulted in increased vapor and aerosol emissions[22]. This is contradictory to the findings by Khakharia et. Al and indicates that it is an increase in magnitude of the bulge temperature and not the lean solvent temperature that increased the emissions. The temperature profiles in both of these studies is included in Figure 3. Figure 3 (a) shows the temperature profiles for Khakharia et. Al and shows that the bulge decreases with increasing lean solvent temperature. While Figure 3 (b) shows the temperature profiles from Yi et. Al which shows that the bulge increases with increasing lean solvent temperature.

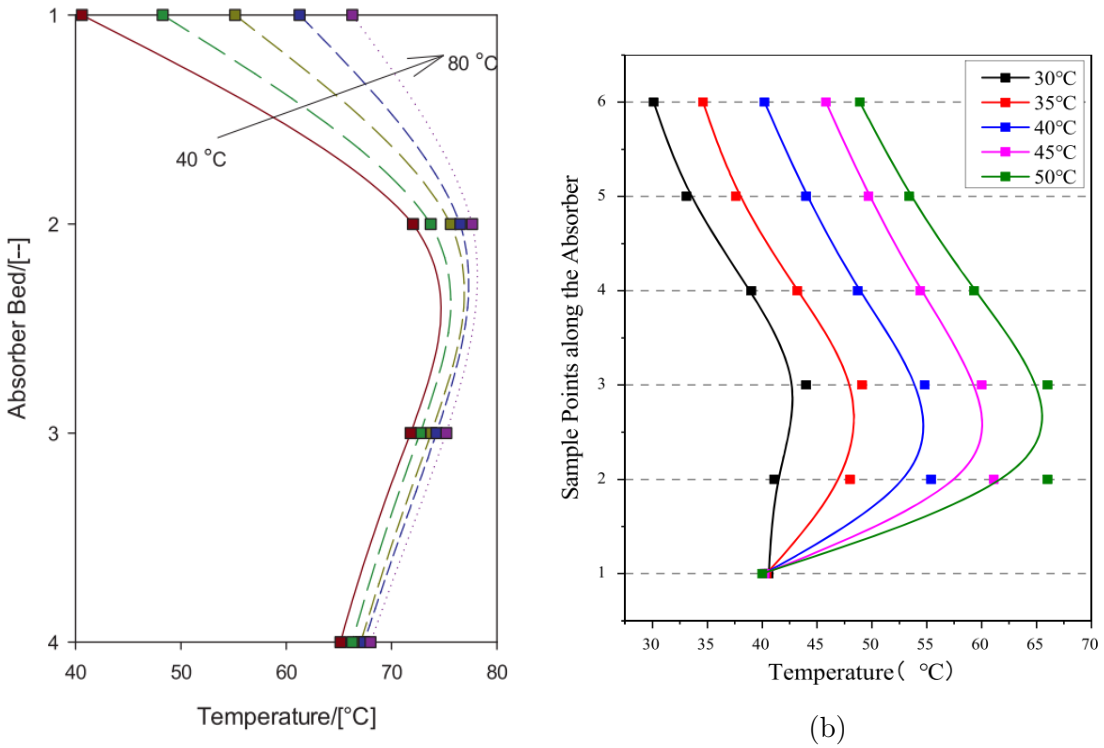

(a) (b)

Figure (3) (a) An example of temperature profiles along the absorber column that shows that the temperature bulge is decreasing when lean solvent temperature is increased from 40°C to 80 °C with 10 °C [37].
(b) Another example of temperature profiles along an absorber column that shows that the temperature bulge is increasing when lean solvent loading is increased from 30 °C to °C with 5 °C intervals [22].

Gupta et. Al has done work on the effect of the temperature bulge on the aerosol emissions and found that an increasing bulge causes a supersaturated environment in the column which accelerates aerosol formation and growth [38]. Thus, this study also suggests that the effect on aerosol is dependent on the size of the bulge temperature.
2.4

A modification that has an effect on the temperature profile in the absorber column is intercooling. The effect of intercooling on energy requirements in amine scrubbing systems is well known and has a desirable effect. The modification is used to reduce the amount of absorbent liquid needed to capture a given amount of CO_2, which

leads to a reduction in the reboiler steam demand. [39], [40] The principle of the modification is to withdraw a fraction of the absorbent liquid some distance down the column, cool it down and insert it back into the column. This will lead to a decrease in the magnitude of the temperature bulge. [41], [42]. The optimal position of the intercooling unit is typically 1/4th-1/5th of the column height from the bottom of the column as this gives the optimal reboiler duty, while 1/3th of the column height is considered to be the conventional choice [43].

However, the effect of intercooling on emissions from amine scrubbing systems is not considerably researched. Fulk and Rochelle performed a study were the effect of intercooling on aerosol based amine emissions using the amine option Piperazine (PZ) as the solvent was investigated. In this work an intercooling unit was placed in the middle of the column, and the absorbent liquid was cooled down to the absorbent liquid inlet temperature. The results showed that the partial pressure of PZ was significantly reduced and that the aerosol droplets showed less growth compared to a non-intercooled absorber [34].

Majeed and Svendsen also studied the effect of intercooling, but on an MEA based absorption system, using flue gas with high CO_2 content and the intercooling section placed at a quarter from the bottom. Their results showed that intercooling lowered the partial pressure of MEA in both the absorber and the water wash section, which reduced MEA emissions overall. They also observed a reduction in droplet growth. [44]

Gupta et. Al performed a study on the effect of intercooling on aerosol emissions, by shifting the intercooling from the bottom of the absorber column to the top. The study found that this decreased the magnitude of the bulge temperature and thus decreased the emissions. However, the study also commented on that if the major fraction of cooling duty is performed above the location of the bulge, it could create a localized supersaturation, due to an increased temperature bulge, which would increase emissions. [38].

Several studies have reported the effect of CO_2 content in the gas on aerosol emissions and commonly reports that this variable has an effect on the temperature profile. Khakharia et. Al also performed a study where aerosol emissions were predicted when varying CO_2 content in the flue gas from 13% to 2%. This study also concluded that

amine emissions and the bulge temperature in the absorber column increased when the CO_2 content of the flue gas was increased [32]. The same was shown by Yi et. Al, who researched the effect of the CO_2 content of the flue gas. Their results showed that the temperature bulge also increased with increasing CO_2 content, which increased the total emissions [22]. Majeed and Svendsen characterized aerosol emissions from CO_2 capture plants treating various industrial flue gases. In their study they investigated a natural gas with 4% CO_2 and a flue gas from a coal based source with 12% CO_2. Their setup included an absorber section with two water wash sections in the same size ranges as the setup in this work. Their findings included that the aerosol amine emissions from the natural gas source after the second water wash was in the 0.9-3400 mg/Nm^3 range, while the emissions were in the range 65-24000 mg/Nm^3 from the coal based flue gas. The authors explained this by more carbamate being formed with increasing CO_2 content in the flue gas. This leads to more MEA being bound up and to a less effective water wash. The increasing CO_2 content also lead to a higher carry-over of amine into the water wash sections [45].

A few studies has been performed on the effect of water wash parameters on the aerosol based emissions from carbon capture plants. Majeed and Svendsen performed a study where the effect of water wash on aerosol based emissions were studied. The authors found that water wash sections were very effective in reducing mist-born emissions. They also found that the water wash can be an effective measure to increase the size of the droplets, so that a demister unit is more effective in removing the droplets. Increasing the temperature in the water wash section increased droplet size and emissions. Increasing the height of the water wash sections did not have a significant effect on the emissions other than increasing residence time [46].

As mentioned in the previous section Fulk and Rochelle modelled aerosol growth in the water wash section and suggested that the growth mechanism of aerosols in the water wash can be exploited by increasing the residence time in the wash or by diluting the wash water [34].

Gupta et. Al investigated the effect of the temperature in the water wash and concluded that reducing the temperature in the water wash resulted in increased aerosol emissions. The authors explained this by the fact that a lower temperature in the water wash causes increased condensation of amine in the vapor phase into the aeorsol phase [38].

To summarize, the reported findings indicate that the temperature profile has a significant effect on the aerosol based emissions, with increasing bulge increasing the emissions. More specifically, is both the growth of the droplets and the MEA content seen to increase. Modifications like intercooling has the effect of reducing the temperature bulge, which leads to decreased growth and MEA contained in the aerosol phase. The amount of MEA emitted with aerosols also increase with increasing CO_2 content in the gas, as higher CO_2 concentration leads to higher temperature which makes the amine more present in vapor form. The water wash is effective in growing the droplets while reducing the MEA content in the aerosol phase. Increasing residence time by increasing the height of the column is effective in increasing these effects.

3 Method

3.1 Aerosol modeling

To research the behaviour of aerosols, a model is needed. Majeed and Svendsen has developed a model in Matlab for predicting the behaviour of multisized droplet swarms. The model predicts size, internal variable profiles for the droplets and the mass and heat transfer fluxes as function of position in the absorber, including the outlet [45],[46]. The modelling work performed in these studies are used for the work in this project.

For the modeling work it is assumed that a droplet size distribution with two different droplet sizes enters the absorber with the gas phase. The droplet diameters is set to 0.15 μm and 1 μm as this is the typical size ranges reported in literature [37], [32].

3.1.1 Mass and heat transfer

The concentration profile for a single droplet is based upon the general balance equation in terms of flux for a spherical particle. Taking into consideration only the radial direction, the dimensionless concentration profile for MEA is modelled as [45]

$$\frac{\delta C_x}{\delta t} = (\frac{D_x}{R^2}(\frac{2}{\xi}\frac{\delta C_x}{\delta \xi} + \frac{\delta^2 C_x}{\delta \xi^2}) - r_x) - \frac{3C_x}{\xi}\frac{\delta \xi}{\delta t} \tag{5}$$

Where ξ is the dimensionless radial position as a function of radius r; $\xi = r/R$, D_x denotes diffusivity, C_x denotes concentration, and r_x is the reaction rate.

The temperature profile for a single droplet is based upon the general energy balance for pure Newtonian fluids, in terms of spherical particles. Considering only radial direction the dimensionless equation for thermal energy is modelled as [45]

$$\frac{\delta T}{\delta t} = \frac{k}{\rho C_p R^2}(\frac{2}{\xi}\frac{\delta T}{\delta \xi} + \frac{\delta^2 T}{\delta \xi^2}) + \frac{r_x \Delta H}{\rho C_p} \tag{6}$$

Where ρ denotes the density, C_p the heat capacity, k the thermal conductivity, T the temperature and ΔH the enthalpy.

The reaction kinetics for CO_2 and MEA is based on the termolecular mechanism, where MEA reacts with one molecule of a base and one molecule of acid (CO_2) simultaneously. The concentration based rate equation for CO_2 is modelled as [45]

$$r_{\mathrm{CO_2}} = k^T_{MEA}[MEA] + k^T_{\mathrm{H_2O}}[\mathrm{H_2O}]([MEA][\mathrm{CO_2}] - \frac{1}{K^T_{eq}}[MEAH^+][MEACOO^-]) \quad (7)$$

Here k represents the kinetic rate constants for MEA and water and K^T_{eq} is the equilibrium kinetic rate constant.

3.1.2 Droplet size distribution

The droplet size distribution is modelled as a population having two moments that are linked to the droplet radii. A logarithmic normal distribution is chosen to approximate the size distribution for the droplets [46].

$$f(V) = \frac{1}{R\sigma\sqrt{2\pi}} exp(-\frac{(lnR - \mu)^2}{2\sigma^2}) \quad (8)$$

σ represents the variance and μ indicates the mean, these are defined as

$$\sigma = \sqrt{ln\frac{\overline{R_2}}{\overline{R_1}}} \quad (9)$$

$$\mu = ln\,\overline{R_1} - \frac{1}{2}ln\frac{\overline{R_2}}{\overline{R_1}} \quad (10)$$

The droplets grow and shrink due to mass transfer, and is described by

$$\frac{d\,\overline{R_1}}{dt} = \langle\frac{dR}{dt}\rangle = \langle\tilde{N}_1\rangle = \tilde{N}_1 \quad (11)$$

$$\frac{d\,\overline{R_2}}{dt} = \frac{2}{\overline{R_1}}\langle R\tilde{N}_2\rangle - \frac{\overline{R_2}}{\overline{R_1}}\langle\tilde{N}_1\rangle = \frac{2}{\overline{R_1}}\tilde{N}_2\langle R\rangle - \frac{\overline{R_2}}{\overline{R_1}}\tilde{N}_1 \quad (12)$$

3.1.3 Assumptions

The aerosol droplets in the model are assumed to enter and travel with the gas phase through the columns. Coalescence and breakage of the droplets are not considered, meaning that the number of droplets entering a column will be the same number that leaves the column. Thus the model does not take formation of aerosols into consideration. In the a demister unit however, the model removes some particles based on the size of the particles. The model uses a log-normal distribution which means that the removal efficiency in the demister unit goes towards zero for the smallest droplets and towards 100 % larger droplets. It is further assumed that the liquid phase is not influenced by the aerosols and that no reactions are taking place in the gas phase.

3.1.4 Predicting aerosol phase behaviour

The model described above was used to predict the aerosol phases for an amine scrubbing system with varying operating conditions. For each simulated case, liquid side profiles including temperature, mole fraction of MEA and water and loading as a function of position in the system were obtained from the simulation tool CO2SIM. The profiles were used by the aerosol model to predict the aerosol phase composition and size.

Professor emeritus at NTNU, Hallvard Fjøsne Svendsen has performed all the simulation work done by the aerosol-model in this project.

3.2 Validation

3.2.1 Validation of CO2SIM against experimental campaign

In previous work by the author, the simulation tool CO2SIM has been validated against the experimental campaign by Sønderby et. Al (2013) [47]. In this campaign, 23 runs were performed where the height of the packing section in the absorber were varied from 1.6 m to 8.2 m and the lean solvent loading were changed from 0.112 to 0.254, 0.271 and 0.3 with packing height at 8.2 m. The same runs were simulated in CO2SIM and during this work it was found that the deviation between the simulated and experimental CO_2 absorption rate were within 20% for 78% of the runs. The results from the validation work can be found in Appendix A, in Figures 33 - 36. The

figures gives the ratio between simulated and experimental CO_2 absorption rate for different operating conditions. Among the results the most significant trend was seen for the CO_2 vol% at the gas inlet where the results indicated that the absorption rate was getting over-predicted for higher CO_2 contents and under-predicted for lower CO_2 contents. For the other conditions there were not found any significant trends.

The temperature profile given by CO2SIM was also compared to experimental temperature data and can be found in Figures 37-42 in Appendix A. It was evident that the temperature bulge in the column was under-predicted for all of the 23 cases. In these cases the temperature bulge is located in the bottom of the column and would mostly effect the amount of CO_2 absorbed and thus the rich loading at the bottom of the column. Towards the top of the column, the deviation from experimental values decreased, but there was still some under-prediction. The overall deviation increased for lower column heights. In this work, the absorber column is almost twice the height of the column used in the Sønderby et. Al (2013) experimental campaign. This could indicate that the temperature deviations are even smaller for the column height used in this work.

Also, the operating range for the experimental campaign is quite different from the operating range used in this work. Therefore, it is difficult to say how precise the results in the operating range used in this thesis are. To make sure that the Base Case used in this thesis gives reliable results, this simulation is validated against in-house experimental data given in Section 3.3. As will be mentioned in Section 3.3, the interfacial coefficient in the column needed to be adjusted to fit the experimental capture rate. This was not done during the Sønderby. et Al (2013) validation and might be another reason for the deviations seen during the validation. Regardless, the validation work can be used to make sure there are not any major defaults in the simulation tool which might effect the results significantly. This was not detected.

3.2.2 Validation of Vapor Liquid Equilibrium in CO2SIM

In this thesis the water wash sections of amine scrubbing systems is of importance. As the concentration of MEA is in the lower ranges in these sections, [48] there is a need to evaluate the equilibrium model in the simulation tool to ensure that the model is fitted to low MEA concentrations.

The equilibrium model in CO2SIM was validated by generating Vapor Liquid Equi-

librium (VLE) curves for different CO_2, MEA and water ratios using the inbuilt template "Ordinary Electrolyte Non-Random Theory", as this was the equilibrium model to be validated. The validation was performed in CO2SIM, using a flash unit to simulate an equilibrium stage. The flash takes a mixture CO_2, MEA and water as input, and gives a resulting vapor and liquid stream as output. The resultant curves was compared to literature and experimental data.

In the water wash sections the loading in the liquid phase is in the higher range as the MEA content is very low. From previous work it is known that the weight fraction of MEA in the water washes is usually less than 0.001. The equilibrium curves were first compared to the CO_2-water equilibrium, as there exists limited literature data for MEA-CO_2-water vapor-liquid equilibrium for low MEA concentrations. The mole fractions for CO_2 in the CO_2-water VLE was calculated using Henry's law through the following equation [49]

$$x_{CO_2} = \frac{H}{P_{CO_2}} \tag{13}$$

where x_{CO_2} is the mole fraction of CO_2 in the liquid phase, H is the Henry constant and P_{CO_2} is the partial pressure of CO_2 in the vapor phase.

Henry's constant was calculated from Equation 14 as proposed by Caroll et. Al as their work covers the temperature and pressure ranges of interest for post combustion carbon capture [50].

$$lnH^{\infty}_{CO_2,water}[MPa] = -6.8346 + \frac{1.2817 \cdot 10^4}{T} - \frac{3.7668 \cdot 10^6}{T^2} + \frac{2.997 \cdot 10^8}{T^3} \tag{14}$$

Where $H^{\infty}_{CO_2,water}$ is the Henry constant and T is the temperature in Celsius. The temperature was set to 40 °C and Henry's constant was calculated to 228730 MPa. The mole fraction in Equation 13 was then calculated by using the Henry's constant and the partial pressure of CO_2 in the resulting vapor stream from the flash unit in CO2SIM.

Three cases with different weight fractions of MEA in the inlet stream were performed. The cases were simulated by changing the weight fraction of MEA in the inlet liquid

stream from 0.01 to 1E-8. The mass fraction of MEA, the mole flow of CO_2, the pressures specified and the results CO_2 fractions are given in Table 11 to 13 in Appendix B. The resultant equilibrium curves is presented in Figure 4 and compared to the CO_2-Water VLE at 40 °C. The curves show that when the weight fraction of MEA in the MEA-water-CO_2 mixture approach zero, the VLE curves approach the VLE curves for CO_2-water. This is expected and ensures that the equilibrium model in the simulation tool is fitted to very low MEA concentrations.

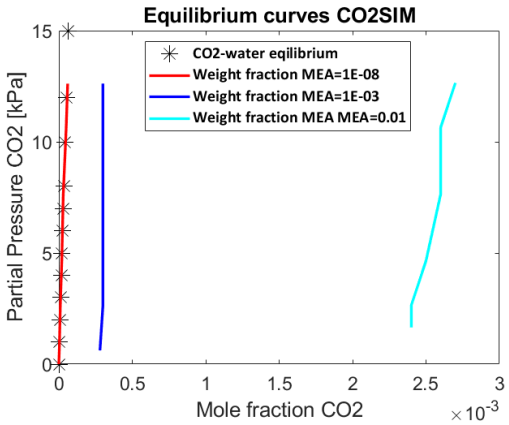

Figure (4) VLE curves generated in CO2SIM for when the weight fraction of MEA approaches zero compared to VLE data for the CO_2-water equilibrium. The VLE data was calculated using Henry's Constant for the CO_2-water equilibrium [50].

Some in-house experimental data when the weight percentage of MEA is in the 0.6-6 wt% range was used to further validate the model. Three cases where the MEA fraction was set to 0.6119, 3.06 and 6.113 wt% were performed. The operating conditions for the flash and the resulting CO_2 vapor fraction, CO_2 liquid fraction and MEA liquid fraction are given in Table 14 to 16 in Appendix B. In these cases the experimental data was given as partial pressure of CO_2 as a function of loading in the liquid phase. The resulting curves is given in Figure 5 together with the experimental data. The curves show that the equilibrium model is fitted for the MEA concentrations in this range. There are some deviations from the experimental data but these are small and not larger than expected when considering experimental uncertainties.

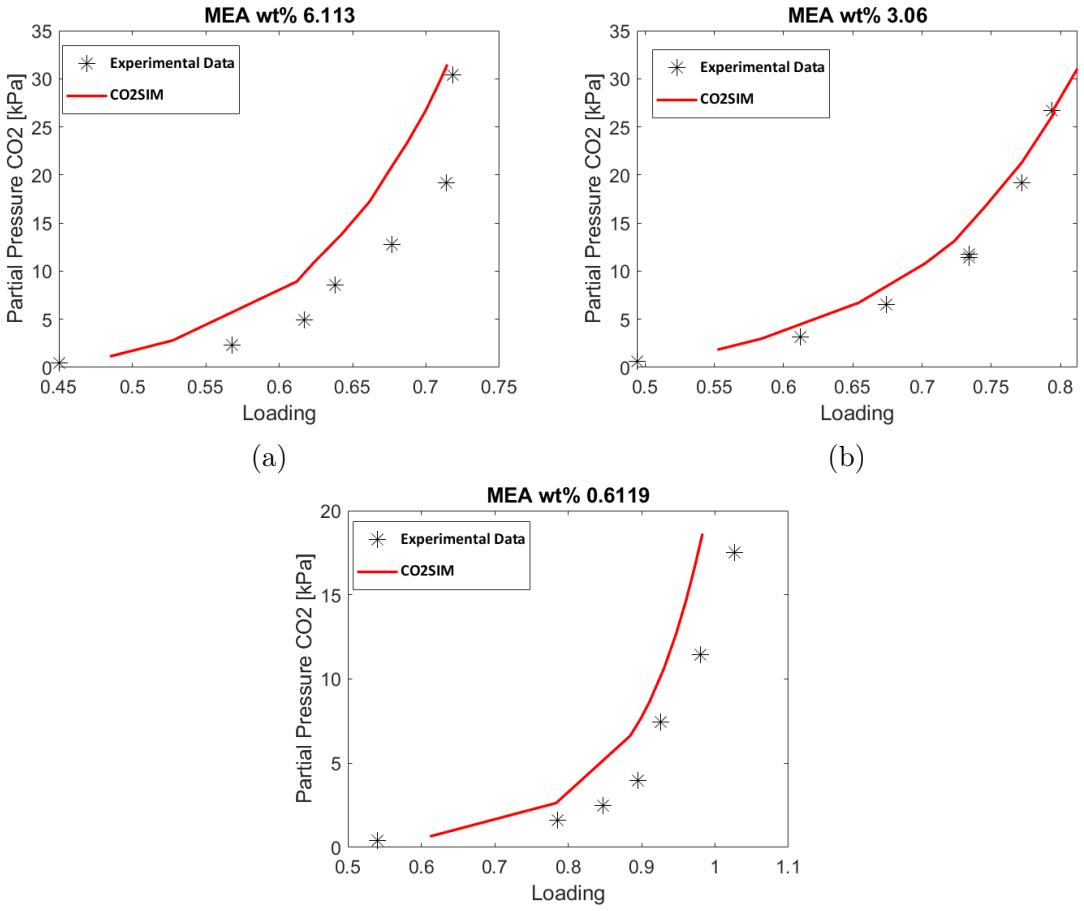

Figure (5) VLE curves generated in CO2SIM compared to experimental data for the weight percentage of MEA being 6.113 wt% (a), 3.06 wt% (b) and 0.6119 wt% (c).

To conclude and summarize, VLE data from CO2SIM has been validated against the CO_2-water equilibrium when the MEA concentration approaches zero and against experimental data for low MEA weight fractions. Both validation cases showed satisfying results, implying that the equilibrium model is fitted for low MEA concentrations and that it approaches the CO_2-water VLE when the MEA concentration approaches zero.

3.3 Defining a base case

The simulations in this project was carried out using the simulation tool CO2SIM, a SINTEF in-house simulator specifically developed for CO_2 absorption processes [51].

A CO_2 absorption process using MEA as the solvent with two water washes stages on top, was simulated in the 7.1.0.5 version of CO2SIM. The simulation does not include a stripper section, as the focus of this work is on the absorber and water wash sections. As a basis for the simulations the inbuilt template "Ordinary Electrolyte Non-Random Theory" model with the mixture "MEA_AMP_CC2_OeNRTL" was used. To get realistic results, the Base Case was set up using in-house data from a carbon capture plant at Tiller in Trondheim. The data can be found in Table 17 in Appendix C. The process flowsheet in CO2SIM is given in Figure 6. The operating conditions for all of the streams in the Flowsheet is given in Table 20 in Appendix D.

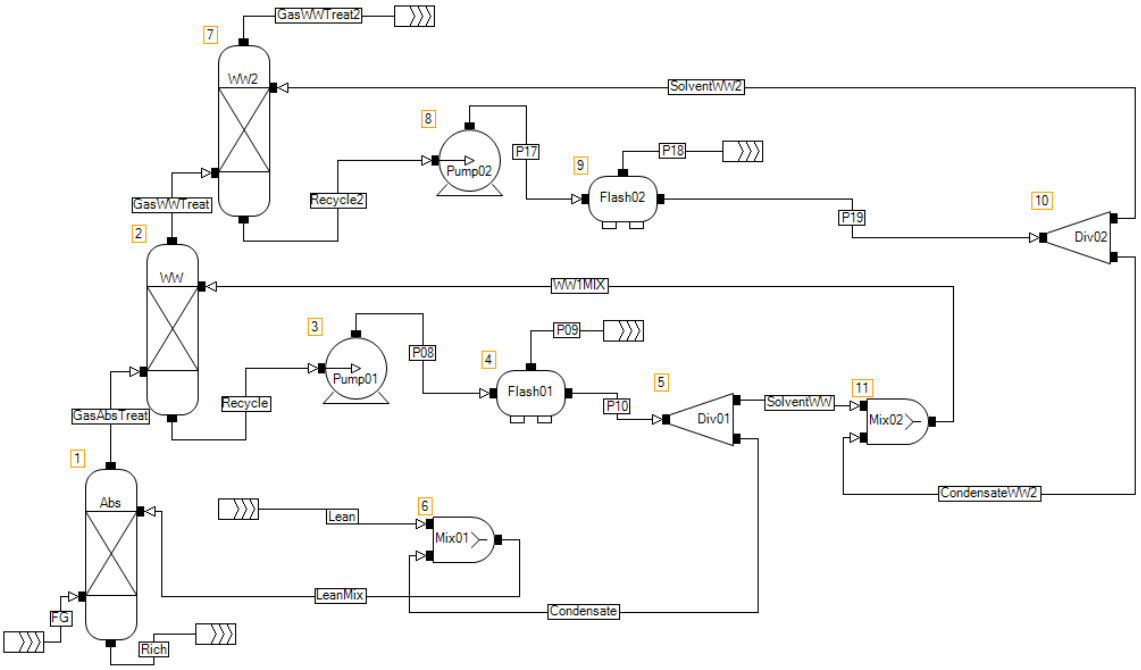

Figure (6) Flowsheet of the simulation in CO2SIM.

The absorber is a 15 m high column with 0.2 m diameter labeled "Abs". The column

is simulated as a mass-transfer-rate-based column. This model calculates the trays on a tray-by-tray basis, considering each tray as a stage of separation. A gas and lean solvent liquid stream was set as inlet streams into the column based on the experimental data. A summary of the inlet conditions is given in Table 1. A trace amount of AMP was added to the lean solvent stream to get the system to converge. However, this amount is so small that it is not expected to effect the results. The packing set in the column is Mellapak 250Y, which is the default packing in CO2SIM.

Table (1) The inlet condition of the flue gas and lean solvent entering the absorber column.

	Flue Gas	Lean Solvent
Temperature [°C]	35	39.4
Flowrate [kmole/hr]	6.14	17.6
Vol% CO_2	13	-
Loading [mole CO2/mole MEA]	-	0.17

The Tiller plant uses Mellapak 2X packing that has a specific geometric surface equal to 205 m^2/m^3 [52]. Mellapak 250Y has a specific geometric surface area equal to 250 m^2/m^3 [53]. The interfacial coefficent is adjustable in the CO2SIM column and based on the packing areas, it should be set to 0.82. However, this gives a column where the absorption efficiency of CO_2 is over predicted compared to the experimental data from the Tiller plant. For this reason, the interfacial coefficient was adjusted to 0.3 to match the experimental capture rate. It is believed that the reason CO2SIM simulates a more effective column than the Tiller plant is due to the low diameter of the column. Even tough liquid is being sampled out of the Tiller column it is likely that such a small diameter causes liquid to be flowing along the walls of the column. This causes a less effective interfacial area between the gas and the liquid and thus the column ends up being less effective than what is theoretically possible. Furthermore, as discussed briefly in Section 3.2.1 the validation performed on the simulation tool in previous work showed a slight indication that the absorption rate might be over-predicted for cases with higher CO_2 content, so this might also explain why the high efficiency of the column is observed.

The Tiller plant has a 2.4 m water wash section, with 0.2 m diameter, at the top of the absorber. This column is also simulated as a mass-transfer-rate-based column and

labeled "WW". The treated flue gas from the absorber and a wash stream is injected into the column. The conditions of the wash stream was set from the experimental data and is listed in Table 18 in Appendix C. The interfacial coefficient was set to 0.3 to be consistent with the absorber column.

As a starting point the liquid stream into the water wash was set as pure water with small amounts of MEA and CO_2 and a trace amount of AMP to get the column to converge. Liquid exiting the water wash sections is being led through a pump where the pressure is specified to 400 kPa. The stream then enters a flash unit, where the temperature and pressure is set equal to the inlet conditions. To avoid flow accumulating a purge stream of excess liquid was taken from the liquid stream. This excess liquid can be considered as condensate from the column and is mixed with the lean solvent liquid entering the absorber. The rest of the liquid is being mixed with condensate from the water wash section above before being inserted back into the water wash column.

The fraction of MEA is close to constant in the top and bottom of the section, as the liquid in the water wash is recirculated. Thus, it is only possible to obtain a single amine/water equilibrium stage from such a column. Another water wash column was added to obtain an extra stage, labeled "WW2", to be able to investigate different water wash conditions. The second water wash stage is a copy of the first stage and the column was set up as described above.

As mentioned, the interfacial coefficient in the absorber was adjusted to match the carbon capture efficiency of the plant. The results for the simulation was also compared to the rich loading and the dry vol% of CO_2 in the outlet gas. There are two experimental values for the vol dry % of CO_2, so the result from CO2SIM was compared to the average of the two values. The results are given in Table 2. There is a constant over prediction of maximum 2 %. Since all of the variables are over-predicted it is expected that by fine tuning the interfacial coefficient one could obtain even more accurate results. However, the results are considered to be adequate as the relative difference is negligible and as there is no indication on consistent errors in the simulation.

For the water wash section the only experimental data available to compare with simulation tool is the liquid loading out of the absorber. The ratio between the

simulated and experimental loading is also given in Table 2. There is a 5% under prediction of the loading in this section. As the equilibrium model was validated in the water wash range, this deviation might be due to experimental uncertainties or from the specified tolerance in the simulation tool, that was set to 2E-07. As the values in the water wash sections are low, this might have an effect on the results.

Table (2) The ratio between the simulated CO_2 capture efficiency, rich loading and CO_2 vol dry % in the treated gas from the absorber and the experimental values from the Tiller plant.

Variable	SIM/EKS
CO_2 capture efficiency	1.01
Rich Loading	1.02
CO_2 vol dry %	1.00
Water wash loading	0.95

3.4 Aerosol Emissions - Case Studies

To gain a better understanding of the behaviour of aerosol amine emissions from amine scrubbing systems, the aerosols were studied during several case studies. In these studies, different system variables were varied and modifications were implemented to research how it effected the aerosol phase. The operating conditions for all of the cases are given in Table 21 in Appendix E, where the changes made to the system are highlighted. The following sections describes the conditions and modifications investigated. An overview of the cases performed in the case study is given in Table 3.

Table (3) Overview of the simulated cases.

Case 1	Height of WW1 doubled
Case 2	Total height of water wash sections decreased to 4m
Case 3	Total height of water wash sections decreased to 2m
Case 4	Intercooling placed at 1/3 from bottom
Case 5	Intercooling placed at 1/3 from top
Case 6	Height of absorber decreased to 13m with intercooling at 1/3 from bottom
Case 7	Height of absorber decreased to 12m with intercooling at 1/3 from bottom
Case 8	Height of absorber decreased to 12m with intercooling at 1/3 from top
Case 9	Isothermally operated absorber
Case 10	Saturated natural gas used as flue gas
Case 11	Unsaturated Natural gas used as flue gas with inlet temperature being 90 °C

3.4.1 Case Study - Water wash height

The first case study investigated the effect of varying the height of the water wash sections. Three cases were performed, one where the height was increased and two where the height was reduced. The cases are given in Table 3 as Case 1, Case 2 and Case 3. For Case 1, the simulation was performed by increasing the height of the first water wash to 4.8 m, giving a total water wash height of 7.2 m. For Case 2 the simulation was performed by reducing the height of both water wash sections from 2.4 m to 2 m each, giving a total height of 4 m. For Case 3 the simulation was done by decreasing the height of both water washes to 1 m each, giving a total height of 2 m.

Previous work reported in literature and mentioned in Section 2.5 indicates that the height of the water washes effects the retention time in the water washes. In the water washes the droplets grow due to uptake of water, and MEA depletes out of the droplets. For the case with increased height the retention time is thus increased, which means that it is likely that the results will show an increased droplet size and a reduction in the MEA carried with the aerosols. For the cases with decreased height the retention time is thus reduced and a decrease in droplet size and the amount of MEA carried with the droplets is expected.

3.4.2 Case Study - Intercooling

The next case study performed was a case study investigating the effect of intercooling, with and without a height reduction of the packing height. The cases simulated is given in Table 3 as Case 4, Case 5, Case 6, Case 7 and Case 8. Two cases were simulated where intercooling was implemented at 1/3 from the bottom of the column, Case 4, and 1/3 from the top of the column, Case 5, with the absorber packing height being the same as for the Base Case. As the absorber column has a 15 m packing height, the intercooling unit is placed at 5 m from the bottom in Case 4 and 10 m from the bottom in Case 5.

The simulations were performed in CO2SIM by simulating two separate absorber columns. For the first case, an absorber of 5 m and 10 m was simulated. The lean solvent liquid was injected into the top of the 10 m column, and the liquid leaving at the bottom was cooled with a flash unit to the lean solvent inlet temperature, before it was inserted into the top of the 5 column. The flue gas was inserted into the bottom of the 5 m column and the gas leaving the column was led into the bottom of the 10 m column. The gas leaving the absorber section was then led into the same water wash system as used in the base case. The set up for the second case was the same but with the 10 m column at the bottom and the 5 m column at the top.

Based on the studies described in Section 2.5, it is expected that an intercooling unit in the absorber column will reduce the magnitude of the temperature bulge and reduce the outlet temperature of the gas from the absorber. This will cause less transport of water and MEA into the aerosols in the absorber. A lower temperature of the treated gas will cause a smaller temperature difference between the cold environment in the water wash and the gas. This will lead to less condensation of water in the water wash, which causes the growth of the droplets to slow down compared to the Base Case. It is also expected that the vapor based emissions are reduced due to the lower temperatures.

Intercooling is usually placed close to the bottom of the column as this gives the highest cyclic capacity in regards to carbon capture. However, it is expected that by placing the intercooling unit close to the top it will have a larger effect on the magnitude of the bulge temperature [38]. As the importance of the bulge temperature in regards to emissions was elaborated in Section 2.5, it is expected that a smaller

difference between gas and liquid will further reduce aerosol emissions.

Three cases where intercooling combined with a reduction of the absorber packing height were also implemented. In Case 6 the absorber packing height was reduced to 13m, and intercooling was placed at 1/3 from the bottom. In Case 7 and Case 8 the height of the absorber packing was reduced to 12 m. Intercooling was implemented at 1/3 from the bottom in Case 7 and 1/3 from the top in Case 8. The set up was implemented the same way as for the intercooling cases without height reduction.

The results from these cases are expected to be the same as for intercooling without height reduction, as it is expected that the intercooling also reduces the magnitude of the temperature bulge in these cases, which reduces both droplet growth and MEA carried with the aerosols. However, in these cases a height reduction in the packing height will also cause a shorter retention time which will cause the growth of the droplets to be reduced. As it is the retention time in the absorber and not in the water washes that it is affected it is expected that less MEA will transfer into the droplets in the absorber section, which will reduce the amount of MEA carried by the droplets. As the cases with 12 m height gives the largest reduction in retention time, the effect is expected to be most significant for these cases.

3.4.3 Case Study - Isotherm Absorber

To further investigate the effect of the temperature profile in the absorber column a case was performed with an isotherm absorber column. The case is given in Table 3 as Case 9.

In CO2SIM such a column is not an option. Therefore, to keep the temperature in the column as constant as possible, the isotherm profile was approximated by splitting the column into several stages and using intercooling between each column. The number of steps and the intercooling temperature was decided by try-and-fail until the temperature change for each step was less then 10 °C. This was done by splitting the column into 6 separate columns with 2.5 m packing height each and cooling the liquid down to 35 °C between each stage. The inlet lean liquid and the inlet gas were the same as in the base case and the diameter of the column also remained unchanged. A flash unit was used to cool down the outlet liquid from each stage, before the solvent was injected into the top of the stage underneath. The flue gas was

injected into the bottom of the first column and the treated gas leaving each column was injected into the bottom of the stage above. The gas leaving the top stage was inserted into the water wash system used in the Base Case.

The modification is expected to reduce both growth of the droplet and the MEA amount transferred into the droplets through the absorber section due to the difference between the gas and liquid temperature being held low like studies described in Section 2.5 suggests.

3.4.4 Case Study - Nature gas

Flue gas typically has a high temperature around 60-100 °C. For this reason the gas usually enters a direct contact cooler (DCC) that cools the gas to around 30-40 °C and saturates the gas with water. In this section two cases was performed using a flue gas from a natural gas source. When flue gas from a natural gas source is used, the CO_2 content is in the lower range of 3-4 vol% CO_2. The gas generally has a low heat capacity and the heat released from reactions in the absorber is less in these cases. Thus, the temperature does not rise as much in the absorber column. Therefore, it is thought as a possibility to not lead such a gas through a DCC unit. In this section the effect of such is case is investigated and an inlet temperature of 65 °C was chosen. The case is compared to another case using the same flue gas, but in this case the gas is thought to be lead through a DCC unit.

Before performing this study, a new base case was set up to validate the simulation tool in this operating range. A simulation based on in-house data from a plant using natural gas with 4.34 vol dry% CO_2 was set up. The specifications for this case is listed in Table 19 in Appendix C. The interfacial coefficient needed to be adjusted to 0.44, to get adequate results. The simulation was compared to in-house experimental data from Tiller and the results are given in Table 4. Both the rich loading and the dry CO_2 vol% are under-predicted but the largest deviation can be seen in the rich loading that is under-predicted with 7 %. During the validation of the Sønderby plant in previous work, the results showed a trend line indicating that the under prediction of the rich loading increased with decreasing vol% of CO_2 in the flue gas. This is show in Figure 33 in Appendix A. The results from this validation also showed that temperature profile was under predicted towards the bottom of the column, which would explain under-predicted rich loadings. However, the deviation is still in the

lower range and could also be explained by experimental uncertainties. Either way, it should be kept in mind when assessing the results, as an under-predicted rich loading may yield over-predicted amine emissions.

Table (4) The ratio between the simulated CO_2 capture efficiency, rich loading and CO_2 vol dry % in the treated gas from the absorber and the experimental values from the Tiller plant with natural gas.

Variable	SIM/EKS
CO_2 capture efficiency	1.00
Rich Loading	0.93
CO_2 vol dry %	0.98

Two cases were simulated with the gas from a natural gas source. The composition of the natural gas was calculated from assuming that methane is burned with oxygen to a resultant volume percentage of 3.5 vol% CO_2. The molar flow and pressure of the gas was the same as in the Base Case. For the first case, Case 10, the inlet temperature of the gas was 35 °C. For the second case, Case 11, the flue gas entered the column at 65 °C. The cases are given in Table 3 as Case 10 and Case 11. For Case 11, the simulation in CO2SIM was run with a 90 °C inlet temperature for the flue gas. However, in the aerosol model, 65 °C was the height possible temperature to get the model to converge, so the temperature was adjusted in the aerosol model.

The lean flow entering the column is the same solvent solution as in the Base Case, but as the CO_2 content in the flue gas is almost 1/3 of the Base Case CO_2 content, the molar flow of the lean flow was adjusted. The lean flow was adjusted to make the rich loading as high as possible while maintaining an absorption rate equal to that of the Base Case. This was done with an L/G [kg/kg] ratio equal to 0.82. The temperature in the last water wash was also adjusted from 31.8 °C to 35 °C to make more water evaporate from the liquid, as to keep the water balance balanced.

As the hot gas is not saturated with water it has a low heat capacity. Thus, it is expected to be cooled down by the absorption liquid relatively quickly and the temperature profile will be maintained quite constant. Also, as the CO_2 content is in the lower range, there is less heat released from the reactions, as less CO_2 is absorbed. This will also contribute to keeping the temperatures low. Thus it is expected that

there will be less vapor emissions and less growth and MEA uptake in the aerosol phase in the absorber section. The gas will leave the absorber with a low temperature, which will also reduce growth in the water wash. For the Case with 65 °C flue gas, the gas temperature is expected to be slightly higher. Thus the aerosols are expected to grow more for this case than for the case with 35 °C.

Using a lower CO_2 content in the gas also means more MEA will be free rather than bound up in carbamate formation, which will give a reduced rich loading for these cases, compared to the Base Case. This means more MEA is available to evaporate in the gas phase, but as the temperatures are low, the emissions is still expected to be reduced compared to from a gas with higher CO_2 content. However, more free MEA means that the water wash section will be more effective, which also contributes to reducing the aerosol emissions.

4 Results and discussion

In this section, the results for the Base Case and the case studies described in Section 3.4 are presented and discussed. First, the results for the Base Case are thoroughly described and discussed. For this case, the internal profiles, including the droplet diameter profiles, the temperature profiles, the partial pressure profiles, the concentration profiles and the droplet distribution are given. All the profiles are given as a function of position in the system, where in the Base Case, the absorber column is from 0 to 15m, the first water wash is from 15 m to 17.4 m and the last water wash is from 17.4 m to 19.8 m.

The other cases are mainly compared to the Base Case. Diameter profiles for the two droplets and MEA amount in the droplets relative to the Base Case after the water wash units and after a demister unit are given for all of the cases. Other profiles are only included if relevant for the discussion. However, all of the internal profiles and raw results used to calculate the relative change in MEA amount for each case are given in Appendix F.2. Also, Table 24 in Appendix F.3 presents the values at the end points of the internal diameter profiles. The raw data from CO2SIM used in the aerosol model, is given as plots for each case in Figures 43-54 in Appendix F.1.

As the focus of this thesis is the behaviour of aerosol emissions this is also the focus for the discussion. Still, vapor based emissions are briefly mentioned to enhance the discussion of the overall emissions. Also, the performance of the system in regards to CO_2 removal is mentioned for some of the cases. These results from CO2SIM, including the removal efficiency in the absorber, the rich loading, the MEA vapor emissions after the absorber and after the second water wash as well as the dry vol% of CO_2 at the outlet are given for all of the cases in Table 22 in Appendix F.1.

4.1 Base Case

In this section the results for the Base Case is thoroughly explained and the internal profiles for the aerosol, liquid and gas phases are presented in this section. Figure 7 includes the change in droplet diameter as a function of position in the system. In Figure 8 the temperature profile for the three phases are presented. The partial pressure profiles for CO_2, MEA and water is given in Figure 9. The concentration profile of MEA in droplet 1 and droplet 2 are given in Figure 11 (a) and (b). The

concentration profile of CO_2 in the two droplets are given in Figure 12 (a), while Figure 12 (b) includes the concentration profile of sulphuric acid in Droplet 1. The sulphuric acid concentration in Droplet 2 can be found in Figure 55 in Appendix F.2. Lastly, the droplet distribution is given as droplet number concentration as a function of droplet diameter in Figure 13.

As mentioned in the aerosol model in Section 3.1, two droplets are assumed to enter the absorber column with the flue gas and are labeled Droplet 1 and Droplet 2. Droplet 1 has an initial diameter of 0.15 μm and Droplet 2 has an initial diameter of 1 μm. When the two droplets enter the absorber column, there is an initial shrinkage of the droplets, before they grow steadily towards the top of the column. This is visible in Figure 7. The initial shrinkage can be explained by the temperature profile in Figure 8. As the liquid phase maintains a higher temperature than the gas and aerosol phase, the droplets gets heated when entering the absorber. This increases the volatility of the H_2O maintained in the droplets, and some of it evaporates from the droplets, causing them to shrink. This is seen in the sulphuric acid profile in Figure 12 (b) as a sharp increase of the sulphuric acid concentration, due to water evaporating, causing the total volume to decrease.

At the inlet, CO_2 is quickly absorbed by the aerosol phase. This is due to the high concentration of CO_2 in the gas phase, driving CO_2 into the droplet. Also, as the droplets has a lower temperature than the liquid phase, CO_2 is more soluble in the aerosol phase, further causing CO_2 to transfer into the droplets. The absorption can be seen in Figure 12 (a), as a sharp increase in the free CO_2 concentration at the absorber inlet. It is also worth mentioning that the CO_2 concentration profile initially shows a negative value for the free CO_2 concentration. This is simply due to the absorption of CO_2 being extremely fast at this point. The integrator used in the aerosol modelling is not able to cope with the speed of the absorption which is why this is seen. It is not expected to effect the results and will not be mentioned again.

After the initial shrinkage of the droplets, there is a slow, but stable growth of the droplets in the absorber column, as findings in literature also suggests [34], [35], [32]. The same can be seen in the partial pressure profiles of water and MEA in Figure 9 (a) and (c). In the partial pressure profile of CO_2 in Figure 9 (b), the situation is the opposite. This is due to the reaction between MEA and CO_2 which forms non-volatile

components like carbamate and bicarbonate and naturally, the partial pressure of CO_2 decreases in both the gas, liquid and aerosol phase. The reactions along the column also releases heat, which increases the temperature along the column. This increases the partial pressure of both MEA and water and their presence in the gas phase increases towards the top of the column. The partial pressure of MEA in the liquid phase also increases along the column because the solvent is entering from the top of the column. Figure 10 shows an enlargement of all the partial pressure profiles around the middle of the absorber column to show the difference between the aerosol phase and the gas phase. In all three of the profiles it is visible that the partial pressure is higher in the gas phase than in the aerosol phase. This causes the driving forces to be towards the droplets, and thus the growth through the absorber is due to a continual uptake of CO_2, MEA and water.

That MEA and CO_2 are entering the droplet along the column is further supported by the MEA and CO_2 concentration profiles in Figures 11 and 12. The free CO_2 molecules that was absorbed by the aerosols when they entered the column reacts with MEA as it enters the droplets. This causes the free CO_2 concentration to decrease, while the bound CO_2 concentration increases. About 3 to 4 meters into the column the concentration of MEA and CO_2 stabilizes as the MEA concentration has reached the same concentration as in the bulk liquid phase. It can be said that the transfer rate of MEA reaches steady state and since the droplets grow at this point the transfer of MEA is so high that it keeps the concentration constant. At the very end of the absorber there is another sharp increase in both MEA and CO_2 concentration which indicates that water depletes out of the droplets. This is seen in the droplet diameter profile in Figure 7 as a small reduction in the droplet size. Further, this is supported by the partial pressures of water in the phases. At the bulge in the temperature profile in Figure 8, the partial pressure in water gets lower than the partial pressure in both the gas and the aerosol phase. This causes water vapor in the gas phase to condense, which decreases the partial pressure of water in the gas, as seen in the profile in Figure 9 (c). Water depleting out of the gas phase causes the driving force of water to be out of the droplets. This results in a reduction of the droplet sizes.

At the end of the absorber, the droplets enter the first water wash section and the growth of the droplets accelerates, again in line with findings in literature [34], [35],

[46]. This is due to the cold environment in the water wash. The gas and aerosol phase leaves the absorber at around 50 °C, while the water wash maintains a temperature of 30 °C. This causes the water vapor in the gas phase to condense and the droplets grow. Mainly water enters the droplets, which is seen by the steep reduction in the CO_2 and MEA concentration profiles. Along the water wash sections it is also evident that MEA depletes out of the droplets as the free CO_2 concentration increases while the bound CO_2 concentration decreases. This is due to a shift in the driving force for MEA. This is supported by the findings in the partial pressure profile of MEA in Figure 9 (a), as the partial pressure in the gas and aerosol phase is practically non existing. However, at the beginning of the water wash the partial pressure in the gas and aerosol phase is higher than in the liquid phase. Thus, the MEA will here transfer out of both the gas and aerosol phase.

Along the entire system the growth of Droplet 2 is steeper than the growth of Droplet 1. This can be explained by the equations given for droplet growth in Section 3.1. The growth of Droplet 1 is only dependent on the mass transfer into the droplet. Droplet 2 however, is dependent on two times the mass transfer into the droplet, minus the mass transfer into Droplet 1. This usually gives Droplet 2 a steeper growth, but if the mass transfer into Droplet 1 one would be higher than two times the mass transfer into Droplet 2, it would reduce the droplet growth for Droplet 2.

In the MEA and CO_2 concentration profiles in Figures 11 and 12, there is a notch that can be observed approximately 1 m into the column. As a basis for the aerosol model described in Section 3.1, two models are used to describe the equilibrium in the aerosol phase. Initially the concentration of sulphuric acid increases quickly when the droplet enters the column, as seen in Figure 12 (b), which makes the environment in the droplet acidic. In the acidic range, an equilibrium model based on sulphuric acid is used. All MEA entering the droplet is converted to $MEAH^+$ and the sulphuric acid is gradually neutralized, forming ${HSO_4}^-$ and eventually ${SO_4}-2$. When all the sulphuric acid has been neutralized, the model shifts to an e-NRTL model for MEA, but included modifications to take the presence of neutralized sulphuric acid into account. The hump seen in the figures is therefore due to the transition between the two models. The models might have a small deviation in the concentrations predicted, but it is not expected to be a deviation large enough to have a significant impact on the results. For this reason it was decided to not work on smoothing out

the transition.

A demister unit was implemented in the aerosol model after the water wash sections. In Figure 13 the change in the droplet distribution before and after the demister is given. As described in the aerosol modelling part of this thesis, a logarithmic normal distribution is used to approximate the size distribution of the droplets. In the aerosol model, the demister is modelled so that the removal efficiency for smaller droplets goes towards zero, while the removal efficiency for larger droplets goes towards 100 %. Thus, after the demister, the distribution is no longer log-normal. In Figure 13 this is shown as "after demister, count", which is the different size classes after the demister. This is used to fit the log-normal model "after demister, model". So, when the deviations between the model and the count is small, there is a good fit between the count and the fitted log-normal model, indicating that very small changes has been done to the distribution entering the demister. This would imply that not many droplets has been removed by the unit.

In this case, after the demister has been implemented, the concentration of droplet diameters below 1 μm increases and the concentration of droplets over 1 μm decreases. The amount of MEA in aerosols after the demister unit is reduced by 50% compared to after the water wash section, as seen in Table 23 in Appendix F.2. This shows that the demister unit is effective in removing larger droplets, but as the profiles are still quite similar, not that many droplets have been removed relative to how much the MEA amount has been reduced. This shows that most of the MEA is being carried with the largest droplets, and that even though only some of the droplets has been removed, it has a significant impact on the amount of MEA being emitted with the aerosols.

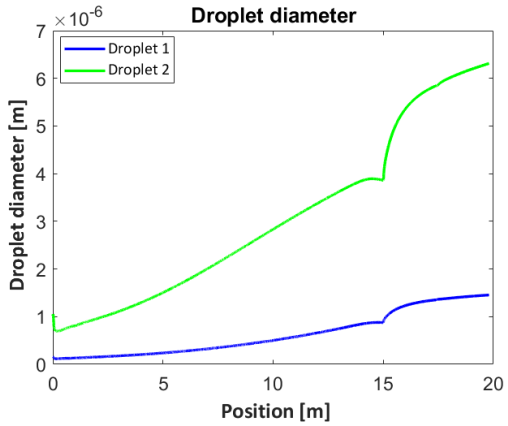

Figure (7) Droplet diameter as a function of position throughout the system for the base case simulation.

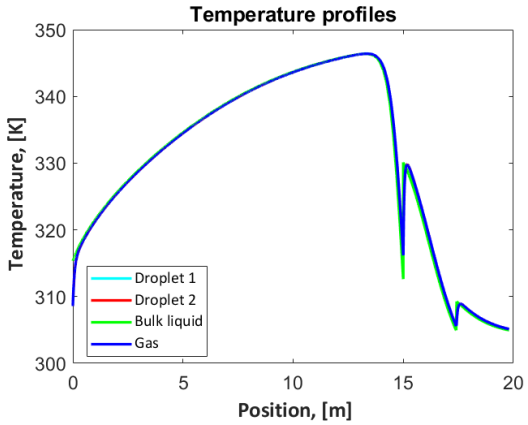

Figure (8) Temperature of the gas and liquid as a function of position in the system for the base case simulation.

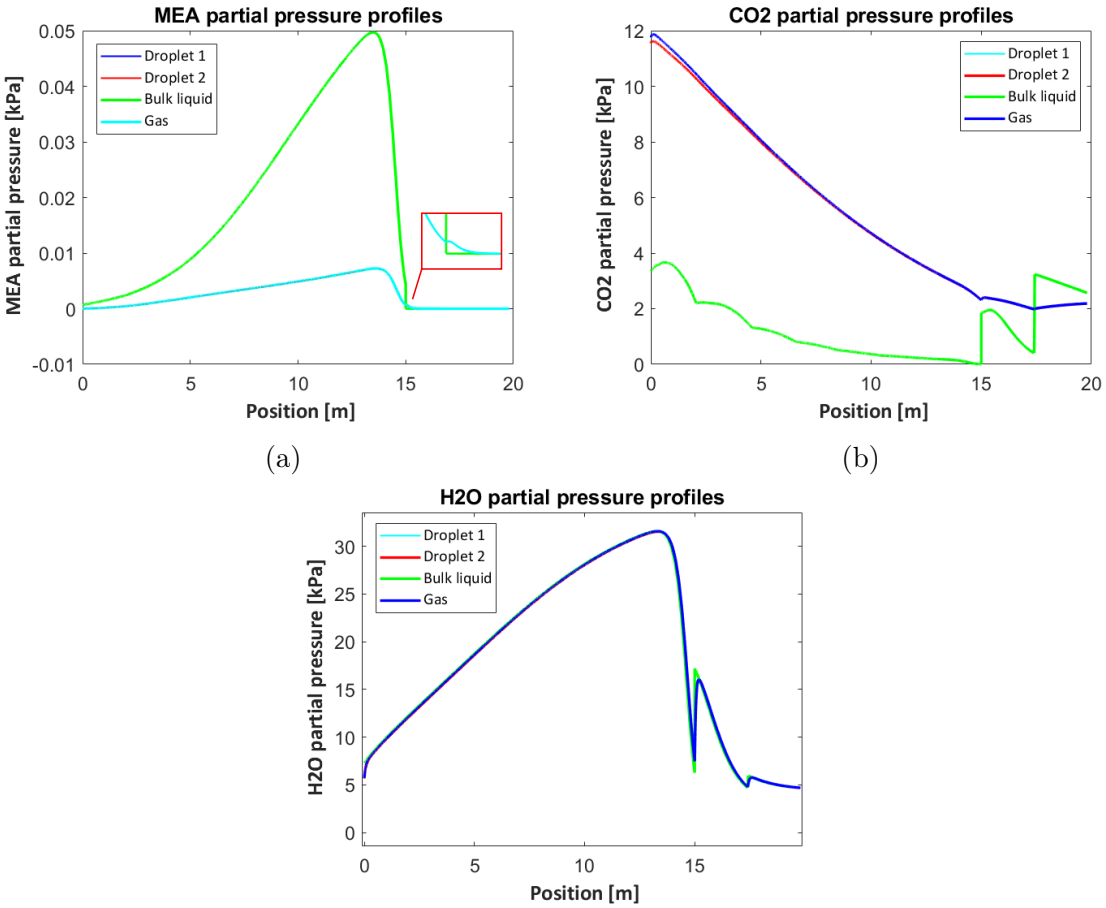

Figure (9) Partial pressure profiles for MEA (a), CO_2 (b) and water (c) as a function of position for the base case simulation.

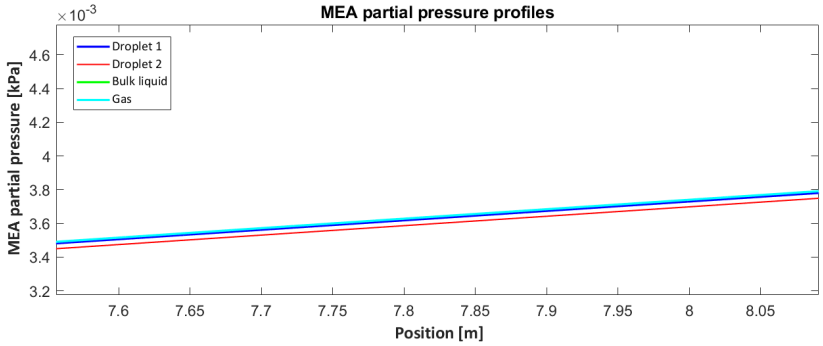

(a)

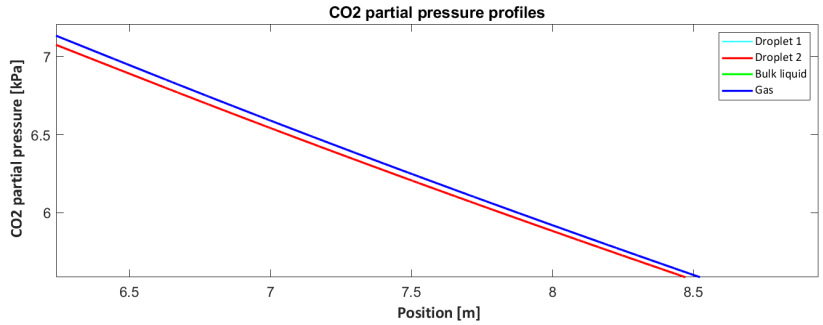

(b)

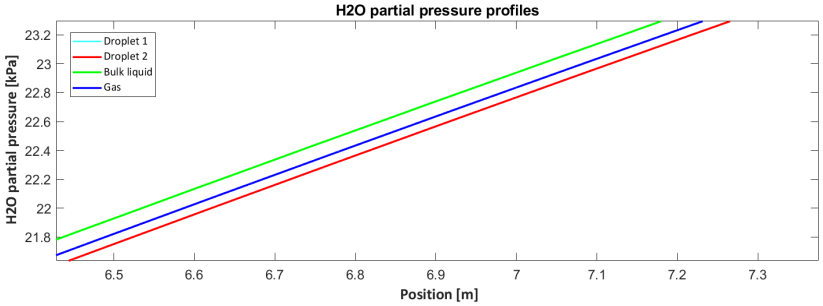

(c)

Figure (10) The partial pressure profiles of MEA (a), CO_2 (b) and H_2O (c) in the middle of the column as a function of position in the system.

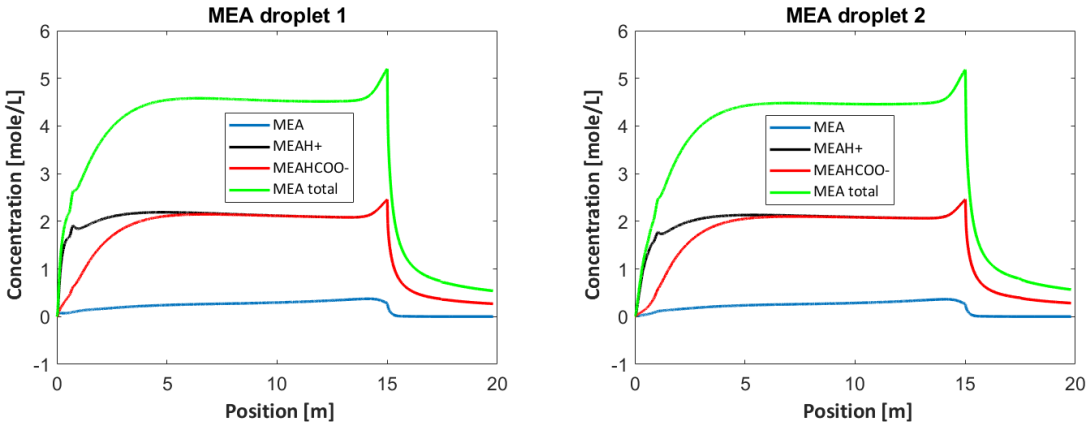

(a) (b)

Figure (11) Concentration of total MEA, free MEA, carbamate and bicarbonate for droplet 1 (a) and droplet 2 (b) as a function of position for the simulated base case.

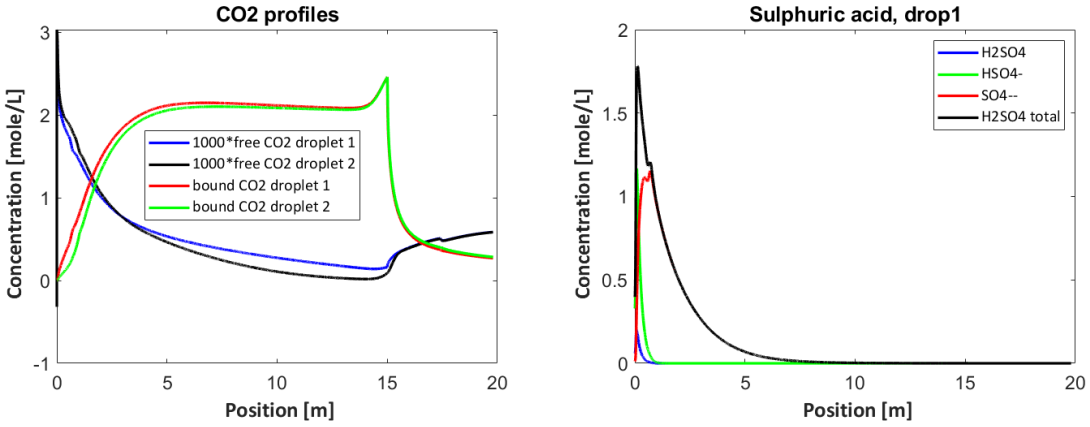

Figure (12) Concentration profiles for free CO_2 and bound CO_2 in the two droplets (a) and concentration profile for sulphuric acid for the droplet 1 (b) as a function of position for the simulated base case

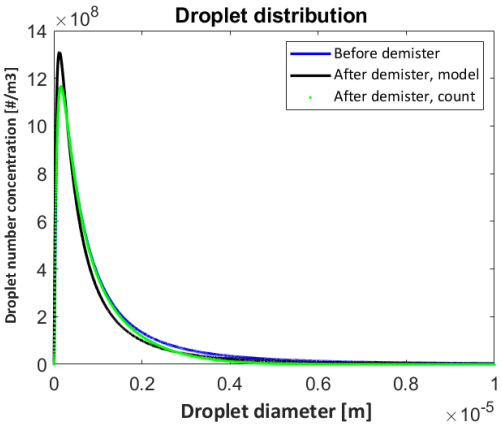

Figure (13) Droplet number concentration before and after the demister unit is implemented for the base case.

4.2 Case Study - Water wash height

The results for the cases with varied height in the water wash section are presented and discussed in this section. In Case 1, the height of the first water wash is doubled from 2.4 m to 4.8 m while the second water wash is not changed from the original height of 2.4 m. In Case 2, the height has been decreased to a total water wash height of 4 m, with each section being 2 m. In Case 3, the height is further decreased to a total water wash height of 2 m, with each section having a height of 1 m. Table 5 gives the amount of MEA in the aerosol phase relative to the Base Case for the three cases. Figure 14 gives the diameter profiles for the three cases.

Case 1 is the case where the total height of the system is the highest, and the case that has the largest final droplet size as seen in Figure 14. This is as expected and as findings in literature suggests, the increased height mainly contributes with an increased retention time [46], [34]. When studying the droplet growth in the water wash section, it is evident that the growth is steepest at the first 3-4 m of the wash column. After this it looks like the growth stabilizes around 18-19 m, which is at the total height for the Base Case. This reasons why increasing the water wash height with 50 % only increases the droplet sizes with approximately 7 %. Looking at the partial pressure profile of H_2O in Figure 15, it is evident that 20 m into the system the difference between the partial pressure in the different phases is reduced, indicating that the transfer of water between the phases goes slower. This causes the droplet growth to slow down. However, there is still an increase in the size and the total MEA amount carried with the droplets is reduced after the water wash compared to the Base Case.

The aerosol emissions for this case are reduced, but for what costs. With a longer column comes increased costs and it can be discussed whether the costs is worth the gain. It is often desirable to grow the droplets to such a size that the demister unit is able to remove them. Comparing the droplet distribution for this case with the base case profile, the distributions are close to identical. Hence, even though some of the droplets grow to a larger size the amount of droplets that are removed in the demister is the same. But, as it is the largest droplets that carry most of the MEA some reduction is seen in the total MEA amount carried by the aerosols after the demister.

In Case 2, a 3 % reduction in the final droplet sizes is seen for both Droplet 1 and Droplet 2. Again this is as expected as a lower height in the wash sections reduces the retention time. The relative amount of MEA is given in Table 5 and a 1 % increase in MEA aerosol emissions is seen after the water wash sections. However, a 5% increase is seen in the relative amount of MEA emitted with the aerosols after the demister unit. This shows that a small reduction in the droplet sizes has a great effect on the amount of MEA that gets removed in the demister unit and implies that in terms of MEA emissions even a small change in the droplet sizes has an impact on the final aerosol emissions.

For Case 3, the final amount of MEA after the demister unit increases with almost 30 % relative to the Base Case and the droplet sizes are reduced by 10.0 % for Droplet 1 and 11 % for Droplet 2. Reducing the water wash height with approximately 50 % compared to increasing the height with 50 % has almost the same but opposite effect on the droplet sizes, but the effect on the total amount of MEA is much more significant for the case with the reduced height. Again indicating that not that many more droplets are removed by increasing the height past the Base Case water wash height, but that decreasing the height has a large effect on the final emissions, due to less droplets being removed in the demister.

Table (5) The amount of MEA in the aerosol phase compared to the Base Case for the case study with varying water wash height.

Amount of MEA in aerosol phase relative to the Base Case	Case 1	Case 2	Case 3
After second Water Wash	-10 %	+1 %	+18 %
After demister unit	-12 %	+5 %	+29 %

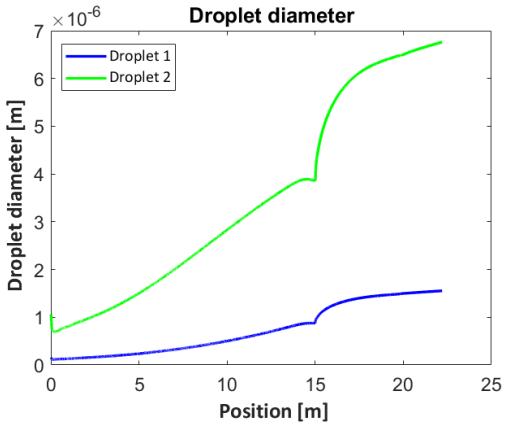

(a) Case 1

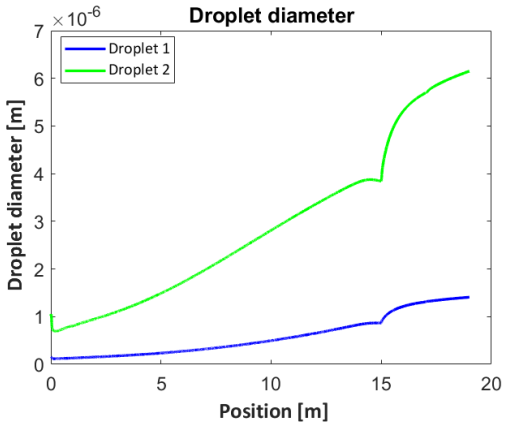

(b) Case 2

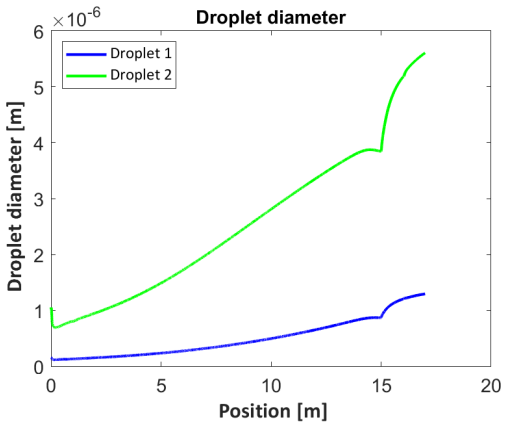

(c) Case 3

Figure (14) Droplet diameter of the two droplets entering the absorber column as a function of position in the column for Case 1 (a), Case 2(b) and Case 3(c).

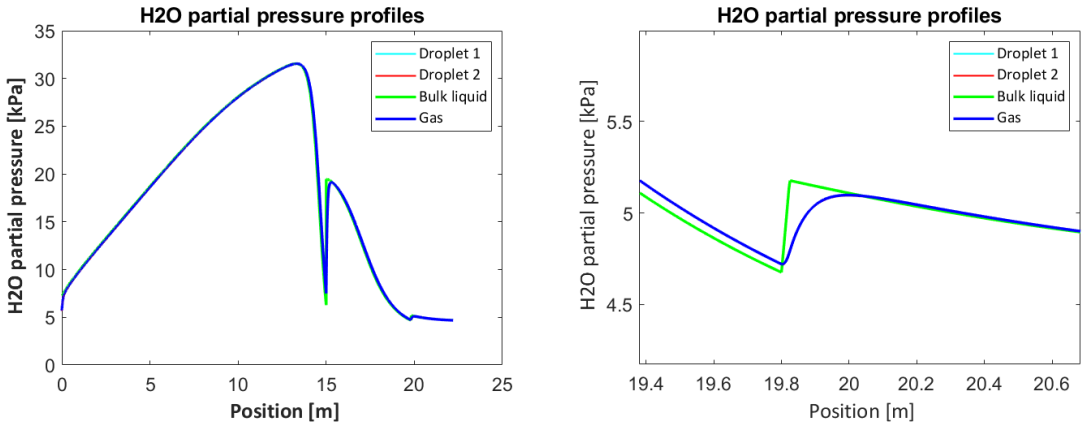

(a) Case 1 (b) Case 1

Figure (15) The partial pressure of H_2O in Case 1 as a function of position in the system in (a), while (b) is an enlargement of the figure at the 20 m mark.

In regards to vapor based emissions the increased height reduces the emissions while the decreased height increases these emissions. This is also due to the residence time in the column as the water wash is effective in reducing vapor based emissions.

As the cases clearly demonstrates the droplets grow and the transfer of MEA out of the aerosol phase is enhanced as the height of the water washes increases. This can be used as an effective measure to reduce the overall MEA emissions from an amine scrubbing system, but at a certain height there is uncertainties in regards to how much more gain to be collected from the measure.

4.3 Case Study - Intercooling

The results for all the cases with implemented intercooling will be presented and discussed in this section.

4.3.1 Case 4 and Case 5

Two intercooling cases were performed at the original height of the absorber and the results are presented and discussed in this section. In Case 4 the intercooling section was placed at 1/3 from the bottom of the column. In Case 5, the section is placed at 1/3 from top of the column.

The temperature profiles for each of the cases compared with the temperature profiles for the Base Case are shown in Figure 16. From the figure it is evident that intercooling has a substantial effect on the temperature profiles, and has the effect of lowering the magnitude of the bulge temperature in the absorber column. This reduces the vapor amine emissions from the system. It can also be seen that placing the intercooling section towards the top of the column gives the most significant reduction of the bulge temperature. Particularly, is the temperature profiles in the water wash sections affected, as the gas enters the water wash sections at a reduced temperature.

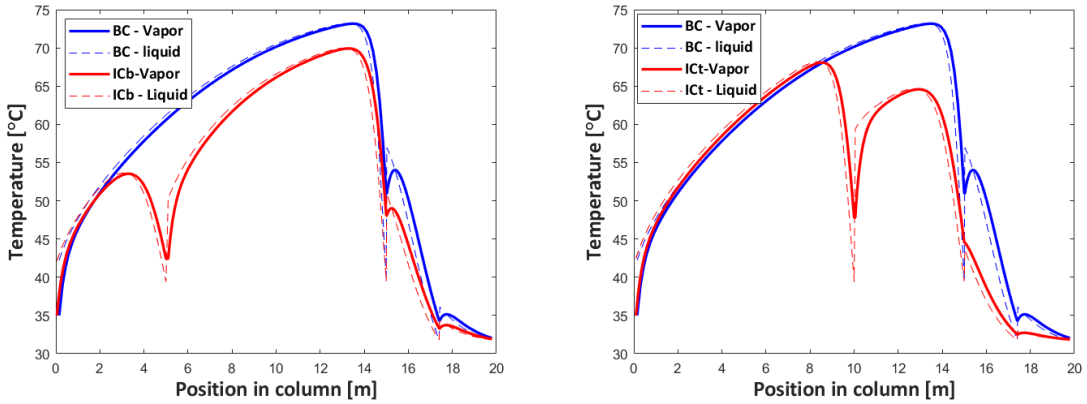

(a) Case 4 (b) Case 5

Figure (16) Temperature profiles in the system. Figure a) shows the temperature profile for the case with intercooling placed at the bottom of the absorber, labeled ICb, compared to the temperature profiles for the Base Case. Figure b) shows the temperature profiles for the case with intercooling placed at the top of the absorber, labeled ICt, compared to the temperature profiles for the Base Case.

Regarding the aerosol emissions, the results are presented by the following figures. The diameter profiles for the two cases are shown in Figure 17. The partial pressure profiles of water in Figure 18 and the concentration profiles of CO_2 are given in Figure 19. Lastly, the droplet distribution profile for Case 5, is given in Figure 20. The relative amount of MEA emitted with the aerosols after the absorber, the water washes and the demister are presented in Table 6.

The modification results in a modest reduction in the final sizes of the aerosol droplets, regardless of whether the intercooling section is placed towards the top or the bottom of the column. This is inline with the findings of Majeed and Svendsen (2017), and as their study reported, the reduction in growth is surprisingly small in comparison to the reduction in MEA partial pressure [45].

The largest effects can be seen on the amount of MEA being emitted with the aerosol phase, as can be seen from Table 6. At the end of the system there is a 26% reduction for Case 4 and a 32% reduction for Case 5, relative to the Base Case. The reduction is more significant before the demister unit, which is due to the reduction in droplet sizes. As can be seen in the droplet distribution in Figure 20, for Case 5, the concentration of the smaller droplets is much higher than in the Base Case. Also, there is a smaller

difference between the distribution before and after the demister from 1 μm and higher, as shown in Figure 20, indicating that since the droplets grow less, less droplets are removed by the demister unit. This is also seen by the good fit between the count and after demister model, as discussed in the Base Case. This reasons why the reduction in MEA relative to the Base Case declines after the demister unit compared to after the water wash section. For Case 4, the droplet distribution is similar to Case 5 and the same reasoning applies for this case. The droplet distribution for Case 4 can be located in Figure 74, in Appendix F.2.

As mentioned, the intercooling has a large effect on the temperature profiles in the columns, as seen in Figure 16. In the absorber column, the magnitude of the bulge temperature is reduced and so the temperature difference between the hot gas at the top of the column and the injected lean solvent is lowered. This effect is the highest for the case were the intercooling is placed towards the top of the column, Case 5. As elaborated in the literature review, a lower bulge temperature is expected to reduce the the growth of the droplets [34]. This is also seen in the results for this thesis and the largest reduction in droplet growth is seen for Case 5, as it has the largest impact on the temperature.

It is also noticeable that there is a sharp decrease in the concentration profiles of CO_2 and MEA as the intercooling sets in. When the intercooling sets in, the cooled liquid enters the absorber again, causing the overall temperature in the column to decrease. The temperature difference between the gas and the liquid phase at this point, causes the droplets to have a increase in size for a limited amount of time. In the CO_2 concentration profile there is a decrease in the bound CO_2 due to the increase in size seen in the droplets at this point, as the volume of the droplets grow due to water uptake. As the water leaves the droplets again, the concentration goes back. An increase in the free CO_2 is also seen at this point. This however, is due to the cold environment increasing the solubility of CO_2, so that it transfer back into the droplets. However, as the temperature increases again, the CO_2 transfers back into the gas phase. Also, as the temperature is decreased, the volatility of MEA is decreased. The concentration of MEA in the gas phase is thus lowered, and the free MEA contained in the droplets transfers out of the droplets. Again, as the temperature starts to increase, the concentration of MEA in the gas phase also increases. Thus, MEA starts to transfer back into the droplets. However, because some MEA transferred

out of the droplets, the amount never reaches the same magnitude as in the Base Case. This also explains why placing the intercooling unit closer to the top, as in Case 5, yields a stronger MEA reduction as there is less time for the MEA amount to build up again. Further, the reduced residence time explains why Case 5 shows the largest reduction in droplet size, as mentioned in the previous paragraph. These findings are in line with the findings of Gupta et. Al (2020), that also observed decreasing aerosol emissions when shifting intercooling from the bottom to the top [38].

The droplets also have a reduced growth in the water wash sections. As described in the beginning of the section, the temperature is lowered in the water wash sections, as seen in Figure 16. This effect is particularly large for Case 5, with intercooling at the top. As elaborated in Section 2.4, growth in the water wash sections is due to elevated partial pressure of water in these columns [34]. However, when the temperature is reduced in this section, the partial pressure of water is also reduced, as seen in Figure 18. As a consequence, the droplet growth is slowed down compared to the growth of aerosols in the water wash section in the Base Case. A reduction in the water wash temperatures also reduces the amount of MEA in the aerosols. This is due to reduced partial pressure of MEA in wash sections, which drives MEA out of the droplets. This is contradictory to the findings by Gupta et. Al (2021), that found that a decreased temperature in the water wash led to increased aerosol emissions [38]. However, in this study the authors did not refer to the difference between the gas and liquid temperatures, and explained that the increase was due to more condensation of MEA into the aerosol phase. In these cases, even though the temperature in the water wash is lowered, so is the difference between the gas an liquid temperature, which is expected to reduce condensation. This makes sense with the observed reduction in droplet growth combined with the reduced MEA content in the aerosols after the water wash.

Table (6) The amount of MEA in the aerosol phase compared to the Base Case.

Amount of MEA in aerosol phase compared to the base case	Case 4	Case 5
After Absorber Section	-29 %	- 37 %
After second Water Wash	-33 %	-43 %
After demister unit	-26 %	-32 %

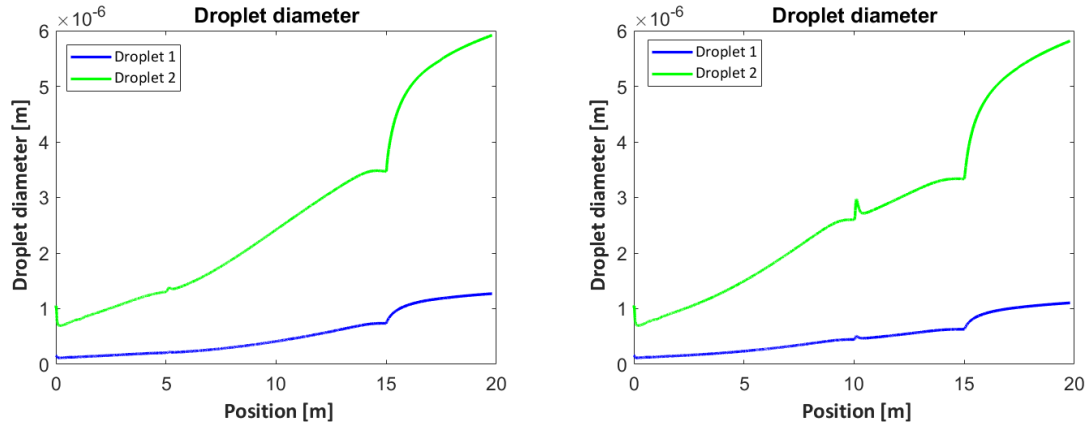

(a) (b)

Figure (17) Droplet diameter of the two droplets entering the absorber column as a function of position in the column

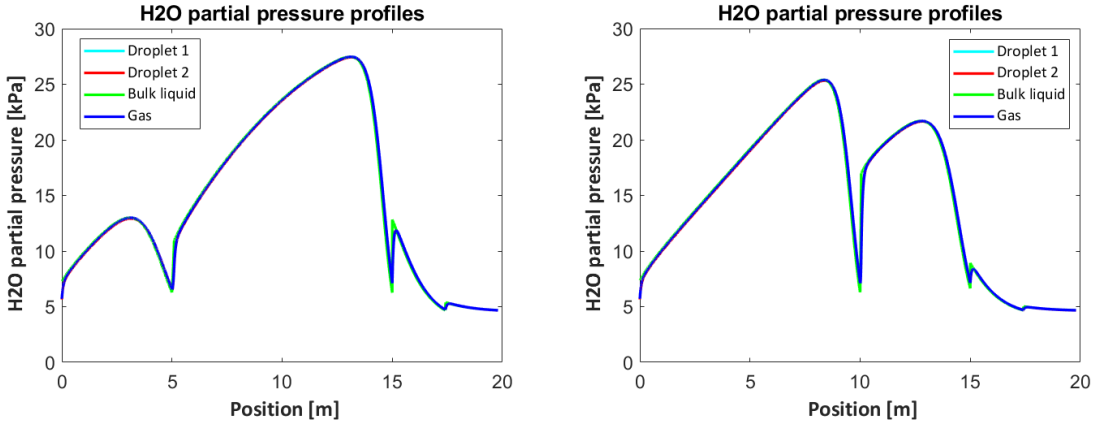

(a) (b)

Figure (18) Partial pressure of H_2O as a function of position in column for Case 4 (a) and Case 5 (b).

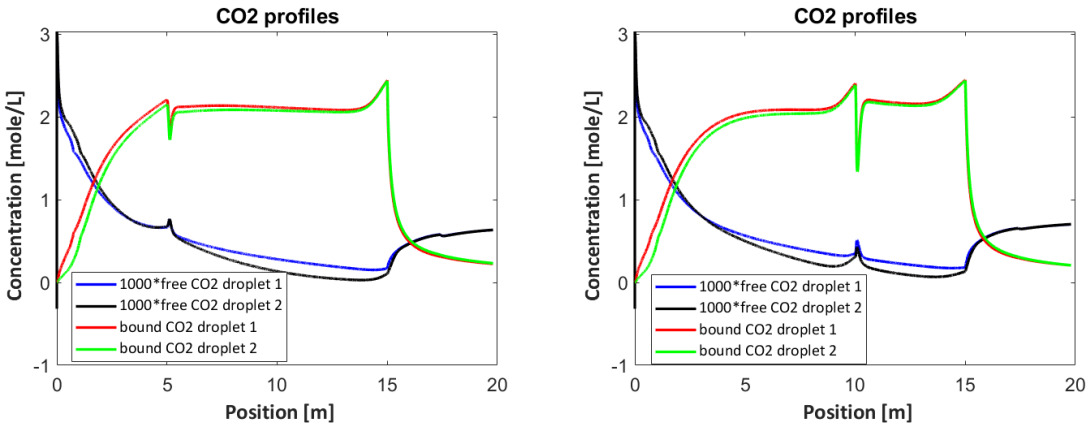

(a) (b)

Figure (19) CO_2 concentration profiles in both droplets for case 4 (a) and Case 5 (b). All concentrations are shown as a function of position in the system.

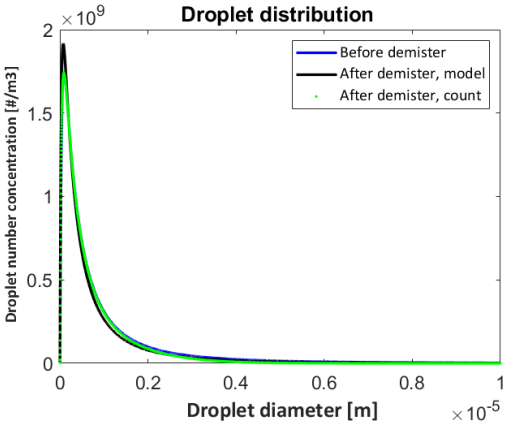

Figure (20) Droplet distribution for Case 5, given as droplet number concentration as a function of droplet diameter.

Intercooling is usually placed somewhere between 1/5 to 1/3 of the column from the bottom, as this gives the most efficient column in regards to absorbing CO_2 from the gas [43], [39], [40]. In these cases, the placement of intercooling was at 1/3 from the bottom and 1/3 from the top. The conventional choice of 1/3 from the bottom, yields the most efficient absorber, but the difference between the two cases is negligible. When placed at the bottom, the absorber column has a CO_2 removal efficiency of 85 %. When placed at the top, the absorber column has a CO_2 removal

efficiency of 84 %. The difference is negligible, but placing the intercooling at the top has a much larger effect on both aerosol and vapor based MEA emissions. Thus, in this particular case the unconventional choice of placing the intercooling towards the top would be the most natural choice. However, this is not necessarily the case for all absorber columns, but the results from these cases seems promising.

4.3.2 Case 6, Case 7 and Case 8

Three cases were also simulated where intercooling was implemented while reducing the packing height in the absorber section. For Case 6 the height has been reduced from 15 m to 13 m, and intercooling is placed at 1/3 from the bottom. For Case 7 and Case 8 the height has been reduced to 12 m, but intercooling is placed at 1/3 from the bottom in Case 7 and at 1/3 from the top in Case 8.

Table 7 shows the amount of MEA in the aerosols after the absorber, the water wash sections and the demister unit for the three cases, all relative to the Base Case. Figure 22 shows the droplet diameter profiles for the three cases, while Figure 21 shows the temperature profiles for the three cases compared to the Base Case.

There is a reduction in amount of MEA emitted with the aerosols for all of the cases, but the most significant effect can be seen in Case 8, as seen in table 7. A reduction in the vapor phase emissions is also observed, this can be seen in Table 22 in Appendix F.1. This is due to Case 8 having the largest effect on the temperature profile, as seen in Figure 21. In the Base Case the maximum temperature is approximately 73 °C. This temperature is around 70 °C for Case 7 and 67 °C for Case 8. This is almost the same temperatures as seen for the intercooling case with 15 m. However, the MEA emissions are more reduced for Case 7 and Case 8 than for Case 4 and 5, showing that the reduction in emissions is also due to decreased retention time, as discussed for the water wash height case study. In Case 6, the maximum temperature is 69 °C which is almost the same as for Case 7, but the height of the column is higher in Case 6. This gives a longer retention time in the absorber in Case 6, and larger MEA amounts is seen in the aerosol phase after the absorber. Also, larger droplet sizes after the absorber is seen for this case, compared to Case 7 and 8.

The results shows that when combined with intercooling, the height of the absorber can be reduced without it causing an increase in the MEA emissions. The height has not been reduced enough to have a particularly significant effect on the rich loading.

However, there is an effect on the rich loading which decreases with decreasing height. Therefore, the reduction in aerosol emissions does not come without a cost of a less effective absorber.

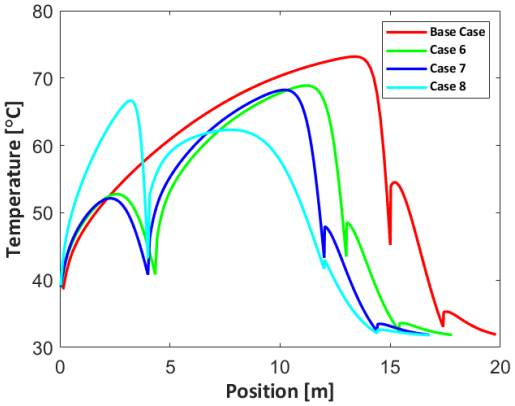

Figure (21) The temperature profiles for Case 6, 7 and 8 comapred to the temperature profile in the Base Case.

Table (7) The amount of MEA in the aerosol phase compared to the Base Case for Case 6, 7 and 8.

Amount of MEA in aerosol phase compared to the Base Case	Case 6	Case 7	Case 8.
After Absorber Section	-41 %	-46 %	-53 %
After second Water Wash	-47 %	-53 %	-60 %
After demister unit	-38 %	-44 %	-49 %

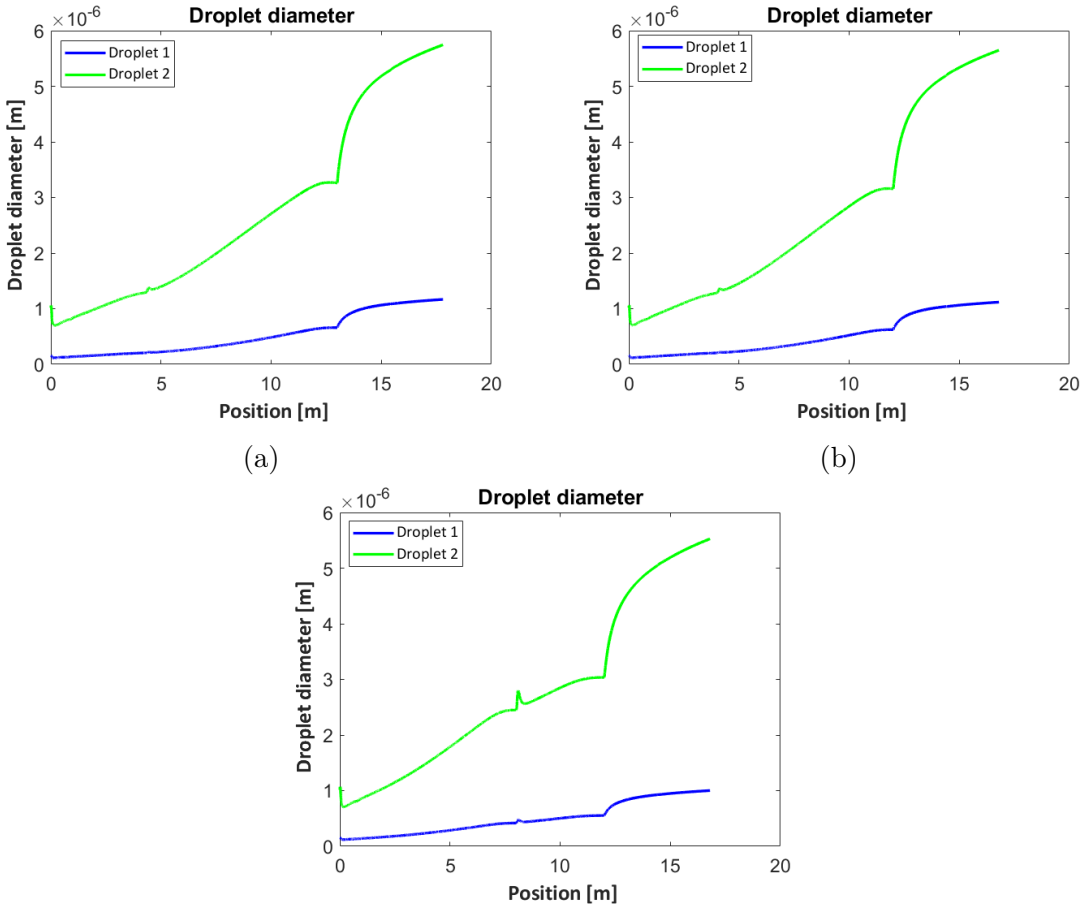

(a)

(b)

(c)

Figure (22) Droplet diameter of the two droplets entering the absorber column as a function of position in the column

4.4 Case Study - Isotherm Absorber

In this section, the results for the case with an isotherm absorber, Case 9, are presented. The relative amount of MEA emitted with the aerosols is presented in Table 8. The droplet diameter profiles are given in Figure 24 (a) and the sulphuric acid concentration profile in Figure 24 (b). The partial pressure profile of MEA and water are given in Figure 25.

As expected, operating the absorber isothermally has a significant effect on the vapor based MEA emissions because the temperature along the column and at the top of the absorber is considerably reduced. In Figure 23 (a) the temperature profile for the isotherm system is compared to the temperature profile of the Base Case. While Figure 23 (b) gives the fugacity profile for MEA in the vapor phase as a function of position compared to the Base Base profile. As the temperature of the gas never reaches more than 43 °C the vapor pressure of MEA is maintained low compared to the base case. This means that the presence of MEA in the gas phase is very low, and the sparse vapor based emissions there are gets removed by the water washes.

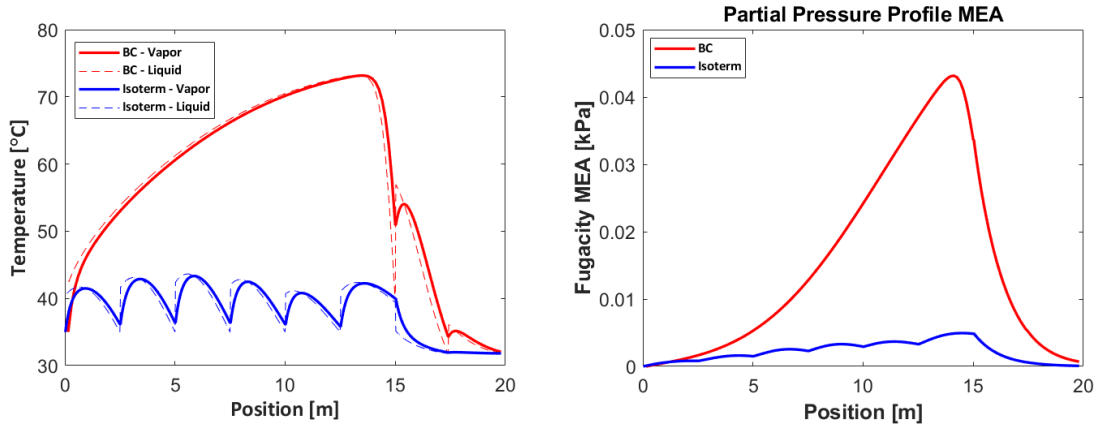

(a) (b)

Figure (23) The temperature profile (a) and the partial pressure profile of MEA (b) for the isotherm absorber compared to the Base Case profiles.

Figure 24 (a) shows the droplet diameter for the two droplets as a function of position in the column. A significant reduction in the droplet diameters compared to the Base Case is observed. For Droplet 1 there is a 62 % reduction after the absorber and a 51 % reduction after the last water wash. Similarly for Droplet 2, there is a 47 %

reduction after the absorber and a 30 % reduction after the last water wash. These numbers signals that the growth of the droplets are limited, especially in the absorber. This is due to the temperature being kept low in the entire column. This causes the partial pressures of water, MEA and CO_2 to be reduced which means their presence in the gas phase is reduced. This is clearly visible in the partial pressure profiles in Figure 25, that shows that the MEA partial pressure is only a 10th of what it is in the Base Case simulation. Equally for water, the partial pressure is only two 10ths of what it is in the Base Case. When the vapor pressures are reduced so significantly, the transfer of the components into the aerosol phase is limited, which is why less droplet growth and lower MEA aerosols emissions are observed. That there is less transfer into the droplets in the absorber is supported by comparing the sulphuric acid profiles for the droplets in Figure 24 (b) to the Base Case profile. The total sulphuric acid concentration reaches zero at the top of the absorber column, while the concentration reaches zero all ready at 6-7 m in the Base Case. This clearly indicates that less liquid is entering the droplets in the isotherm absorber leading to slower growth. This is similar to the results seen in the intercooling cases, as the cold intercooling liquid causes the vapor phases to decrease. As intercooling is implemented several times in Case 9, the growth is further reduced compared to the cases with one intercooling unit.

When the droplets enter the water wash, the growth gets steeper due to the elevated partial pressure of water. The growth of the droplets is still very limited compared to the Base Case. This is caused by the low temperature of the gas after the absorber, and thus the partial pressure of water is low in the water wash sections. As discussed for the intercooling cases, the low temperature also enhances the driving force of MEA out of the droplets. After the water wash a 91 % relative reduction in the MEA amount is observed. As the droplets are smaller than in the Base Case, less droplets is removed in the demister. However, at the end of the system the amount of MEA leaving with the aerosols is almost completely eliminated.

The results from the isotherm absorber column is very promising and arguments that when the temperature bulge in the absorber column is almost eliminated, the growth of aerosol and the transfer of MEA into the droplets is also almost eliminated. This fits nicely with the expectations and what the studies described in Section 2.5 indicated. That reducing the magnitude of the temperature bulge leads to reduced aerosol

emissions is extensively referred to in the literature [22], [38], [37]. The modification needs to be considered as a effective counter measure against overall amine emissions. There are of course large costs linked to cooling down the liquid several times in an absorber column. However, there are also large costs associated with handling the amine emissions and the modification may be realistic in some cases. Reducing the number of sections will still have a promising effect on reducing the emissions and may be more realistic in terms of costs. Nonetheless, that is up to future work to determine.

Table (8) The amount of MEA in the aerosol phase for the isotherm absorber case relative to the Base Case.

Amount of MEA in aerosol phase compared to the base case	Case 9
After Absorber Section	-86 %
After second Water Wash	-91 %
After demister unit	-86 %

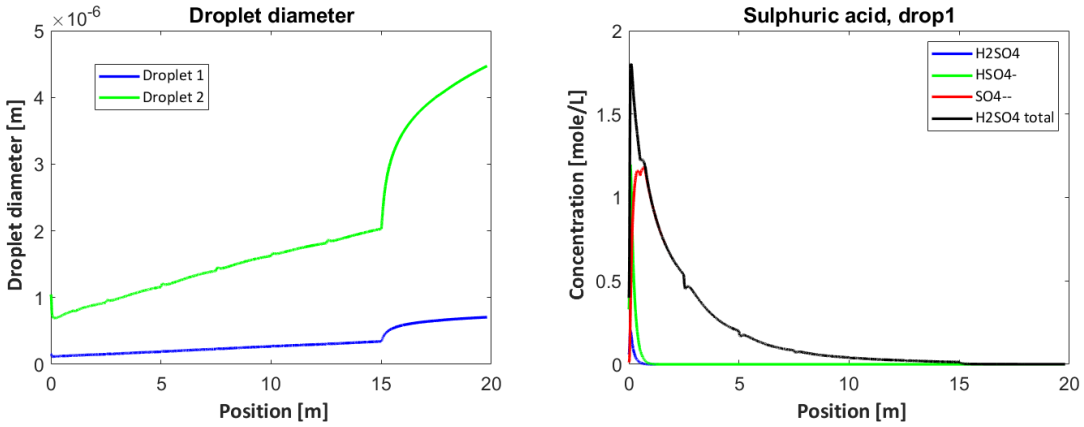

(a) (b)

Figure (24) The droplet diameter profiles (a) and the sulphuric acid profile for Droplet 1 (b) as functions of position in the system for the isotherm absorber case.

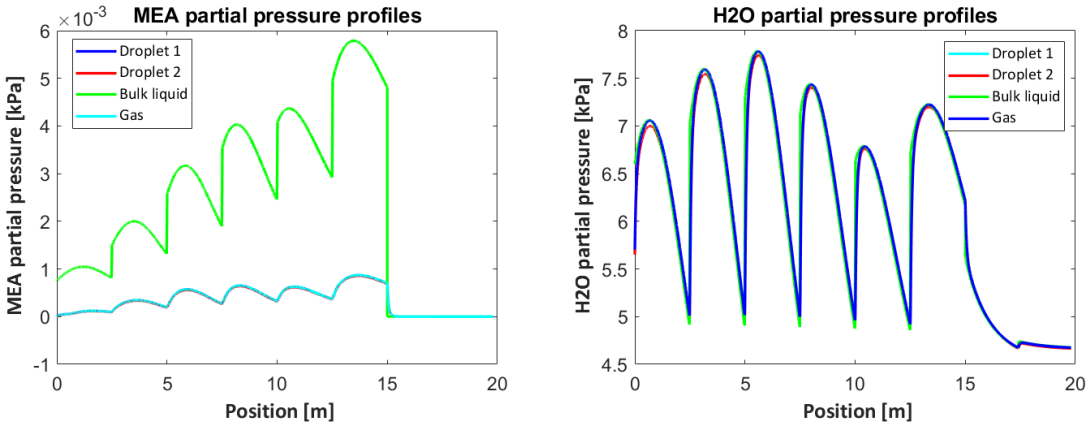

(a) (b)

Figure (25) The partial pressure profile of MEA (a) and H_2O (b) as a function of position in the system for the isotherm absorber case.

4.5 Case Study - Natural Gas Based Flue Gas

In this study the effect of using a natural gas based flue gas and the effect of such a gas not entering a direct contact cooler (DCC) is investigated. In this study two cases were performed. Case 10 acts as a base case for this study and the flue gas is from a natural gas source entering the absorber at 35 °C. In the other case, Case 11, the flue gas is thought to not enter a DCC. This makes the flue gas be unsaturated with water, and the gas enters the absorber at 65 °C.

The flue gas used in Case 10 and Case 11 has a lower CO_2 content than the flue gas used in the Base Case. To investigate the effect of this, Case 10 is compared to the Base Case. The MEA amount carried with the droplets is given for Case 10 relative to the Base Case in Table 9. As the table shows, the amount of MEA carried with the aerosols are significantly less when a flue gas with lower CO_2 content is used rather than a coal based flue gas. This is in line with findings in the literature [32], [22] and as Majeed et. Al (2018) suggests, the emissions are in a smaller size range because a reduced CO_2 content in the flue gas makes less MEA be bound up in carbamate formation as less CO_2 is available for reactions [44]. This makes more of the MEA be in free state which makes the water wash section more effective in reducing the MEA amount. The reduced emissions is also due to the flue gas having a lower heat capacity. As a consequence, the liquid flow is able to obtain a lower temperature in the column and the magnitude of the bulge is strongly reduced. This will cause a reduction in the partial pressure of MEA compared to coal based flue gas cases, which reduces both aerosol based and vapor based MEA emissions.

Table (9) The amount of MEA in aerosols after the absorber section, water wash section and demister unit relative to the Base Case for Case 10.

MEA amount in aerosols relative to base case	
After absorber	-71 %
After Water Wash	-78 %
After Demister	-72 %

The effect of having a unsaturated hot flue gas is seen by comparing the results for Case 10 and Case 11. Table 10 gives the amount of MEA contained in the aerosols for Case 11 relative for Case 10. The internal temperature profiles for the cases are

given in Figure 26 and Figure 27. The droplet size profiles are given in Figure 28 and the partial pressure profiles of H_2O are given in Figure 29.

The final droplet sizes after the absorber and water wash sections are almost the same for both of the cases, as seen in Table 24 in Appendix F.3. However, for the first meter of the absorber column the situation is very different in the two cases. For Case 10 there is an initial increase in droplet size, while there is a initial decrease in droplet size for Case 11. For Case 10 the droplets enter at a lower temperature than the bulk liquid. The temperature profile for this case is given in Figure 26. Both the gas phase and the aerosol phase enters the column at 35 °C, while the bulk liquid has a temperature of approximately 50 °C. Water will thus evaporate from the liquid phase, causing the water vapor pressure in the gas to increase. This increase makes the gas phase partial pressure higher than the condensation pressure on the surface of the droplets. This causes the evaporated water to condense on the droplets and the sharp increase in the droplet diameter is seen. For Case 11 however, the gas and aerosol phase enters the column at 65 °C. Figure 27 (a) shows the temperature profile for this case, while Figure 27 shows the inlet temperature profile enlarged, to better shows what is happening. From the figure it is visible that the liquid bulk phase also here has a temperature of 50 °C. Thus, as the droplets enter at 65 °C, they have a higher temperature than the liquid bulk phase and water evaporates from the droplets. This can also be seen in the partial pressure profile for water in Figure 29 (b). Here it is seen that the partial pressure in the droplets are much higher than the partial pressure over the gas and liquid phase and naturally water evaporates from the aerosol phase. This causes the initial decrease in the droplet diameter. Also, since the droplets are entering at such a high temperature the evaporation rate is extremely fast and the temperature of the droplets decreases quickly before the temperature rises again as MEA, CO_2 and water is entering the droplet.

After the initial increase and decrease in the droplet diameters, the droplets have a stable growth towards the end of the absorber. After the first 1-2m into the column, the temperature profiles are exactly the same for the column. This is probably due to the liquid having a higher heat capacity than the gas, so the inlet temperature does not affect the temperature profile more than at the inlet. For Case 10, the gas is saturated with water, but the water composition is still not different enough for it to have an effect on the temperatures. Even though the droplets show the same

growth and final sizes there is a difference in the amount of MEA that is let out with the aerosol phase. As reported in Table 10, Case 11 shows a 4% reduction in MEA content contained in the droplets after the absorber and a 6% reduction after the demister. As the droplets has the same sizes in both of the cases the droplet distributions are identical for the two cases. The reduction in MEA amount after the demister unit is thus due to the droplets in Case 11 having lower MEA content before the demister.

Table (10) The amount of MEA in aerosols after the absorber section, water wash section and demister unit for Case 11 relative to Case 10.

MEA amount in aerosols relative to Case 10	
After absorber	-4 %
After Water Wash	-5 %
After Demister	-6 %

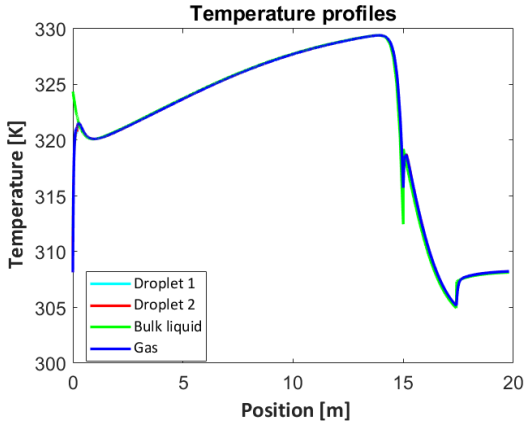

Figure (26) The temperature profile of Case 10 as a function of position in the system.

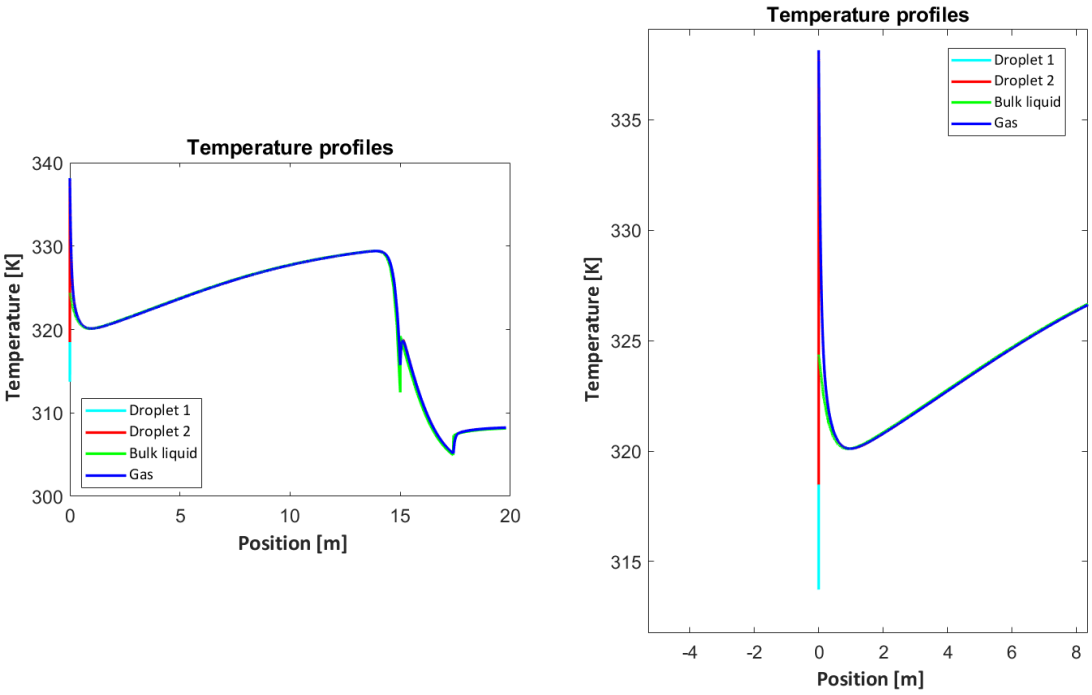

Figure (27) Temperature profile for Case 11 as a function of position in the column (a). An enlargement of the temperature profile at the inlet of the column (b).

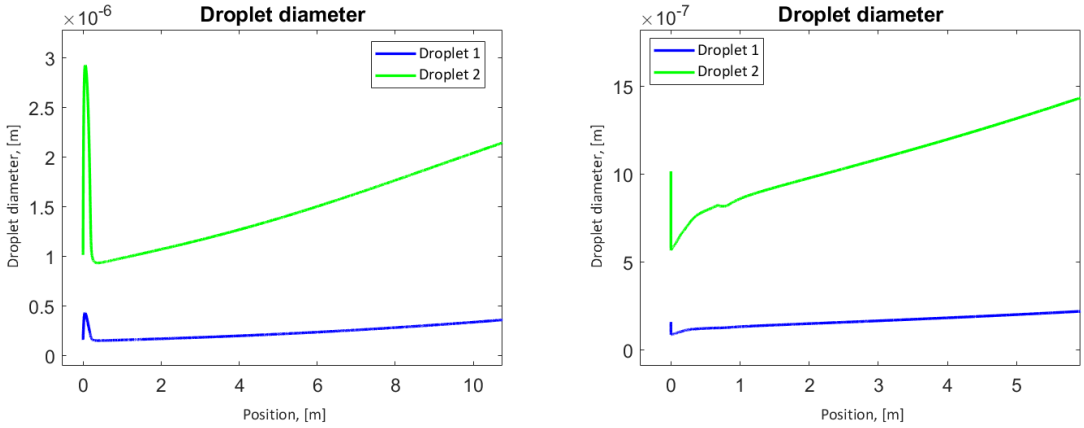

(a) Case 10 (b) Case 11

Figure (28) Droplet diameter profiles as a function of position in the column, enlarged at the inlet of the absorber for Case 10 (a) and Case 11 (b).

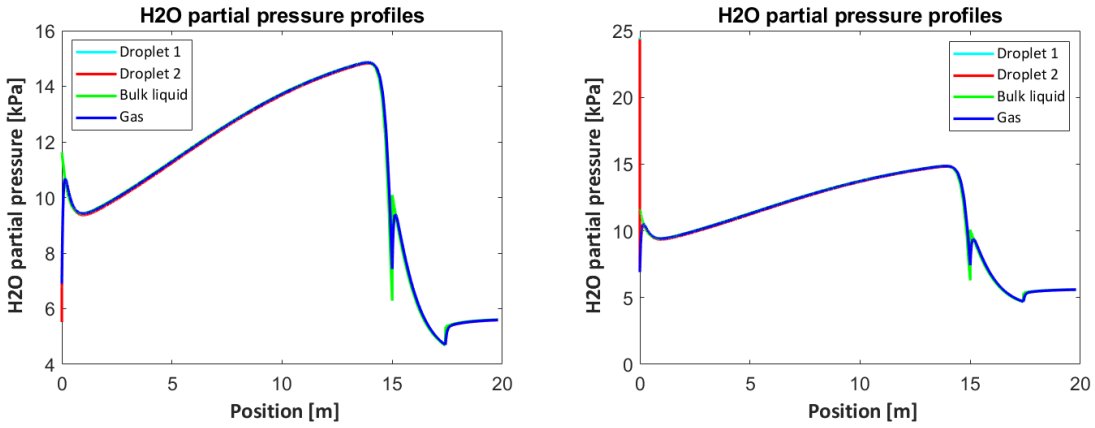

(a) Case 10 (b) Case 11

Figure (29) Partial pressure profile of H_2O as a function of position in the column for Case 10 (a) and Case 11 (b).

To explain why Case 11 has a lower MEA content in the aerosol phase than Case 10, it is necessary to take a closer look at the inlet internal profiles in the cases. Figure 30 gives the loading in the two droplets for both cases. From these results it is evident that loading goes towards maximum almost immediately for Case 10 while the same loading is not reached before a few meters into the column for Case 11. This implies that the transfer of CO_2 is much faster in Case 10. This is not very surprising taking the temperature profiles into account. That the solubility of CO_2 is higher at low temperatures is one of the fundamentals of amine scrubbing. For Case 10, the temperature is maintained quite a lot lower than in Case 11. Thus, the solubility of CO_2 in the liquid phase, but also in the aerosol phase, is higher in Case 10, causing the aerosols to absorb CO_2 faster.

Moving on to the MEA partial pressure profiles given in Figure 31. At the inlet of the column the partial pressure of MEA is close to zero, and the transfer of MEA into the droplets is slow in both cases. However, for Case 10, a small but sharp increase can be seen in the partial pressure of MEA at 0.15 m into the column. The small increase in MEA pressure is due to the small increase of the gas temperature as visible in the temperature profile. At this point, the pressure of MEA is slightly higher in Case 10 then Case 11. Also, as there is more CO_2 in the droplets in Case 10, the transfer of MEA into the droplets is slightly faster in Case 10. This can be observed in Figure 32, that shows the MEA concentration profiles for Droplet 1 at the inlet for both of the

cases. The carbamate formation is faster in Case 10 than in Case 11. As known from the chemical equilibrium in amine scrubbing, the formed Carbamate, is non-volatile. As a consequence of this reaction, the partial pressure of MEA decreases and more MEA can transfer into the droplets.

In the aerosol model, 65 °C was the highest temperature possible in the gas phase, to get the model to converge. When the flue gas is not treated in a DCC, this temperature is in the lower limits of the temperature range and it is realistic that these gases can have even higher temperatures. From the results in this case it is likely that the effect would be even larger for higher temperatures. As the gas temperature does not effect the temperature profile considerably with low CO_2 content, but the solubility of CO_2 would be even lower for higher temperatures. Thus, less MEA would be bound up in carbamate formation, causing the water wash to be more effective, and less MEA would be expected to be emitted with the aerosol phase. Either way, this is up to further work to investigate closer.

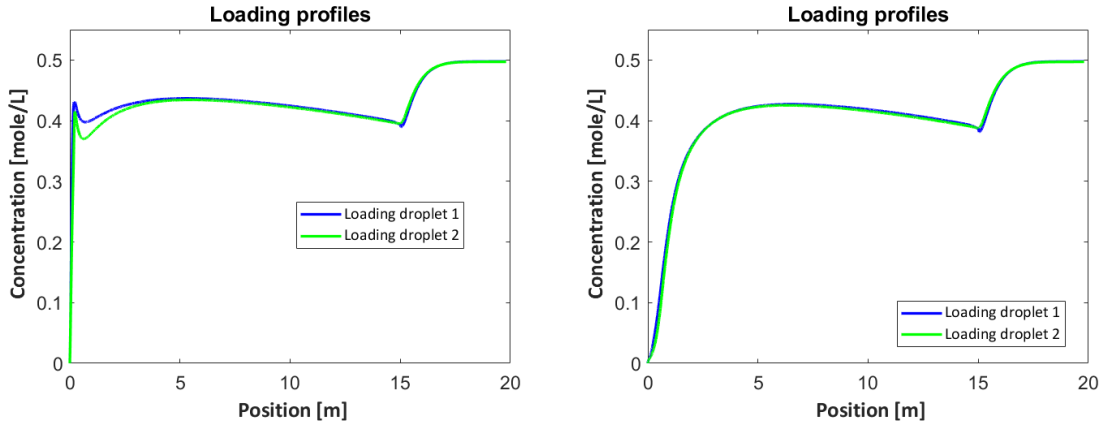

(a) Case 10 (b) Case 11

Figure (30) The loading in the aerosol phase as a function of position in the system for Case 10 (a) and Case 11 (b).

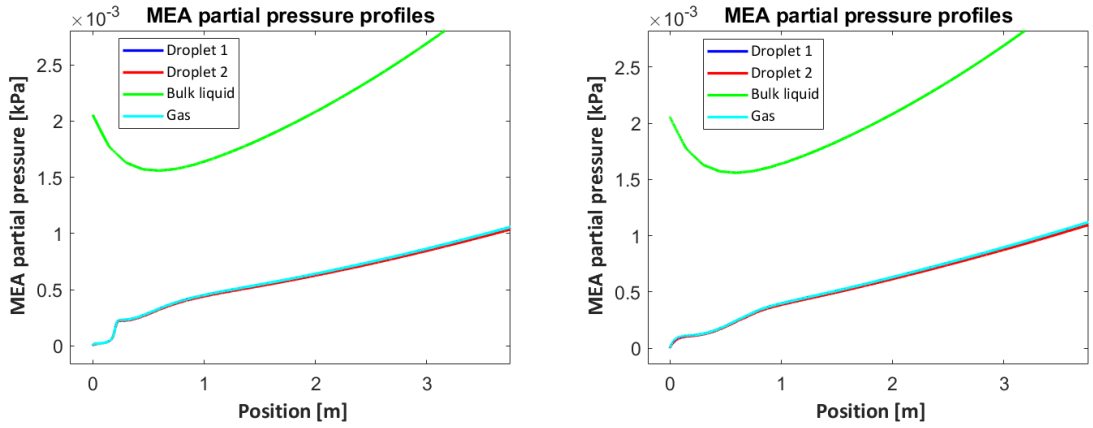

(a) Case 10 (b) Case 11

Figure (31) Enlargment of the partial pressure profiles of MEA at the inlet of the absorber column for Case 10 (a) and Case 11 (b).

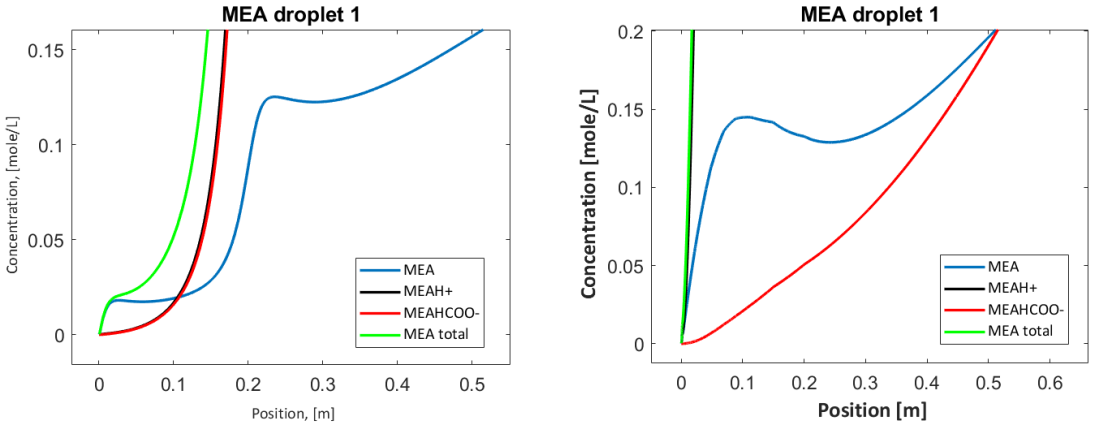

(a) Case 10 (b) Case 11

Figure (32) Enlargement of MEA concentration profiles for Droplet 1 as a function of position in the system for Case 10 (a) and Case 11 (b).

4.6 Further Work

Further work is still needed to characterize the growth mechanisms of aerosol emissions in post combustion amine scrubbing systems. The report has given a thorough explanation of the growth of aerosols in an amine scrubbing system, both in the absorber column and in the water wash sections. The report also investigates some system variables, operating conditions and modifications of the system. The temperature profiles along the system has been paid significant attention, as it is believed that the parameter significantly effects the emissions. Still, it is recommended to further investigate how to affect the temperature profile. Amine scrubbing systems operating in a different range does not necessarily show the same temperature profile as in the cases performed during this thesis and several variables can effect both the placement and magnitude of the temperature bulge. Validating the results through experimental runs in a pilot plant would also be recommended, and would ensure even better understanding of the behaviour of aerosols.

It is also recommended that the modifications like intercooling and the isotherm absorber, that showed to impact the emissions significantly is further researched. Gupta et. Al suggested that intercooling placed above the bulge temperature could created a local supersaturated environment and would further lead to increased aerosol emissions [38]. It is recommended that this is further researched, and it would be interesting to see the effect of intercooling on an absorber where the bulge temperature is localized in the bottom of the column. Further, is it recommended that a cost assessment is performed on the isotherm absorber, to investigate if the modification could be realistic.

This work focuses mostly on coal based flue gas, but also makes an effort to investigate different volumes of CO_2 in the gas phase. It would however be interesting to investigate the effect of different modifications and system variables on systems with different CO_2 content, as the results deviated a lot between high and low CO_2 content in the gas.

Lastly, in the aerosol model used in this work aerosol are assumed to enter with the flue gas entering the absorber, and formation of aerosols are not considered. To get a fuller picture of the aerosol emissions it is recommended to either do simulated or experimental work taking the formation of aerosols into consideration, as it might

give a different picture of the emissions.

5 Conclusion

The main objective of this thesis was to contribute to the understanding of aerosol emissions in amine scrubbing systems. This was done by researching how different system variables and modifications to the system affected the behaviour of the aerosol phase. Several case studies were performed where the effect of water wash height, the effect of the intercooling modification with and without a height reduction in the absorber, the effect of operating the absorber isothermally and the effect of CO_2 content as well as the effect of not cooling the flue has before entering the absorber was investigated. These case studies was compared to a Base Case consisting of an absorber and two water wash stages. All the cases were simulated in the simulation tool CO2SIM, and the behaviour of the aerosol phase was predicted using a model by Majeed et. Al (2017) [45].

Before performing the case studies, a validation was performed on the equilibrium model "Ordinary Electrolyte Non-Random Theory" in CO2SIM to ensure that the model was fitted to the low MEA concentration ranges seen in the water wash sections. The results from the validation were satisfactory as the results showed that the equilibrium model was well fitted to low MEA concentrations.

It was found that the height of the wash sections mainly influenced the retention time of the gas in the column. Increasing the height increased the retention time. As the aim of the water wash is to reduce both aerosol and vapor based emissions, a increased retention time contributes with making the wash column more effective in reducing the overall emissions. The aerosols initially grow rapidly in the water wash sections. However, the growth in seen to slow down towards the top of the water wash columns. This implies that there is an optimal height of the water wash, and that increasing the height past this optimum does not give much gain.

The intercooling modification showed a large impact on the temperature profile in the absorber column, reducing the magnitude of the bulge, which reduced the overall emissions. The intercooling was placed at the conventional choice of 1/3 from the bottom and the unconventional choice of 1/3 from the top. The largest reduction in emissions was seen from the unconventional choice, without affecting the efficiency of the absorber. The two placement choices were also implemented while reducing the height of the absorber. This showed further reduction in the emissions due to

decreased retention time, yet, the reduced height of the absorber causes the column to be less efficient.

The isotherm absorber has the same effects as the intercooling modification had on the temperature profile, just more significant. This reduced the emissions significantly and is considered to be a promising modification to reduce the emissions. However, as the modification is thought to be expensive to implement, questions arise about weather the modification is realistic or not.

Lastly, the reduced CO_2 content of the flue gas showed reduced overall emissions, as less MEA is bound up in carbamate. This reduced the emissions as well as making the water wash more effective. The case with elevated temperature in the flue gas showed a further reduction in the emissions. This was due to the CO_2 being less soluble in the droplets, due to the higher temperature. As CO_2 has the effect of accelerating the transfer of MEA into the aerosol phase, less CO_2 in the droplets caused limited transfer of MEA into the aerosols.

Overall, the study has gained a better understanding of the behaviour of the aerosol emissions. From the case studies performed it is clear that the temperature profile has a significant effect on the overall emissions, and variables and modification to the system that reduced the bulge temperature also showed a reduction in the aerosol emissions. Concerning both the growth of the aerosols, and the amount of MEA emitted with the aerosols. It is also confirmed that the emissions can be affected such that the water wash and demister unit are effective in removing them. Of all the cases, the isotherm absorber showed the largest reduction in overall emissions.

Recommendations for further work included investigating the variables and modifications further, with systems using different operating ranges. As well as confirming the findings in this thesis with experimental campaigns. It is also recommended to investigate the intercooling modification with absorber column where the bulge is located at the bottom of the column. Lastly, it is recommended to do a cost assessment on the isotherm absorber, as this modification showed promising results.

References

[1] J. G. J. Olivier and J. A. H. W. Peters, "Trends in global CO2 and total greenhouse gas emissions 2019 Report," Tech. Rep., 2020. [Online]. Available: https://www.pbl.nl/sites/default/files/downloads/pbl-2020-trends-in-global-.

[2] T. Wilberforce, A. Baroutaji, B. Soudan, A. H. Al-Alami, and A. G. Olabi, "Outlook of carbon capture technology and challenges," *Science of the Total Environment*, vol. 657, pp. 56–72, Mar. 2019, ISSN: 18791026. DOI: 10.1016/j.scitotenv.2018.11.424. [Online]. Available: https://doi.org/10.1016/j.scitotenv.2018.11.424.

[3] J. G. Speight, *Gas Processing: Environmental Aspects and Methods*. Butterworth-Heinemann, 1993, ISBN: 0750611324.

[4] A. B. Rao, E. S. Rubin, and M. B. Berkenpas, "An integrated modeling framework for carbon management technologies - Volume 1-Technical Documentation: Amine-Based CO 2 Capture and Storage Systems for Fossil Fuel Power Plant Final Report of," Tech. Rep.

[5] B. Dutcher, M. Fan, and A. G. Russell, "Amine-Based CO 2 Capture Technology Development from the Beginning of 2013A Review," 2015. DOI: 10.1021/am507465f. [Online]. Available: www.acsami.org.

[6] G. T. Rochelle, "Amine Scrubbing for CO2 Capture," *Science*, vol. 325, pp. 1652–1654, 2009.

[7] D. Aaron and C. Tsouris, "Separation of CO 2 from Flue Gas: A Review," *Separation Science and Technology*, vol. 40, pp. 321–348, 2005, ISSN: 1520-5754. DOI: 10.1081/SS-200042244. [Online]. Available: https://www.tandfonline.com/action/journalInformation?journalCode=lsst20.

[8] G. Puxty and M. Maeder, *The fundamentals of post-combustion capture*. Elsevier Ltd, 2016, pp. 13–33, ISBN: 9780081005156. DOI: 10.1016/B978-0-08-100514-9.00002-0. [Online]. Available: http://dx.doi.org/10.1016/B978-0-08-100514-9.00002-0.

[9] H. Majeed, H. Knuutila, M. Hillestad, and H. F. Svendsen, "Effect of Amine Volatility on Aerosol Droplet Development in Absorption Columns," *Energy Procedia*, vol. 114, no. 1876, pp. 977–986, 2017, ISSN: 18766102. DOI: 10.1016/j.egypro.2017.03.1243. [Online]. Available: http://dx.doi.org/10.1016/j.egypro.2017.03.1243.

[10] S. A. Mazari, B. Si Ali, B. M. Jan, I. M. Saeed, and S. Nizamuddin, "An overview of solvent management and emissions of amine-based CO2 capture technology," *International Journal of Greenhouse Gas Control*, vol. 34, pp. 129–140, Mar. 2015, ISSN: 17505836. DOI: 10.1016/j.ijggc.2014.12.017.

[11] H. Bartsch and R. Montesano, *Relevance of nitrosamines to human cancer*, Nov. 1984. DOI: 10.1093/carcin/5.11.1381.

[12] M. K. Wong, A. M. Shari, and M. A. Bustam, "Raman spectroscopic study on the equilibrium of carbon dioxide in aqueous monoethanolamine †," pp. 10 816–10 823, 2016. DOI: 10.1039/c5ra22926j.

[13] Y. Maree, S. Nepstad, and G. d. Koeijer, "Establishment of Knowledge base for Emission Regulation for the CO2 Technology Centre Mongstad," *Energy Procedia*, 2013.

[14] the Norwegian Institute of Public Health (NIPH), "Health effects of amines and derivatives associated with CO2 capture: Nitrosamines and nitramines," vol. 10, pp. 1–15, 2011.

[15] Scottish Environment Protection Agency, "Review of amine emissions from carbon capture systems," Tech. Rep., 2015.

[16] J. Monteiro, J. Ros, E. Skylogiani, H. F. Svendsen, H. Knuutila, P. Moser, A. Hartono, G. Wiechers, C. Charalambous, and S. Garcia, "Accelerating Low carbon Industrial Growth through CCUS," vol. 691712, no. 271501, pp. 3–9, 2020.

[17] T. Nguyen, M. Hilliard, and G. T. Rochelle, "Amine volatility in CO2 capture," *International Journal of Greenhouse Gas Control*, vol. 4, no. 5, pp. 707–715, Sep. 2010, ISSN: 17505836. DOI: 10.1016/j.ijggc.2010.06.003.

[18] J. Mertens, L. Brachert, D. Desagher, M. L. Thielens, P. Khakharia, E. Goetheer, and K. Schaber, "ELPI+ measurements of aerosol growth in an amine absorption column," *International Journal of Greenhouse Gas Control*, vol. 23, pp. 44–50, 2014, ISSN: 17505836. DOI: 10.1016/j.ijggc.2014.02.002. [Online]. Available: http://dx.doi.org/10.1016/j.ijggc.2014.02.002.

[19] P. Khakharia, L. Brachert, J. Mertens, A. Huizinga, B. Schallert, K. Schaber, T. J. Vlugt, and E. Goetheer, "Investigation of aerosol based emission of MEA due to sulphuric acid aerosol and soot in a Post Combustion CO2 Capture process," *International Journal of Greenhouse Gas Control*, vol. 19, pp. 138–144, Nov. 2013, ISSN: 17505836. DOI: 10.1016/j.ijggc.2013.08.014. [Online]. Available: http://dx.doi.org/10.1016/j.ijggc.2013.08.014.

[20] E. F. Da Silva, H. Kolderup, E. Goetheer, K. W. Hjarbo, A. Huizinga, P. Khakharia, I. Tuinman, T. Mejdell, K. Zahlsen, K. Vernstad, A. Hyldbakk, T. Holten, H. M. Kvamsdal, P. Van Os, and A. Einbu, "Emission studies from a CO2 capture pilot plant," *Energy Procedia*, vol. 37, pp. 778–783, 2013, ISSN: 18766102. DOI: 10.1016/j.egypro.2013.05.167. [Online]. Available: http://dx.doi.org/10.1016/j.egypro.2013.05.167.

[21] G. Richner and G. Puxty, "Assessing the chemical speciation during CO 2 absorption by aqueous amines using in situ FTIR," *Industrial and Engineering Chemistry Research*, vol. 51, no. 44, pp. 14 317–14 324, 2012, ISSN: 08885885. DOI: 10.1021/ie302056f.

[22] N. Yi, M. Fang, W. Di, Z. Xia, T. Wang, and Q. Wang, "Aerosol Emissions of Amine-Based CO 2 Absorption System: Effects of Condensation Nuclei and Operating Conditions," DOI: 10.1021/acs.est.0c04630. [Online]. Available: https://dx.doi.org/10.1021/acs.est.0c04630.

[23] T. Spietz, T. Chwoła, A. Krótki, A. Tatarczuk, L. Wicław-Solny, and A. Wilk, "Ammonia emission from CO2 capture pilot plant using aminoethylethanolamine," *International Journal of Environmental Science and Technology*, vol. 15, no. 5, pp. 1085–1092, May 2018, ISSN: 17352630. DOI: 10.1007/s13762-017-1475-z.

[24] E. da Silva, H. Kolderup, T. Mejdell, A. Tobiesen, G. Haugen, K. Hoff, K. Josefsen, T. Strøm, O. Furuseth, K. Hanssen, H. Wirsching, T. Myhrvold, and K. Johnsen, *Emission Reducing Technologies*. 2011, p. 123, ISBN: 9788214050240.

[25] M. Fang, N. Yi, W. Di, T. Wang, and Q. Wang, *Emission and control of flue gas pollutants in CO2 chemical absorption system – A review*, Feb. 2020. DOI: 10.1016/j.ijggc.2019.102904.

[26] H. Gretscher and K. Schaber, "Aerosol formation by heterogeneous nucleation in wet scrubbing processes," *Chemical Engineering and Processing: Process Intensification*, vol. 38, no. 4-6, pp. 541–548, Sep. 1999, ISSN: 02552701. DOI: 10.1016/S0255-2701(99)00051-3.

[27] R. K. Srivastava, C. A. Miller, C. Erickson, and R. Jambhekar, "Journal of the Air & Waste Management Association Emissions of Sulfur Trioxide from Coal-Fired Power Plants Emissions of Sulfur Trioxide from Coal-Fired Power Plants," 2012, ISSN: 2162-2906. DOI: 10.1080/10473289.2004.10470943. [Online]. Available: https://www.tandfonline.com/action/journalInformation?journalCode=uawm20.

[28] L. Brachert, J. Mertens, P. Khakharia, and K. Schaber, "The challenge of measuring sulfuric acid aerosols: Number concentration and size evaluation using a condensation particle counter (CPC) and an electrical low pressure impactor (ELPI+)," *Journal of Aerosol Science*, vol. 67, pp. 21–27, Jan. 2014, ISSN: 18791964. DOI: 10.1016/j.jaerosci.2013.09.006.

[29] K. Schaber, "Aerosol formation in absorption processes," *Chemical Engineering Science*, vol. 50, no. 8, pp. 1347–1360, 1995, ISSN: 00092509. DOI: 10.1016/0009-2509(95)98846-7.

[30] H. Vehkama¨kivehkama¨ki and I. Riipinen, "Thermodynamics and kinetics of atmospheric aerosol particle formation and growth," *This journal is Cite this: Chem. Soc. Rev*, vol. 41, pp. 5160–5173, 2012. DOI: 10.1039/c2cs00002d. [Online]. Available: http://blogs.helsinki.fi/aerosoltrain/.

[31] K. Schaber, J. Körber, O. Ofenloch, R. Ehrig, and P. Deuflhard, "Aerosol formation in gas-liquid contact devices-Nucleation, growth and particle dynamics," *Chemical Engineering Science*, vol. 57, no. 20, pp. 4345–4356, Nov. 2002, ISSN: 00092509. DOI: 10.1016/S0009-2509(02)00350-0.

[32] P. Khakharia, J. Mertens, T. J. Vlugt, and E. Goetheer, "Predicting aerosol based emissions in a post combustion CO2 capture process using an aspen plus model," in *Energy Procedia*, vol. 63, Elsevier Ltd, 2014, pp. 911–925. DOI: 10.1016/j.egypro.2014.11.101. [Online]. Available: www.sciencedirect.com.

[33] G. Puxty and M. Maeder, "The fundamentals of post-combustion capture," in *Absorption-Based Post-Combustion Capture of Carbon Dioxide*, Elsevier Inc., Jun. 2016, pp. 13–33, ISBN: 9780081005156. DOI: 10.1016/B978-0-08-100514-9.00002-0.

[34] S. M. Fulk and G. T. Rochelle, "Modeling aerosols in amine-based CO2 capture," *Energy Procedia*, vol. 37, pp. 1706–1719, 2013, ISSN: 18766102. DOI: 10.1016/j.egypro.2013.06.046. [Online]. Available: http://dx.doi.org/10.1016/j.egypro.2013.06.046.

[35] J. L. Kang, Y. Zhang, S. Fulk, and G. T. Rochelle, "Modeling Amine Aerosol Growth in the Absorber and Water Wash," in *Energy Procedia*, vol. 114, Elsevier Ltd, Jul. 2017, pp. 959–976. DOI: 10.1016/j.egypro.2017.03.1241.

[36] H. M. Kvamsdal and G. T. Rochelle, "Effects of the Temperature Bulge in CO 2 Absorption from Flue Gas by Aqueous Monoethanolamine," 2008. DOI: 10.1021/ie061651s. [Online]. Available: www.pseenterprise.com.

[37] P. Khakharia, L. Brachert, J. Mertens, C. Anderlohr, A. Huizinga, E. S. Fernandez, B. Schallert, K. Schaber, T. J. Vlugt, and E. Goetheer, "Understanding aerosol based emissions in a Post Combustion CO2 Capture process: Parameter testing and mechanisms," *International Journal of Greenhouse Gas Control*, vol. 34, pp. 63–74, 2015, ISSN: 17505836. DOI: 10.1016/j.ijggc.2015.01.001. [Online]. Available: http://dx.doi.org/10.1016/j.ijggc.2015.01.001.

[38] V. Gupta, P. Mobley, J. Tanthana, L. Cody, D. Barbee, J. Lee, R. Pope, R. Chartier, J. Thornburg, and M. Lail, "Aerosol emissions from water-lean solvents for post-combustion CO2 capture," *International Journal of Greenhouse Gas Control*, vol. 106, Mar. 2021, ISSN: 17505836. DOI: 10.1016/j.ijggc.2021.103284.

[39] A. Cousins, L. T. Wardhaugh, and P. H. Feron, *A survey of process flow sheet modifications for energy efficient CO 2 capture from flue gases using chemical absorption*, Jul. 2011. DOI: 10.1016/j.ijggc.2011.01.002.

[40] Y. Le Moullec and M. Kanniche, "Screening of flowsheet modifications for an efficient monoethanolamine (MEA) based post-combustion CO2 capture," *International Journal of Greenhouse Gas Control*, vol. 5, no. 4, pp. 727–740, 2011, ISSN: 17505836. DOI: 10.1016/j.ijggc.2011.03.004. [Online]. Available: http://dx.doi.org/10.1016/j.ijggc.2011.03.004.

[41] H. Ahn, M. Luberti, Z. Liu, and S. Brandani, "Process configuration studies of the amine capture process for coal-fired power plants," *International Journal of Greenhouse Gas Control*, vol. 16, pp. 29–40, Aug. 2013, ISSN: 17505836. DOI: 10.1016/j.ijggc.2013.03.002. [Online]. Available: http://dx.doi.org/10.1016/j.ijggc.2013.03.002.

[42] Y. L. Moullec and T. Neveux, "Process modifications for CO2 capture," in *Absorption-Based Post-Combustion Capture of Carbon Dioxide*, Elsevier Inc., Jun. 2016, pp. 305–340, ISBN: 9780081005156. DOI: 10.1016/B978-0-08-100514-9.00013-5.

[43] M. Karimi, M. Hillestad, and H. F. Svendsen, "Capital costs and energy considerations of different alternative stripper configurations for post combustion CO2 capture," 2011.

[44] H. Majeed and H. F. Svendsen, "Characterization of aerosol emissions from CO2 capture plants treating various power plant and industrial flue gases," *International Journal of Greenhouse Gas Control*, vol. 74, pp. 282–295, Jul. 2018, ISSN: 17505836. DOI: 10.1016/j.ijggc.2018.04.016. [Online]. Available: https://doi.org/10.1016/j.ijggc.2018.04.016.

[45] H. Majeed, H. K. Knuutila, M. Hillestad, and H. F. Svendsen, "Characterization and modelling of aerosol droplet in absorption columns," *International Journal of Greenhouse Gas Control*, vol. 58, pp. 114–126, 2017, ISSN: 17505836. DOI: 10.1016/j.ijggc.2017.01.006. [Online]. Available: http://dx.doi.org/10.1016/j.ijggc.2017.01.006.

[46] H. Majeed and H. F. Svendsen, "Effect of water wash on mist and aerosol formation in absorption column," *Chemical Engineering Journal*, vol. 333, no. September 2017, pp. 636–648, 2018, ISSN: 13858947. DOI: 10.1016/j.cej.2017.09.124. [Online]. Available: https://doi.org/10.1016/j.cej.2017.09.124.

[47] T. L. Sønderby, K. B. Carlsen, P. L. Fosbøl, L. G. Kiørboe, and N. von Solms, "A new pilot absorber for CO2 capture from flue gases: Measuring and modelling capture with MEA solution," *International Journal of Greenhouse Gas Control*, vol. 12, pp. 181–192, Jan. 2013, ISSN: 17505836. DOI: 10.1016/j.ijggc.2012.10.010.

[48] S. Pierucci, J. J. Klemeš, L. Piazza, C. Madeddu, M. Errico, D. Porcu, and R. Baratti, "Solvent Recovery System for a Co 2-Mea Reactive Absorption-Stripping Plant," in *CHEMICAL ENGINEERING TRANSACTIONS*, vol. 74, 2019, ISBN: 978-88-95608-71-6. DOI: 10.3303/CET1974135. [Online]. Available: www.cetjournal.it.

[49] J. G. Monteiro and H. F. Svendsen, "The N2O analogy in the CO2 capture context: Literature review and thermodynamic modelling considerations," *Chemical Engineering Science*, vol. 126, pp. 455–470, 2015, ISSN: 00092509. DOI: 10.1016/j.ces.2014.12.026. [Online]. Available: http://dx.doi.org/10.1016/j.ces.2014.12.026.

[50] J. J. Carroll, J. D. Slupsky, and A. E. Mather, *The Solubility of Carbon Dioxide in Water at Low Pressure*, 1991. DOI: 10.1063/1.555900.

[51] F. A. Tobiesen, M. Hillestad, H. Kvamsdal, and A. Chikukwa, "A general column model in CO2SIM for transient modelling of CO2 absorption processes," *Energy Procedia*, vol. 23, no. 1876, pp. 129–139, 2012, ISSN: 18766102. DOI: 10.1016/j.egypro.2012.06.071.

[52] A. Zakeri, A. Einbu, and H. F. Svendsen, "Post Combustion Capture Conference," Tech. Rep., 2011.

[53] R. Billet and M. Schultes, "Prediction of Mass Transfer Columns with Dumped and Arranged Packings," *Chemical Engineering Research and Design*, vol. 77, no. 6, pp. 498–504, 1999, ISSN: 02638762. DOI: 10.1205/026387699526520.

Appendices

A Validation against experimental campaign

This section gives the validation results from the validation of CO2SIM against an experimental campaign by Sønderby et. Al (2013) [47] performed in previous work by author. Figure 33 gives the ratio between the simulated and experimental rich loading as a function of vol% CO_2 at the gas inlet. The ratio between simulated and experimental absorption rate is given as a function of column height, flue gas inlet temperature, liquid gas ratio, vol% CO_2 at the gas inlet, lean solvent loading and lean solvent inlet temperature in Figures 34, 35 and 36.

The temperature profiles generated from the runs in CO2SIM is compared to the experimental temperature profiles in Figures 37, 38, 39, 40, 41 and 42.

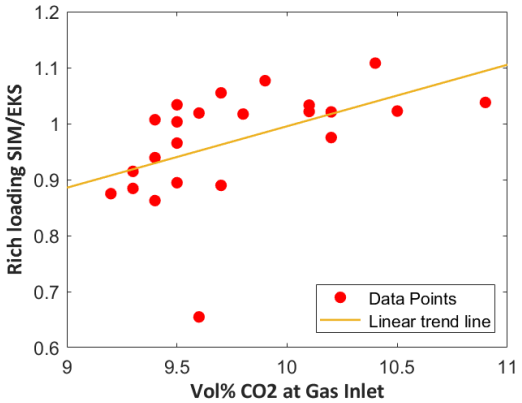

Figure (33) The ratio between simulated and experimental rich loading as a function of CO_2 content in the gas at the inlet.

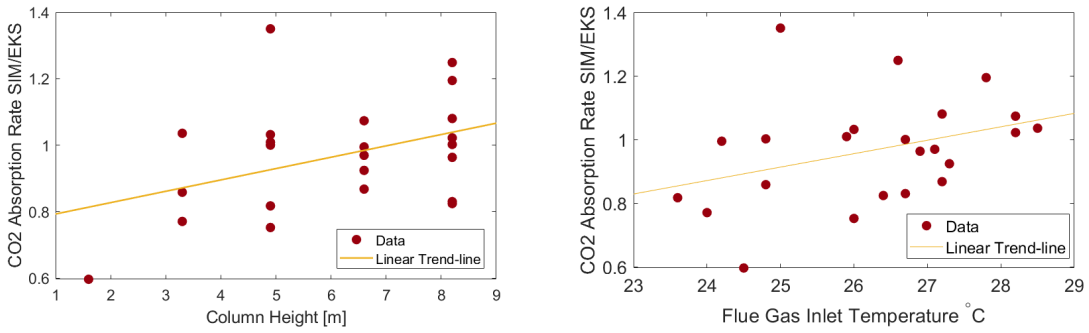

(a) (b)

Figure (34) Ratio of the simulated CO_2 absorption rate to the experimental rate plotted against height of column (a) and flue gas inlet temperature (b)

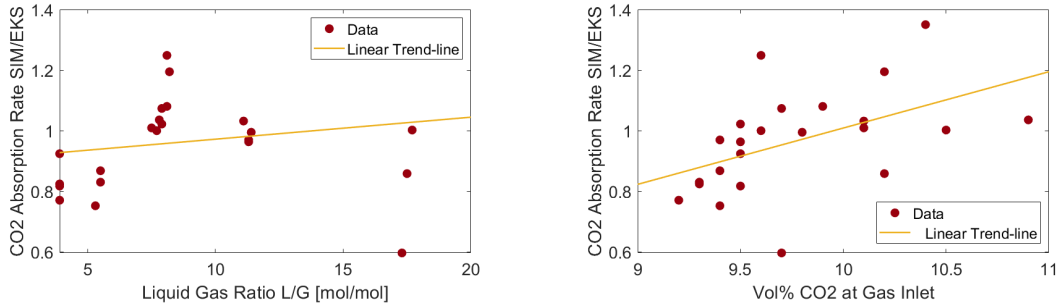

(a) (b)

Figure (35) Ratio of the simulated CO_2 absorption rate to the experimental rate plotted against liquid gas ratio (a) and vol% CO_2 in the flue gas (b).

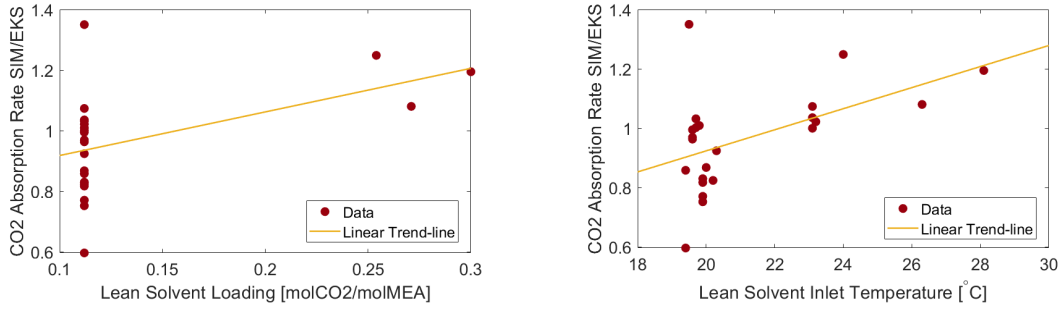

(a) (b)

Figure (36) Ratio of the simulated CO_2 absorption rate to the experimental rate plotted against lean solvent loading (a) and lean solvent temperature (b).

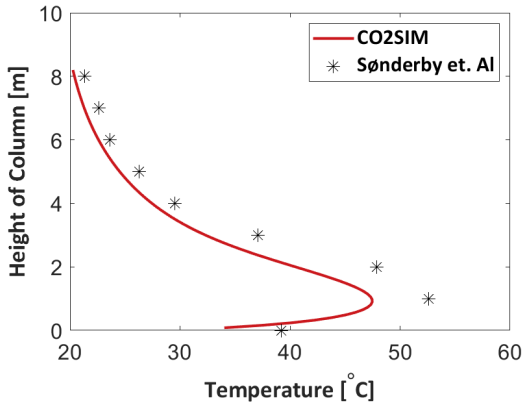

(a) Run 1

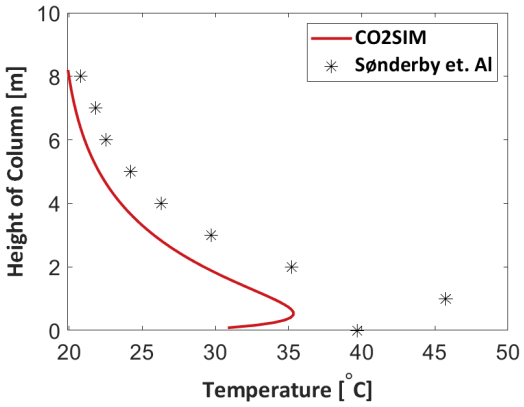

(b) Run 2

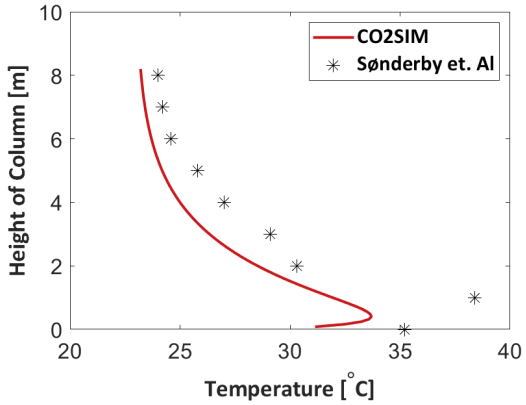

(c) Run 3

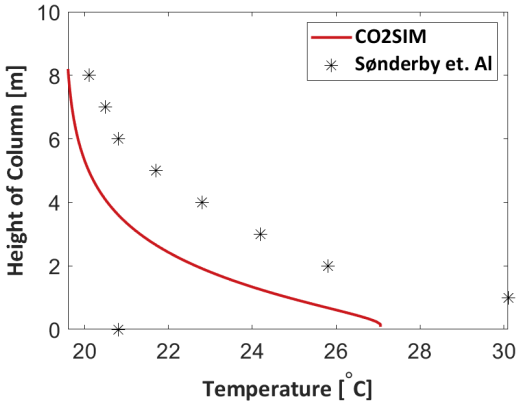

(d) Run 4

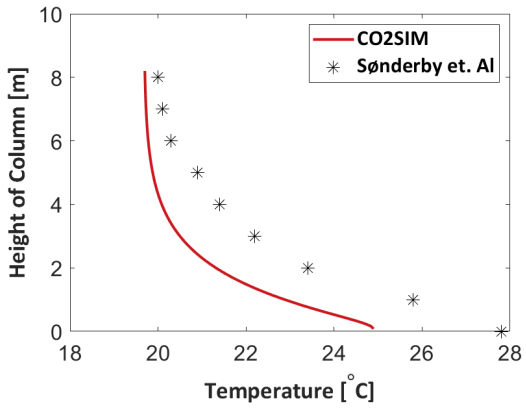

(e) Run 5

Figure (37) Internal temperature profiles for runs with height packing height equal to 8.2m given by CO2SIM and experimental data

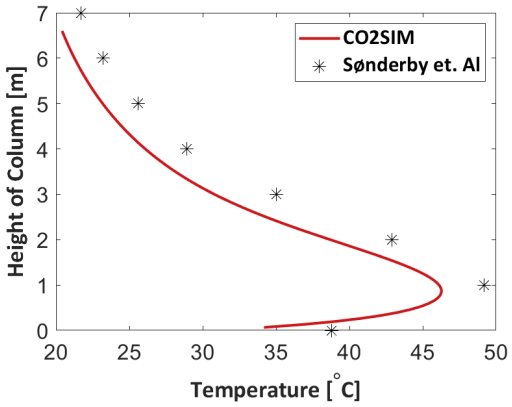

(a) Run 6

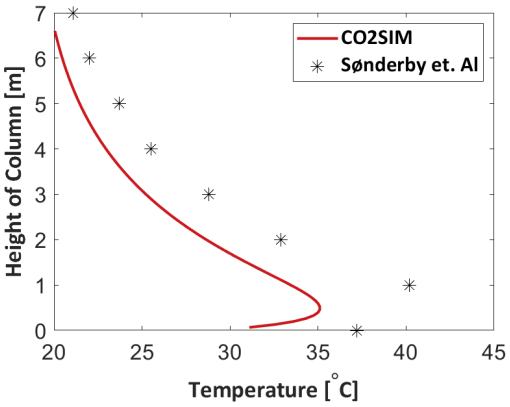

(b) Run 7

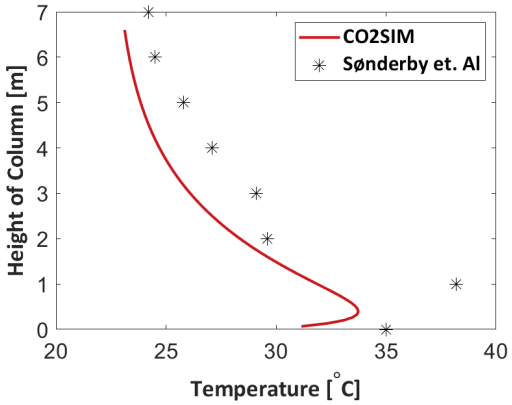

(c) Run 8

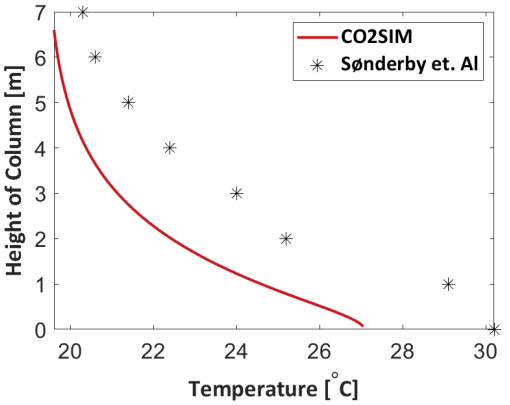

(d) Run 9

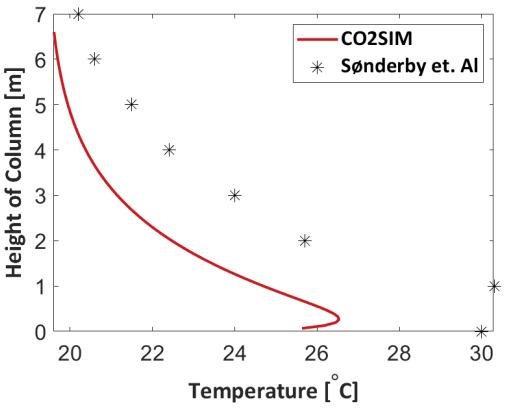

(e) Run 10

Figure (38) Internal temperature profiles for runs with height packing height equal to 6.4m given by CO2SIM and experimental data

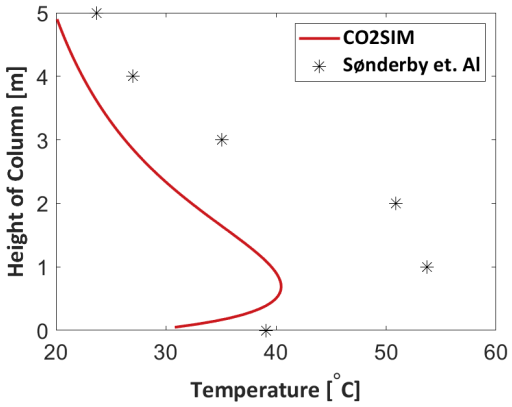

(a) Run 11

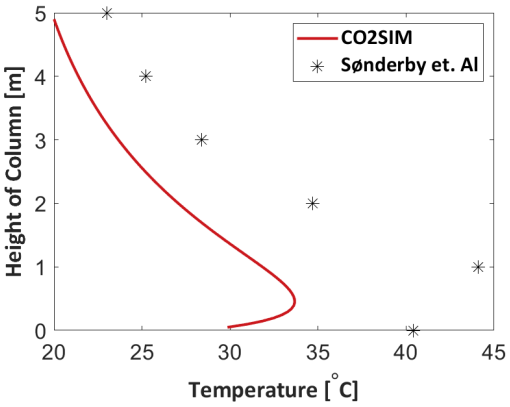

(b) Run 12

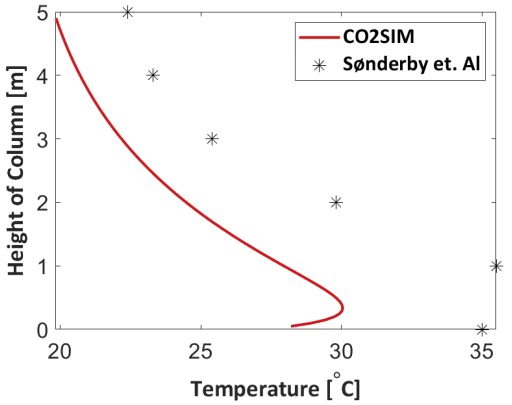

(c) Run 13

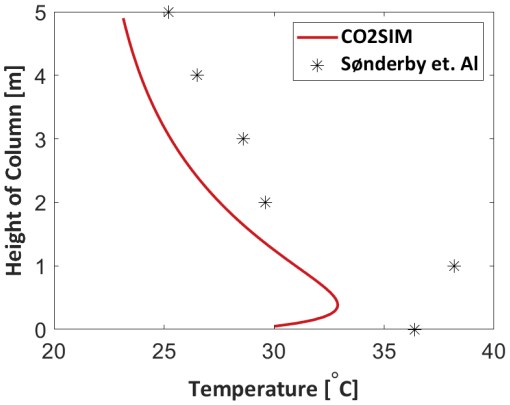

(d) Run 14

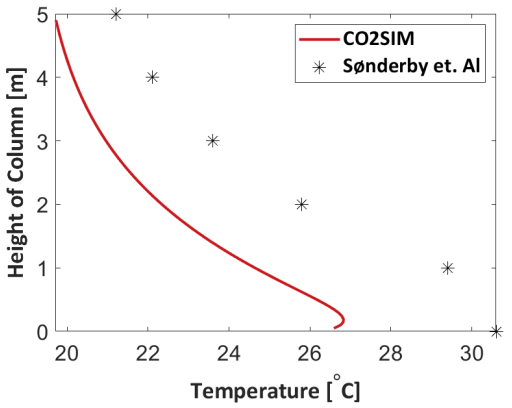

(e) Run 15

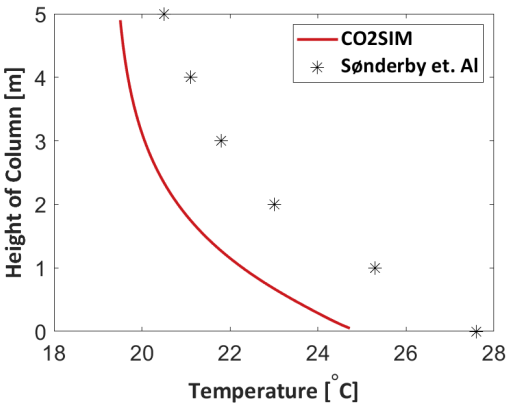

(f) Run 16

Figure (39) Internal temperature profiles for runs with height packing height equal to 4.9m given by CO2SIM and experimental data

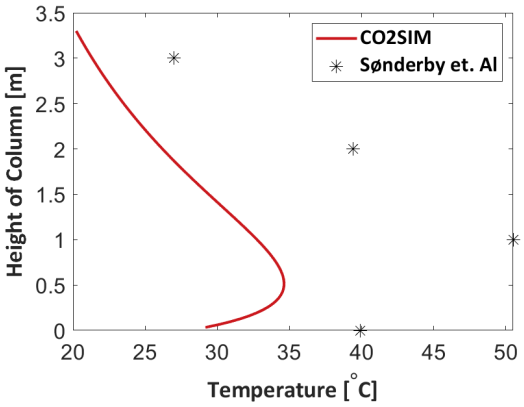

(a) Run 17

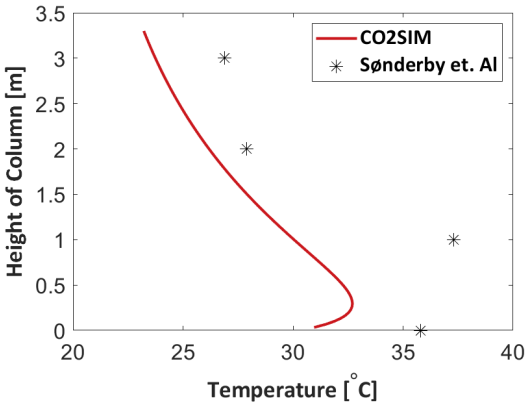

(b) Run 18

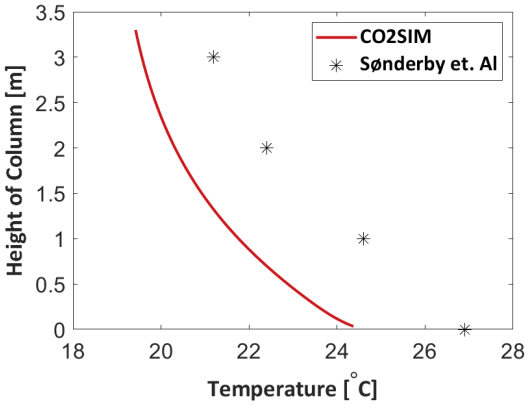

(c) Run 19

Figure (40) Internal temperature profiles for runs with height packing height equal to 3.3m given by CO2SIM and experimental data

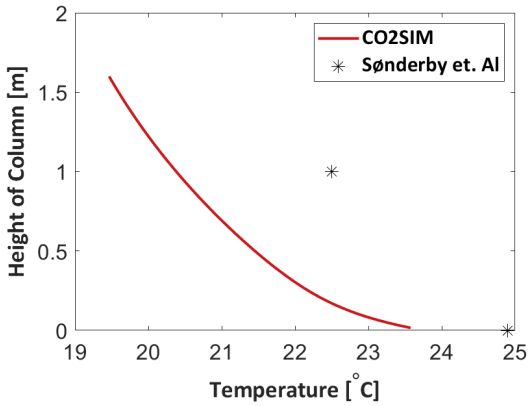

Figure (41) Internal temperature profile for run 20 with height packing height equal to 1.6m given by CO2SIM and experimental data

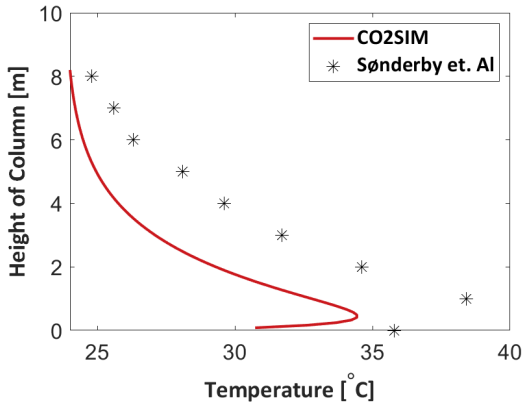

(a) Run 21

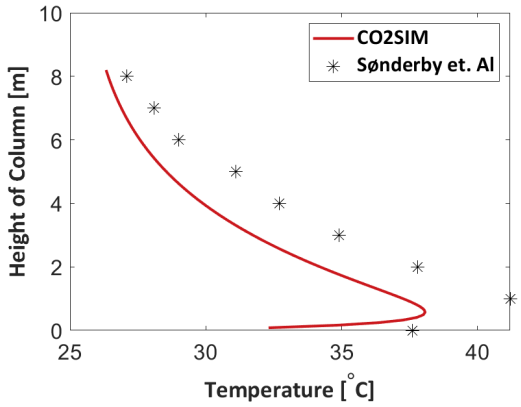

(b) Run 22

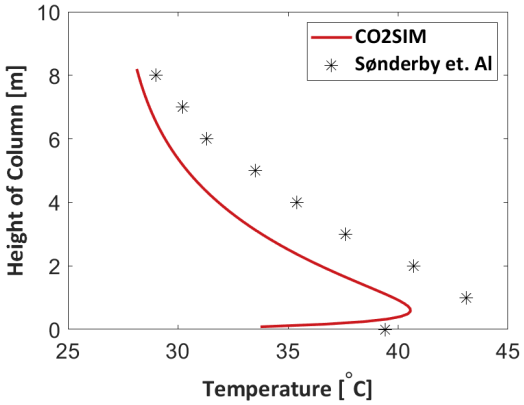

(c) Run 23

Figure (42) Internal temperature profiles for runs with height packing height equal to 8.2m and varied lean loading.

B Vapor Liquid Equilibrium Validation

The specifications for the validation runs in CO2SIM that were compared to the CO_2-water VLE is given in Tables 11, 12 and 13. The specifications for the runs compared to the MEA-CO_2-water VLE is given in Tables 14, 15 and 16.

Table (11) The specified conditions in the flash unit and the results used to generate VLE for when the mass fraction of MEA was set to 1E-8.

Flow CO_2 [kmole/hr]	Flash Pressure [kPa]	Mole fraction CO_2 Vapor	Mole fraction CO_2 Liquid
0.01	100	0.92	4.0E-04
0.01	50	0.85	1.8E-04
0.01	20	0.63	5.6E-05
0.01	18	0.59	4.7E-05
0.01	15	0.51	3.4E-05
0.01	12	0.38	2.1E-05
0.01	10	0.26	1.2E-05
0.01	8	0.08	2.8E-06

Table (12) The specified conditions in the flash unit and the results used to generate VLE for when the mass fraction of MEA was set to 1E-3

Flow CO_2 [kmole/hr]	Flash Pressure [kPa]	Mole fraction CO_2 Vapor	Mole fraction CO_2 Liquid
0.01	100	0.93	7.0E-04
0.01	60	0.88	5.2E-04
0.01	20	0.63	3.5E-04
0.01	18	0.59	3.4E-04
0.01	15	0.51	3.3E-04
0.01	12	0.38	3.1E-04
0.01	10	0.26	3.0E-04
0.01	8	0.09	2.8E-04

Table (13) The specified conditions in the flash unit and the results used to generate VLE for when the mass fraction of MEA was set to 1E-1

Flow CO_2 [kmole/hr]	Flash Pressure [kPa]	Mole fraction CO_2 Vapor	Mole fraction CO_2 Liquid
0.05	100	0.93	0.023
0.05	20	0.64	0.019
0.05	18	0.60	0.019
0.05	15	0.52	0.018
0.05	12	0.40	0.018
0.05	10	0.29	0.016
0.05	9	0.28	0.020
0.05	8	0.12	0.047

Table (14) The specified conditions in the flash unit and the results used to generate VLE for when the weight % of MEA was set to 6.113 wt%.

Flow CO_2 [kmole/hr]	Flash Pressure [kPa]	Mole fraction CO_2 Vapor	Loading Liquid
0.01	40	0.79	0.72
0.01	38	0.78	0.71
0.01	35	0.76	0.70
0.01	31	0.75	0.69
0.01	28	0.74	0.68
0.01	25	0.69	0.66
0.01	21	0.66	0.64
0.01	18	0.60	0.63
0.01	15	0.60	0.61
0.01	10	0.28	0.53
0.01	8	0.14	0.49

Table (15) The specified conditions in the flash unit and the results used to generate VLE for when the weight % of MEA was set to 3.06 wt%.

Flow CO_2 [kmole/hr]	Flash Pressure [kPa]	Mole fraction CO_2 Vapor	Loading Liquid
0.01	36	0.86	0.81
0.01	34	0.79	0.80
0.01	32	0.83	0.80
0.01	28	0.76	0.77
0.01	24	0.70	0.75
0.01	20	0.66	0.72
0.01	18	0.60	0.70
0.01	14	0.48	0.65
0.01	10	0.30	0.58
0.01	8	0.23	0.55

Table (16) The specified conditions in the flash unit and the results used to generate VLE for when the weight % of MEA was set to 0.6119 wt%.

Flow CO_2 [kmole/hr]	Flash Pressure [kPa]	Mole fraction CO_2 Vapor	Loading Liquid
0.01	2	0.72	0.98
0.01	24	0.69	0.97
0.01	22	0.67	0.96
0.01	20	0.63	0.95
0.01	18	0.59	0.93
0.01	16	0.54	0.91
0.01	15	0.51	0.90
0.01	14	0.47	0.90
0.01	10	0.26	0.78
0.01	8	0.08	0.61

C Tiller Plant Data

This sections gives the operating conditions in the Tiller Plant used to set up the Base Case and the natural gas Base Case. The operating conditions in the absorber and in the water wash used to set up the Base Case is given in Tables 17 and 18. The operating conditions from the Tiller Plant used to set up the natural gas base case is given in Table 19.

Table (17) The operating conditions in the absorber column at the Tiller plant used as a basis for the Base Case.

Variable [Unit]	Value
Height [m]	15
Diameter [m]	0.2
Gas Flow Inlet [m^3/h]	160
CO_2 inlet vol% dry	13
CO_2 outlet Absorber vol% dry	2.32/2.44
CO_2 recovery %	83
Lean loading [mole/mole]	0.17
Lean amine [mole/kg]	5.19
Liquid inlet absorber [kg/min]	7.03
Temperature Gas inlet [°C]	35
Temperature Lean inlet [°C]	39.4
Rich loading [mole/mole]	0.47

Table (18) The operating conditions in the water wash section at the Tiller plant used as a basis for the Base Case.

Variable [Unit]	Value
Height [m]	2.4
Diameter [m]	0.2
Temperature liquid inlet [°C]	31.79
Flowrate liquid inlet [$kmole/hr$]	23.22
Loading liquid bottom [mole/mole]	0.68

Table (19) The operating conditions in the absorber column at the Tiller plant used as a basis for the natural gas Base Case.

Variable [Unit]	Value
Height [m]	15
Diameter [m]	0.2
Gas Flow Inlet [m^3/h]	250
CO_2 inlet vol% dry	4.34
CO_2 outlet Absorber vol% dry	0.96
CO_2 recovery %	79
Lean loading [mole/mole]	0.16
Lean amine [mole/kg]	5.08
Liquid inlet absorber [kg/min]	4.04
Temperature Gas inlet [°C]	35
Temperature Lean inlet [°C]	42.5
Rich loading [mole/mole]	0.45

D Base Case Data

Table (20) Summary of conditions in the streams in the Base Case. The stream names corresponds to the labels in Figure 6.

Stream	Temperature [°C]	Pressure [kPa]	Flow [kmole/hr]	Mole fraction CO_2	Mole fraction H_2O	Mole fraction MEA	Mole Fraction N_2	Loading [-]
FG	35	98.38	6.14	0.1224	0.0578	0	0.8197	-
Lean	40	97.88	16.4568	0.0209	0.8559	0.1232	0	0.1696
GasAbsTreat	50.94	97.68	6.5713	0.0188	0.215	0.0003	0.7659	-
Rich	42.21	98.38	17.1658	0.0567	0.8251	0.1181	0	0.4803
GasWWTreat	34.32	97.68	5.5957	0.0218	0.0787	1.00E-04	0.8994	-
Recycle	56.96	97.68	24.3603	0.0013	0.9968	0.002	0	0.6437
P08	56.96	400	24.3603	0.0013	0.9968	0.002	0	0.6437
P09	31.79	97.68	0	0	0	0	0	-
P10	31.79	97.68	24.3603	0.0013	0.9968	0.002	0	0.6437
Condensate	31.79	97.68	1.1403	0.0013	0.9968	0.002	0	0.6437
SolventWW	31.79	97.68	23.22	0.0013	0.9968	0.002	0	0.6437
LeanMix	39.468	97.68	17.5971	0.0196	0.865	0.1154	0	0.1701
GasWWTreat2	32.04	97.68	5.431	0.0224	0.0508	0	0.9267	-
Recycle2	36.12	97.68	23.3847	0.0013	0.9971	0.0016	0	0.8177
P17	36.12	400	23.3847	0.0013	0.9971	0.0016	0	0.8177
P19	31.79	97.68	23.3847	0.0013	0.9971	0.0016	0	0.8177
CondensateWW2	31.79	97.68	0.1647	0.0013	0.9971	0.0016	0	0.8177
SolventWW2	31.79	97.68	23.22	0.0013	0.9971	0.0016	0	0.8177
WW1MIX	31.79	97.68	23.3847	0.0013	0.9968	0.002	0	0.6447

E Case Study operating conditions

Table (21) Some of the operating conditions in all of the cases performed in this study, to give an overview of the differences in the cases.

Case	Height	Temperature Gas in	Vol % CO_2 Gas in	Lean Solvent Flow	Intercooling	WW Height	Temperature in "WW2"
BC	15	35	13	17.64	No	4.8	31.79
Case 1	15	35	13	17.64	No	**7.2**	31.79
Case 2	15	35	13	17.64	No	**4**	31.79
Case 3	15	35	13	17.64	No	**2**	31.79
Case 4	15	35	13	17.64	**Yes**	4.8	31.79
Case 5	15	35	13	17.64	**Yes**	4.8	31.79
Case 6	**13**	35	13	17.64	**Yes**	4.8	31.79
Case 7	**12**	35	13	17.64	**Yes**	4.8	31.79
Case 8	**12**	35	13	17.64	**Yes**	4.8	31.79
Case 9	15	35	13	17.64	**Yes**	4.8	31.79
Case 10	15	35	**3.5**	**5.6**	No	4.8	**35**
Case 11	15	**65**	**3.5**	**5.6**	No	4.8	**35**

F Case Study Results

F.1 Case Study CO2SIM results

Table 22 gives the summary results from CO2SIM for each of the runs performed in this thesis.

Table (22) Summary of the CO2SIM results for all the cases performed in this study.

	CO_2 removal efficiency [%]	Rich Loading [-]	MEA emissions "Abs" [ppmv]	MEA emissions "WW2" [ppmv]	CO_2 outlet [vol% dry]
BC	84	0.48	0.775	0.017	2.4
Case 1	84	0.48	0.775	0.002	2.4
Case 2	84	0.48	0.775	0.033	2.4
Case 3	84	0.48	0.775	0.182	2.4
Case 4	85	0.48	0.580	0.011	2.3
Case 5	84	0.48	0.359	0.006	2.2
Case 6	81	0.47	0.520	0.010	2.7
Case 7	79	0.46	0.500	0.009	3.0
Case 8	78	0.46	0.292	0.005	3.0
Case 9	84	0.46	0.114	0.002	2.3
Case 10	84	0.45	0.220	0.001	0.6
Case 11	84	0.45	0.253	0.001	0.6

Figures 43 through 54 gives the liquid side profiles from CO2SIM, including temperature and mole fractions of MEA and water as a function of position in the column for each of the runs.

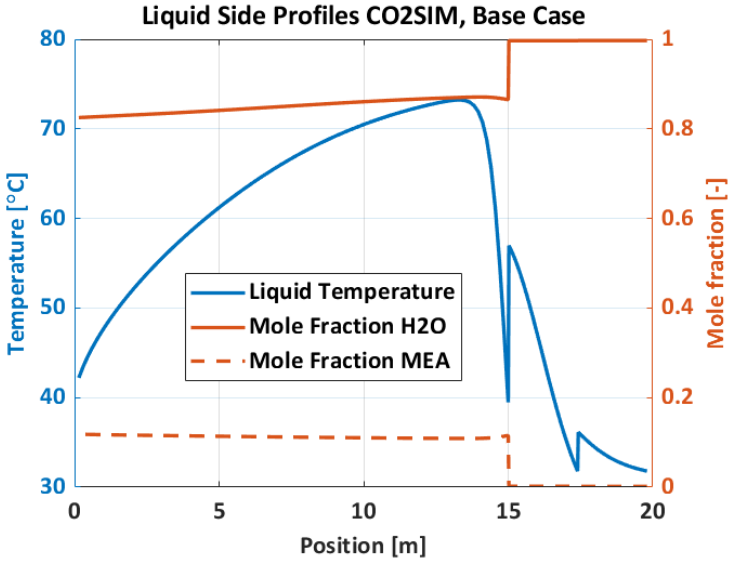

Figure (43) Liquid side profiles for Base Case, including the temperature, mole fraction of H_2O and mole fraction of MEA as a function of position in the system obtained from CO2SIM and used in the aerosol model to predict the aerosol phase.

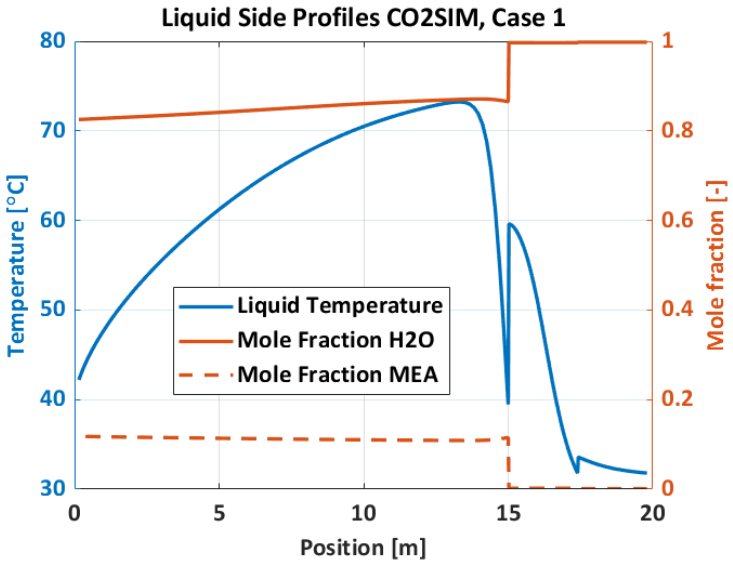

Figure (44) Liquid side profiles for Case 1, including the temperature, mole fraction of H_2O and mole fraction of MEA as a function of position in the system obtained from CO2SIM and used in the aerosol model to predict the aerosol phase.

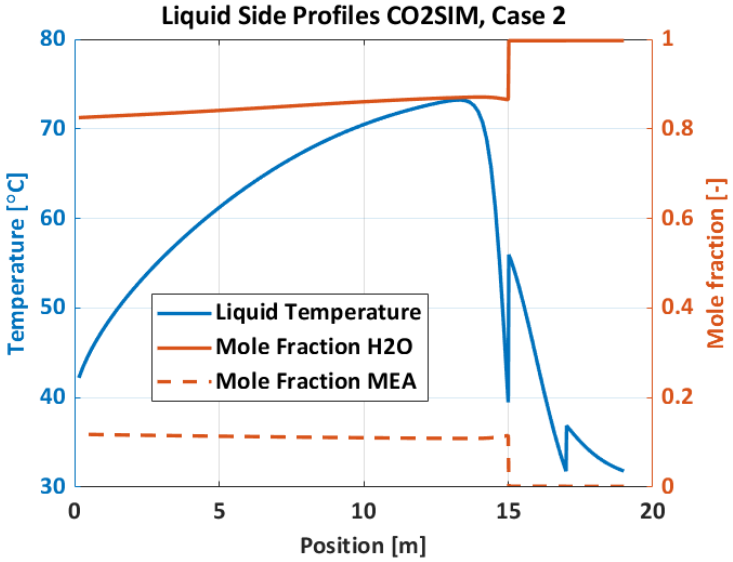

Figure (45) Liquid side profiles for Case 2, including the temperature, mole fraction of H_2O and mole fraction of MEA as a function of position in the system obtained from CO2SIM and used in the aerosol model to predict the aerosol phase.

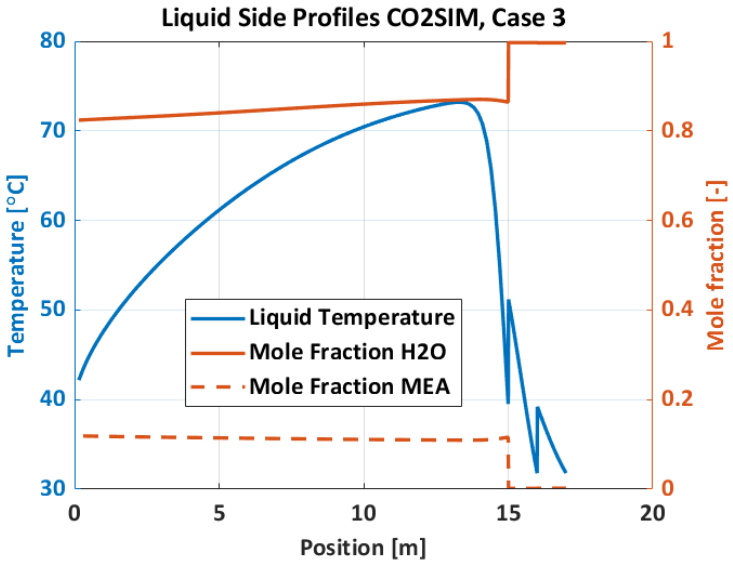

Figure (46) Liquid side profiles for Case 3, including the temperature, mole fraction of H_2O and mole fraction of MEA as a function of position in the system obtained from CO2SIM and used in the aerosol model to predict the aerosol phase.

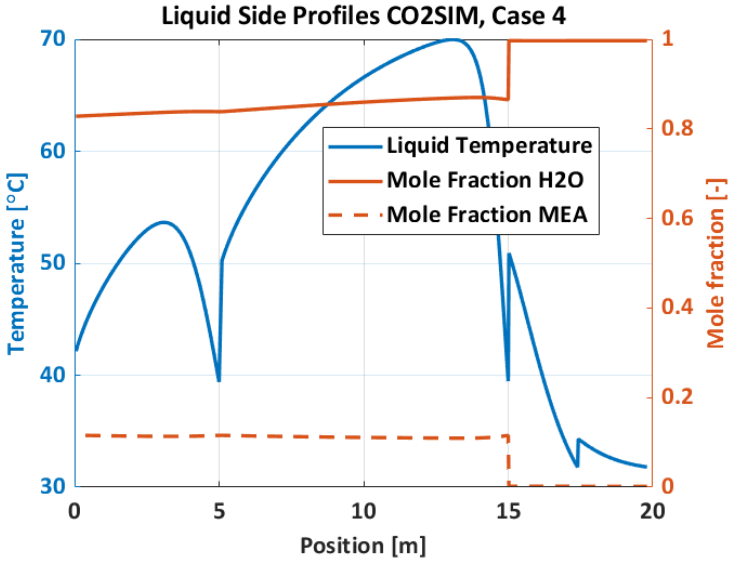

Figure (47) Liquid side profiles for Case 4, including the temperature, mole fraction of H_2O and mole fraction of MEA as a function of position in the system obtained from CO2SIM and used in the aerosol model to predict the aerosol phase.

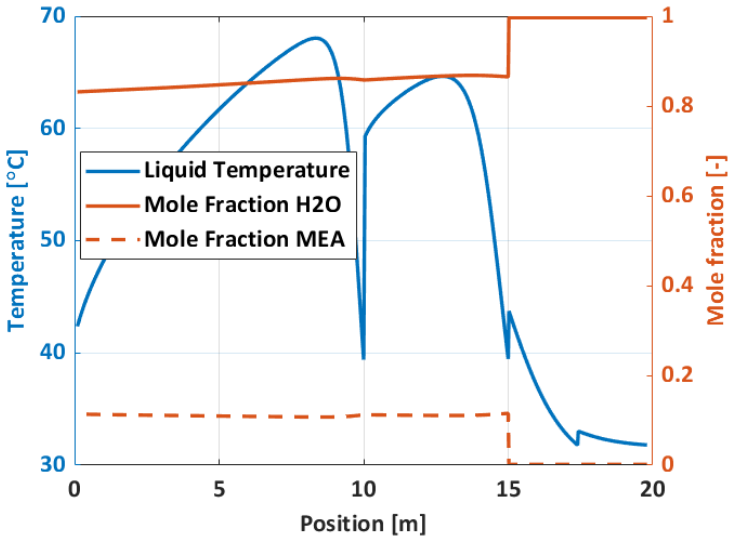

Figure (48) Liquid side profiles for Case 5, including the temperature, mole fraction of H_2O and mole fraction of MEA as a function of position in the system obtained from CO2SIM and used in the aerosol model to predict the aerosol phase.

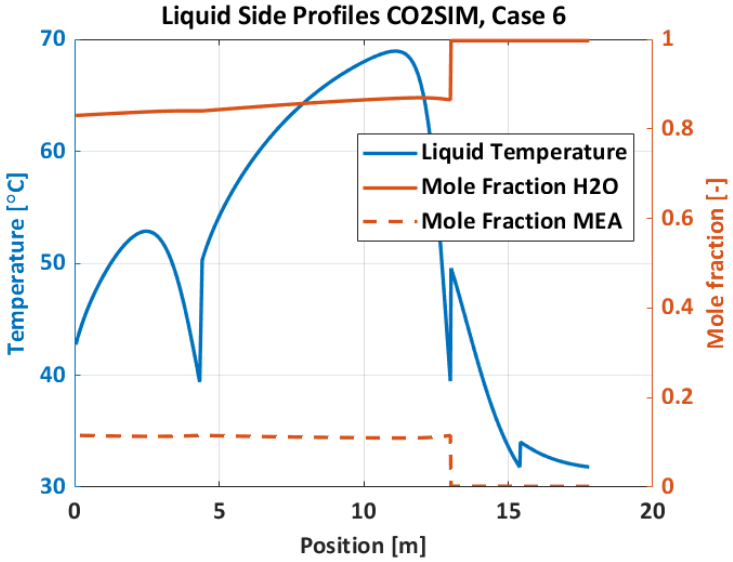

Figure (49) Liquid side profiles for Case 6, including the temperature, mole fraction of H_2O and mole fraction of MEA as a function of position in the system obtained from CO2SIM and used in the aerosol model to predict the aerosol phase.

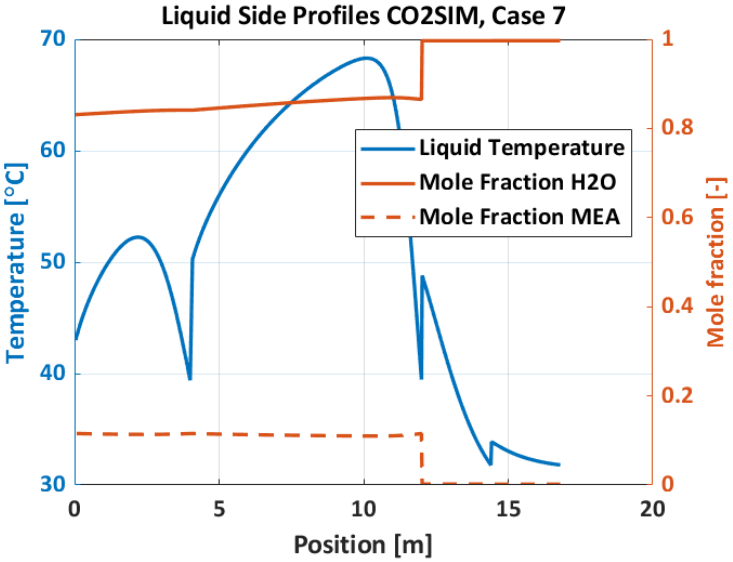

Figure (50) Liquid side profiles for Case 7, including the temperature, mole fraction of H_2O and mole fraction of MEA as a function of position in the system obtained from CO2SIM and used in the aerosol model to predict the aerosol phase.

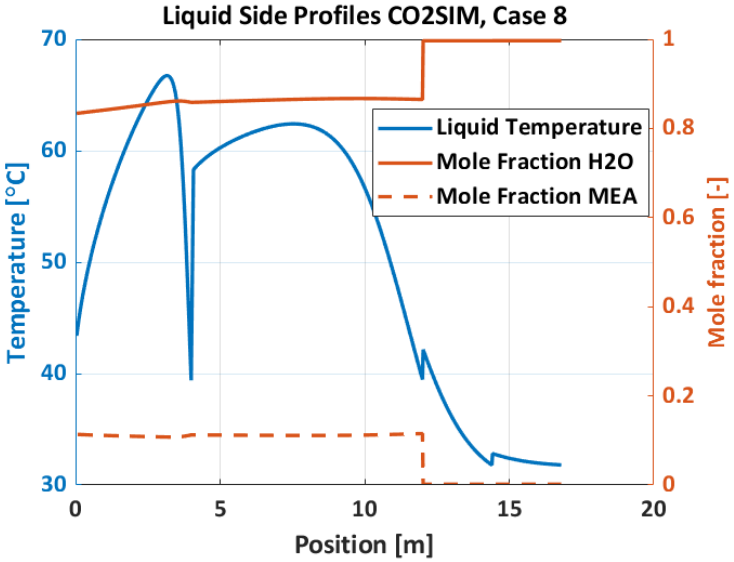

Figure (51) Liquid side profiles for Case 8, including the temperature, mole fraction of H_2O and mole fraction of MEA as a function of position in the system obtained from CO2SIM and used in the aerosol model to predict the aerosol phase.

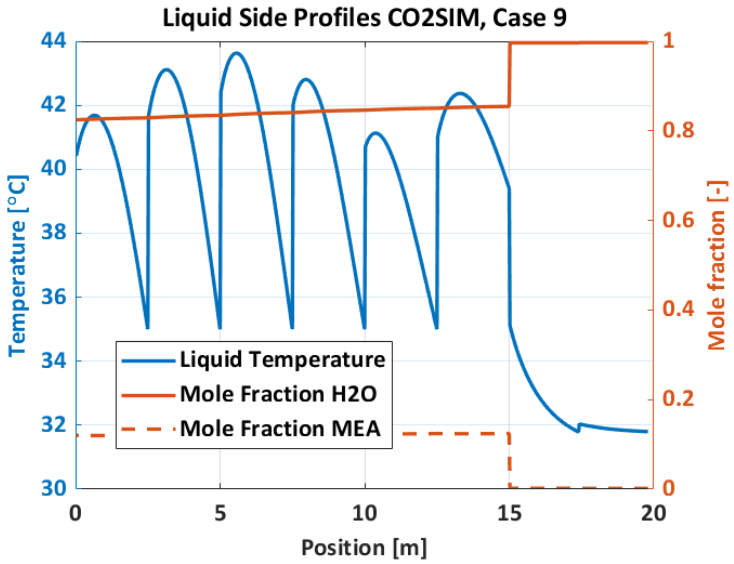

Figure (52) Liquid side profiles for Case 9, including the temperature, mole fraction of H_2O and mole fraction of MEA as a function of position in the system obtained from CO2SIM and used in the aerosol model to predict the aerosol phase.

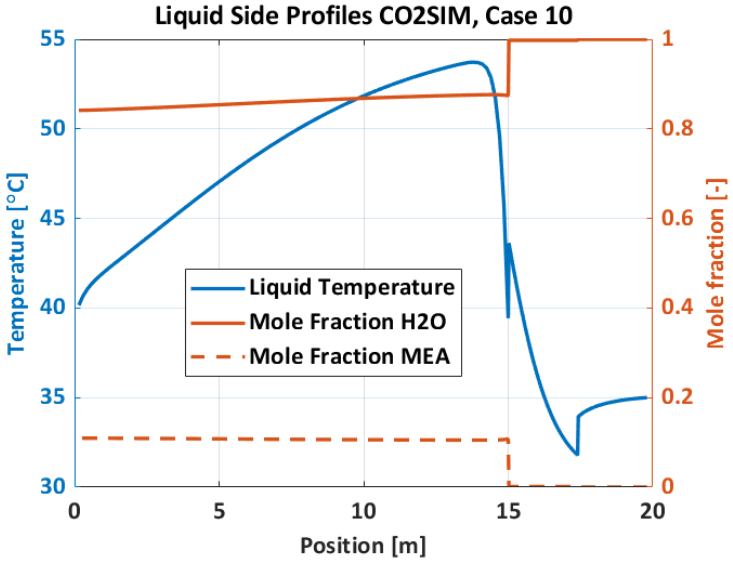

Figure (53) Liquid side profiles for Case 10, including the temperature, mole fraction of H_2O and mole fraction of MEA as a function of position in the system obtained from CO2SIM and used in the aerosol model to predict the aerosol phase.

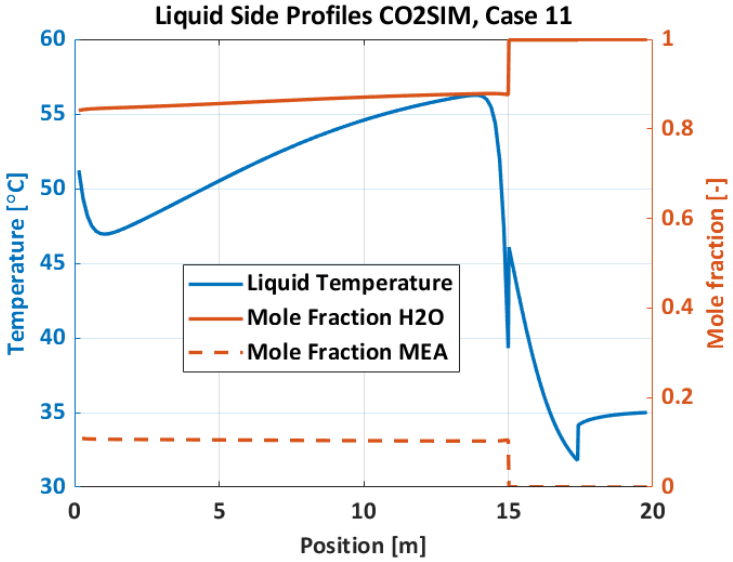

Figure (54) Liquid side profiles for Case 11, including the temperature, mole fraction of H_2O and mole fraction of MEA as a function of position in the system obtained from CO2SIM and used in the aerosol model to predict the aerosol phase.

F.2 Case Study Aerosol Results

The results for the vapor based MEA emissions from CO2SIM is given as pmm in the gas phase after the absorber, the first and second water wash for all of the cases in Table 23. The following subsections includes the aerosol profiles for all of the cases.

Table (23) The raw results for the amount of MEA in the aerosol given in ppm, after the absorber column, after the water wash sections and after the demsiter unit.

Case	MEA in aerosol from abs [ppm]	MEA in aerosol from WW [ppm]	MEA in aerosol from WW, after demister [ppm]
BC	1172.6	543.1	268.8
Case 1	1172.6	489.6	228.3
Case 2	1157.1	553.5	281.4
Case 3	1160.5	638.1	347.7
Case 4	850.5	368.8	200.9
Case 5	723.3	305.0	180.0
Case 6	541.8	214.4	134.2
Case 7	607.5	245.1	143.8
Case 8	687.3	286.3	164.1
Case 9	168.9	51.6	38.1
Case 10	337.1	119.6	75
Case 11	322.6	113	71.5

F.2.1 Base Case

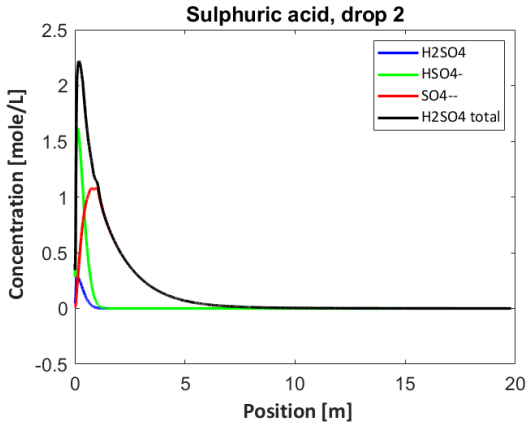

Figure (55) Sulphuric acid concentration as a function of position in the system for Droplet 2, for the Base Case.

F.2.2 Case 1

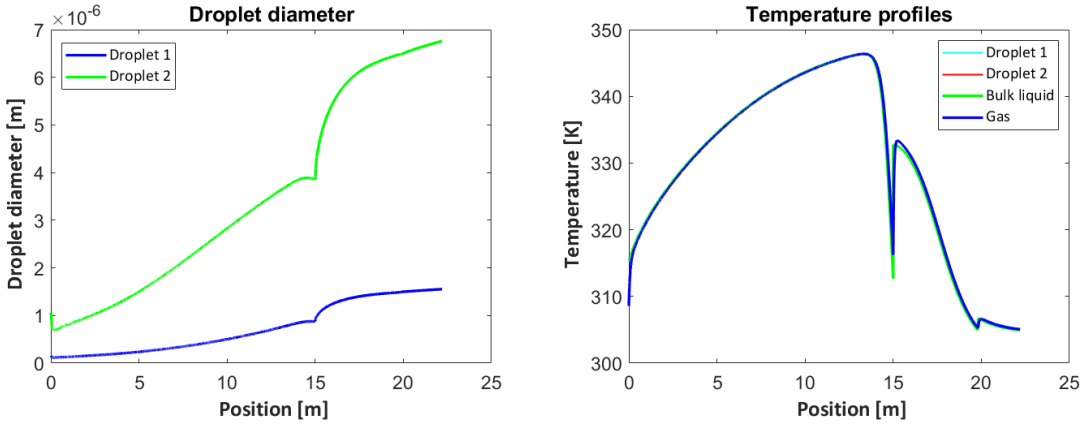

Figure (56) Droplet diameter for the two droplets (a) and the temperature profiles for the three phases (b) as a function of position in the system, for Case 1.

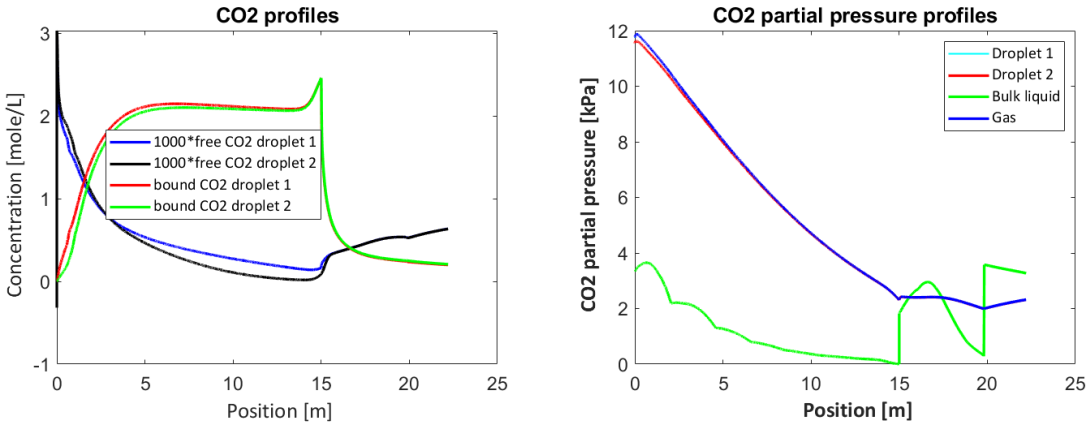

Figure (57) The concentration profile of CO_2 (a) and the partial pressure profile of CO_2 (b) as a function of position in the system, for Case 1.

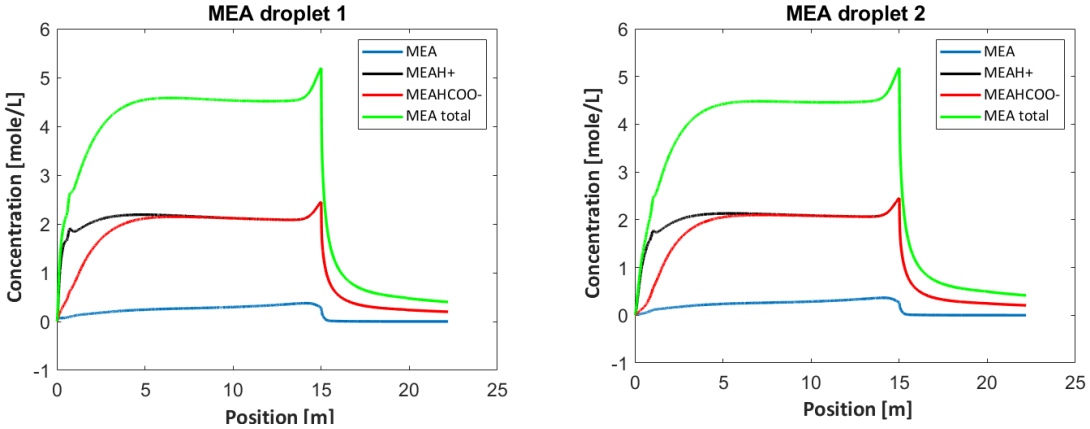

Figure (58) The concentration profile of MEA for Droplet 1 (a) and Droplet 2 (b) as a function of position in the system, for Case 1.

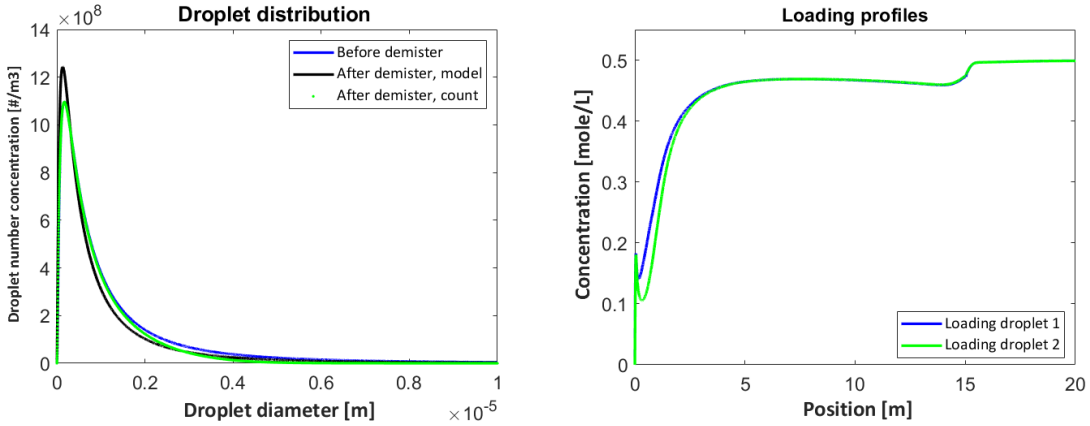

Figure (59) Droplet number concentration as a function of droplet diameter before and after the demister (a) and the loading as a function of position in the system (b), for Case 1.

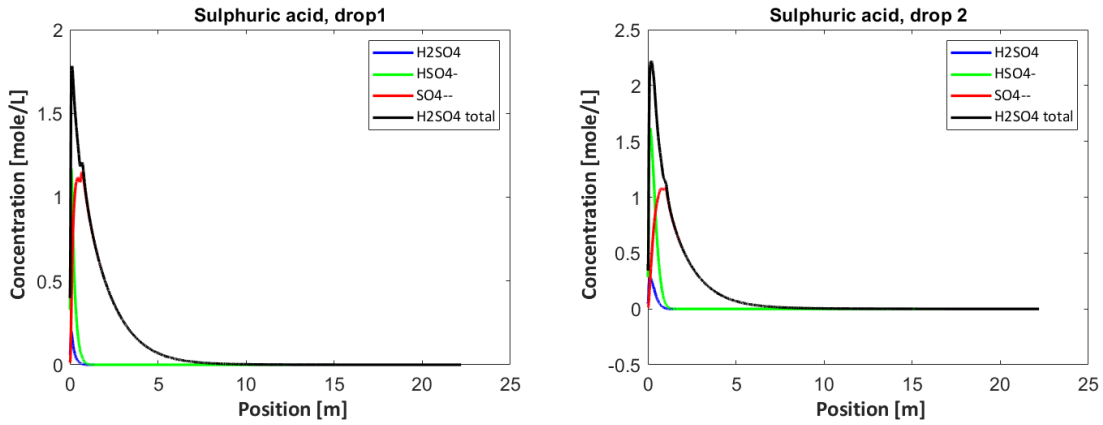

Figure (60) Sulphuric acid concentration as a function of position in the system for Droplet 1 (a) and Droplet 2 (b), for Case 1.

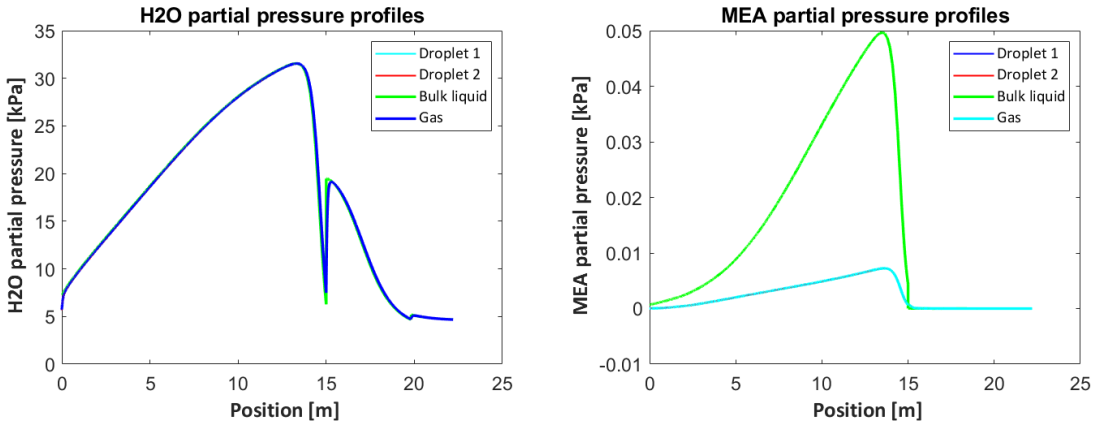

Figure (61) The partial pressure of H_2O (a) and the partial pressure of MEA (b) as a function of position in the system, for Case 1.

F.2.3 Case 2

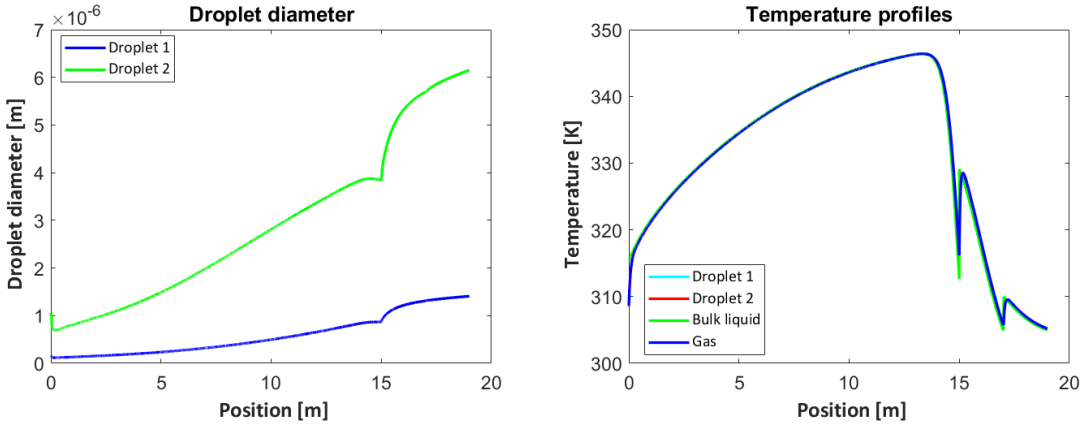

Figure (62) Droplet diameter for the two droplets (a) and the temperature profiles for the three phases (b) as a function of position in the system, for Case 2.

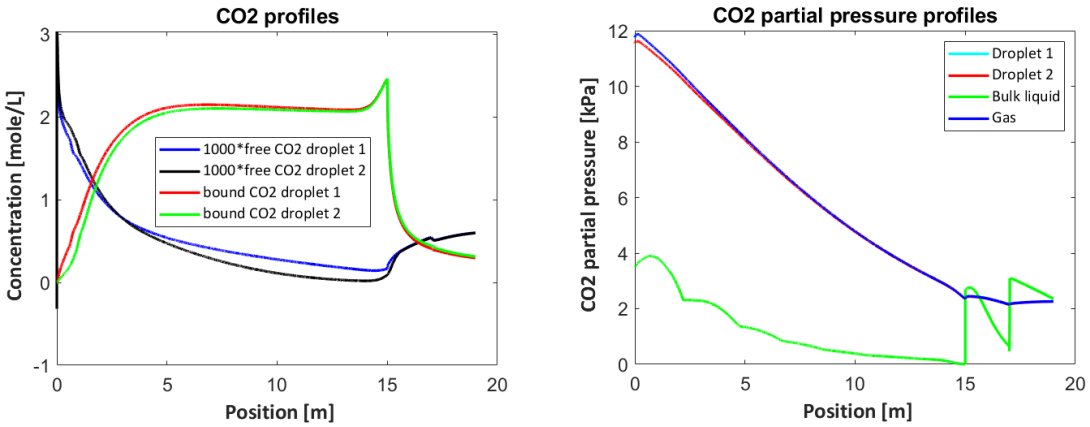

Figure (63) The concentration profile of CO_2 (a) and the partial pressure profile of CO_2 (b) as a function of position in the system, for Case 2.

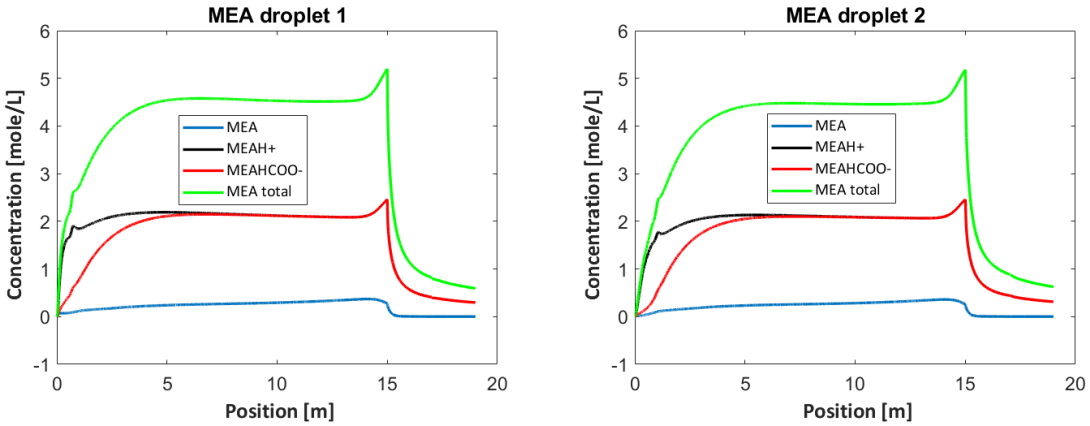

Figure (64) The concentration profile of MEA for Droplet 1 (a) and Droplet 2 (b) as a function of position in the system, for Case 2.

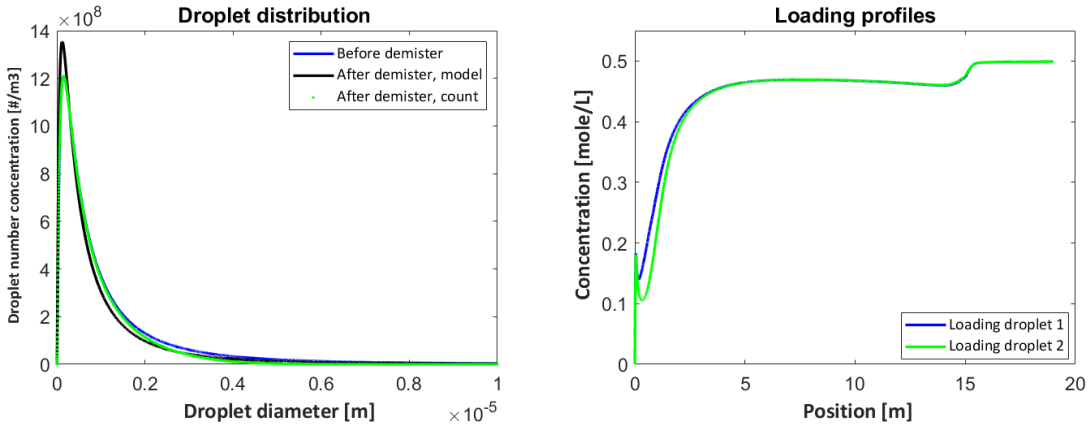

Figure (65) Droplet number concentration as a function of droplet diameter before and after the demister (a) and the loading as a function of position in the system (b), for Case 2.

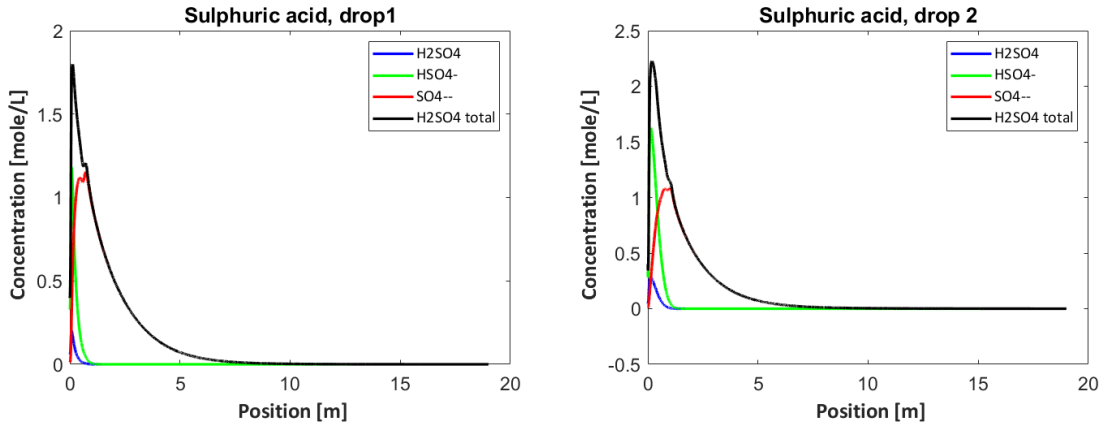

Figure (66) Sulphuric acid concentration as a function of position in the system for Droplet 1 (a) and Droplet 2 (b), for Case 2.

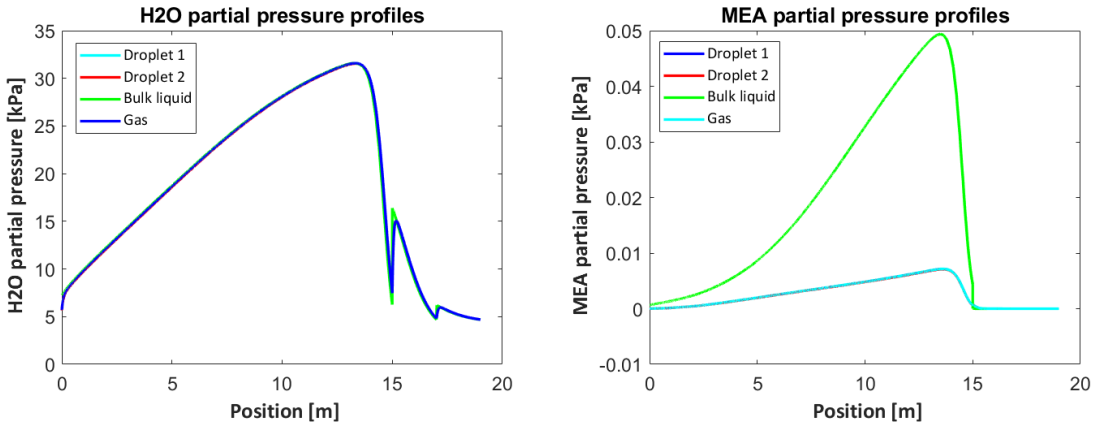

Figure (67) The partial pressure of H_2O (a) and the partial pressure of MEA (b) as a function of position in the system, for Case 2.

F.2.4 Case 3

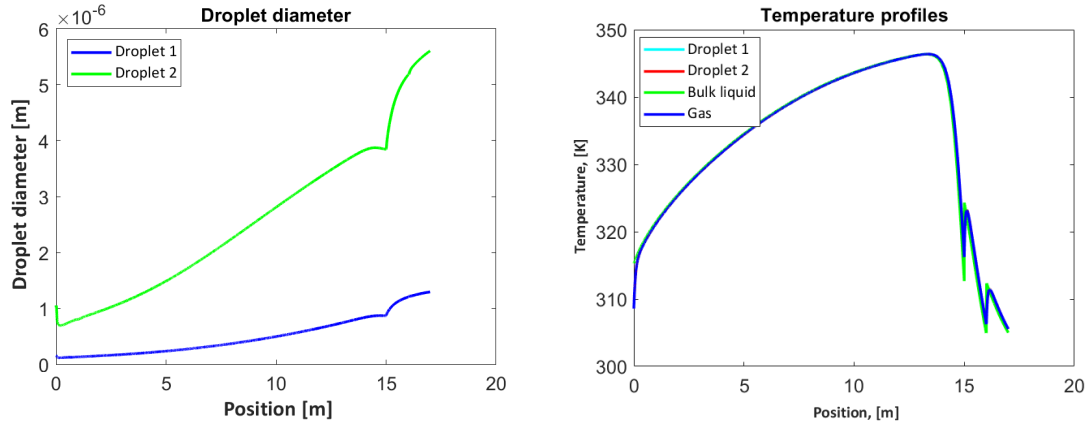

Figure (68) Droplet diameter for the two droplets (a) and the temperature profiles for the three phases (b) as a function of position in the system, for Case 3.

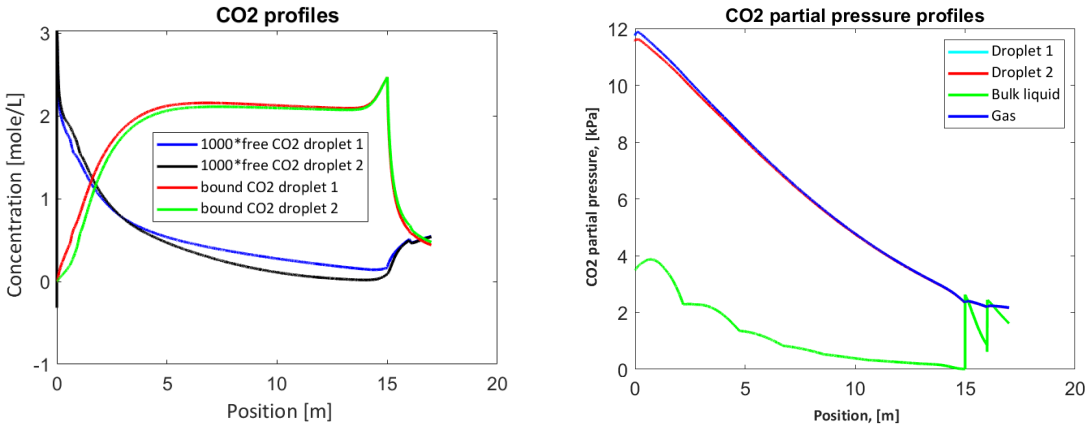

Figure (69) The concentration profile of CO_2 (a) and the partial pressure profile of CO_2 (b) as a function of position in the system, for Case 3.

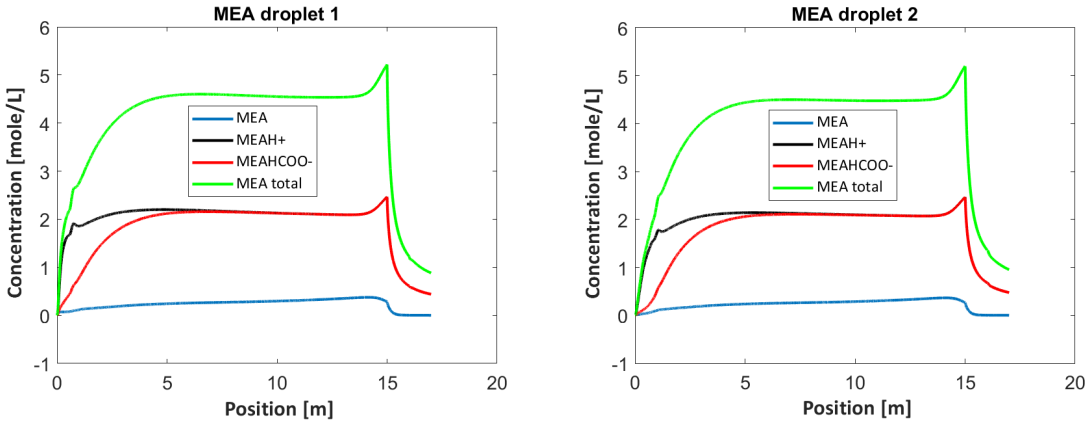

Figure (70) The concentration profile of MEA for Droplet 1 (a) and Droplet 2 (b) as a function of position in the system, for Case 3.

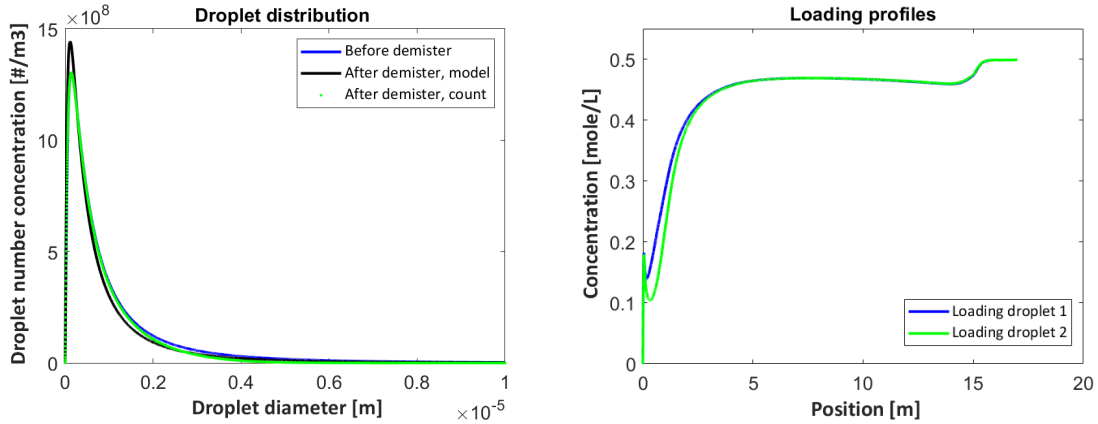

Figure (71) Droplet number concentration as a function of droplet diameter before and after the demister (a) and the loading as a function of position in the system (b), for Case 3.

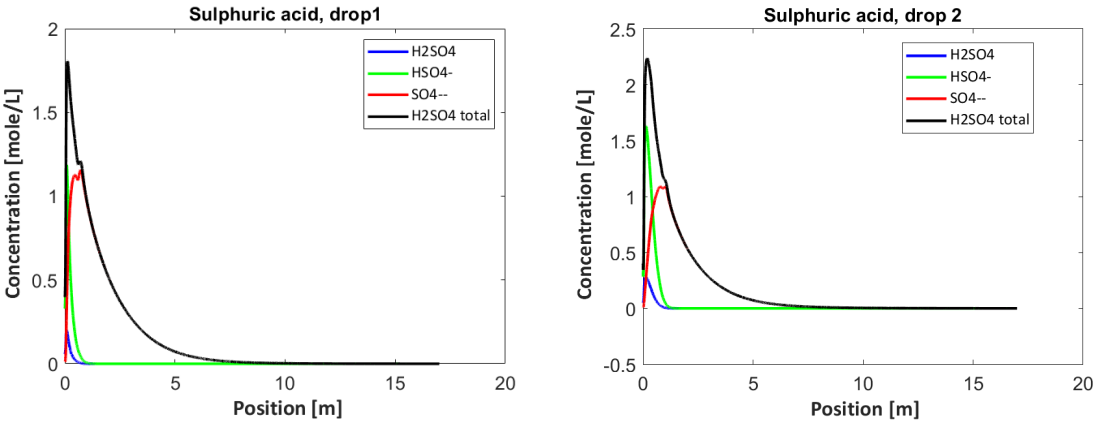

Figure (72) Sulphuric acid concentration as a function of position in the system for Droplet 1 (a) and Droplet 2 (b), for Case 3.

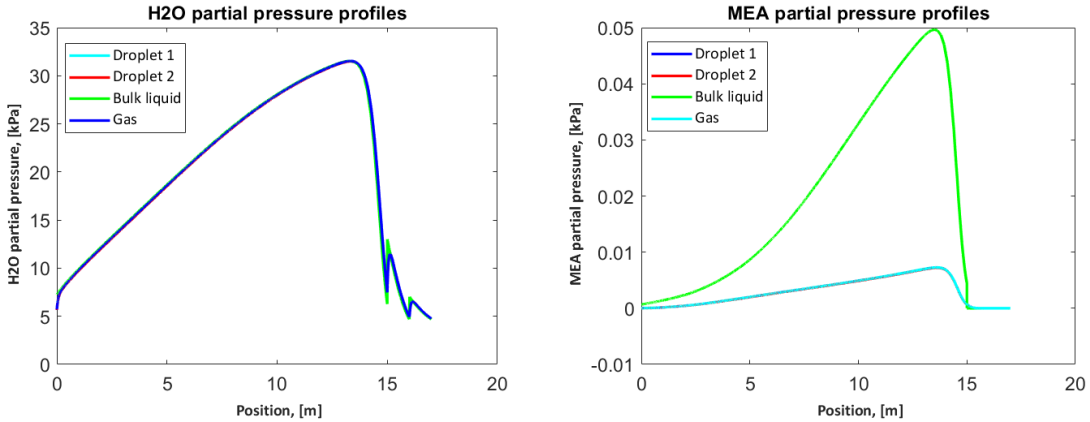

Figure (73) The partial pressure of H_2O (a) and the partial pressure of MEA (b) as a function of position in the system, for Case 3.

F.2.5 Case 4

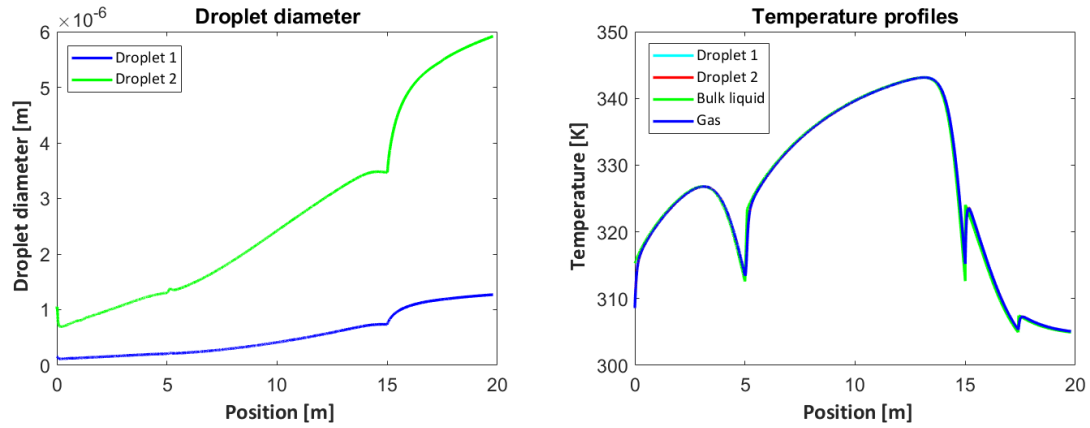

Figure (74) Droplet diameter for the two droplets (a) and the temperature profiles for the three phases (b) as a function of position in the system, for Case 4.

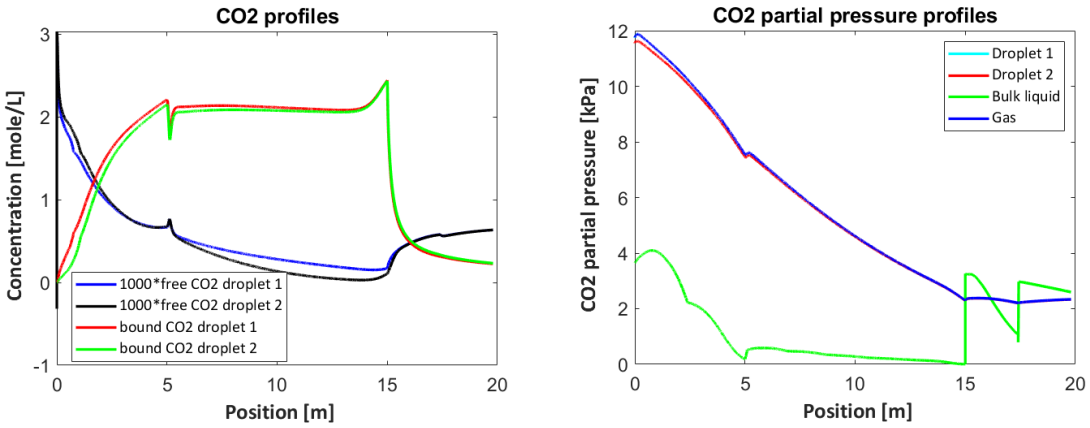

Figure (75) The concentration profile of CO_2 (a) and the partial pressure profile of CO_2 (b) as a function of position in the system, for Case 4.

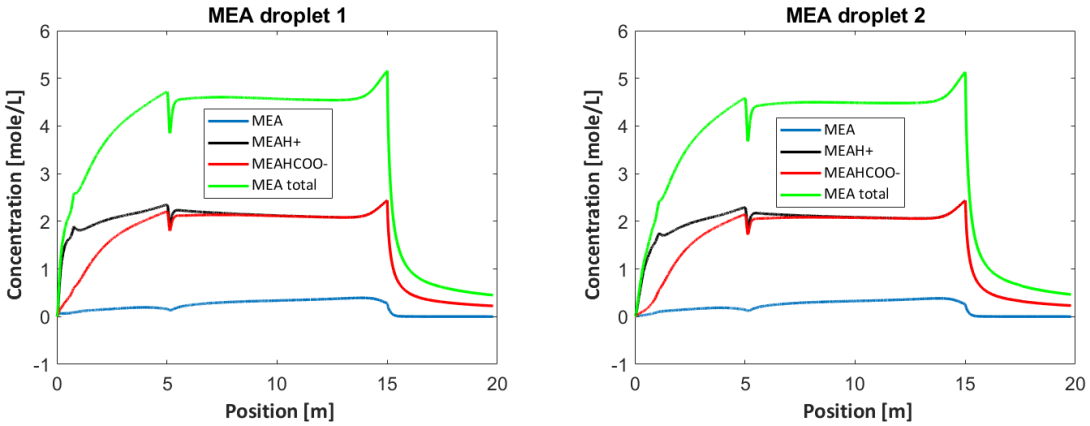

Figure (76) The concentration profile of MEA for Droplet 1 (a) and Droplet 2 (b) as a function of position in the system, for Case 4.

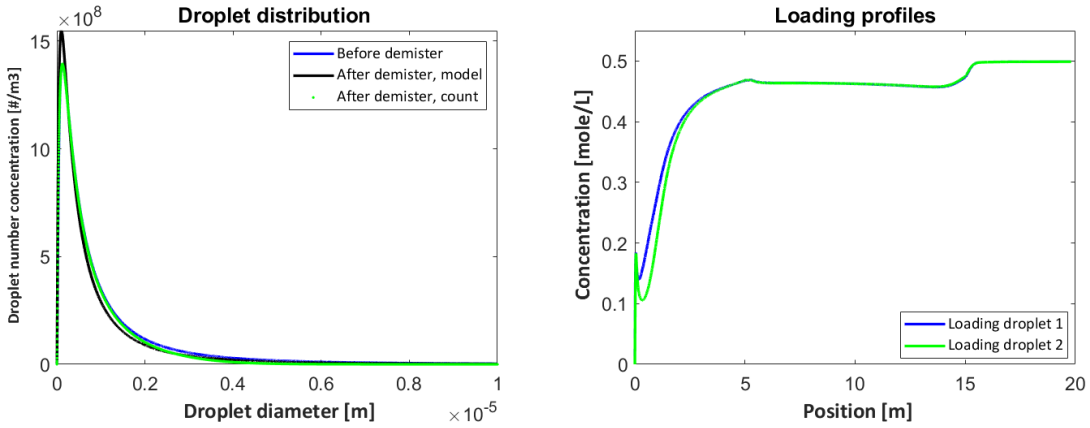

Figure (77) Droplet number concentration as a function of droplet diameter before and after the demister (a) and the loading as a function of position in the system (b), for Case 4.

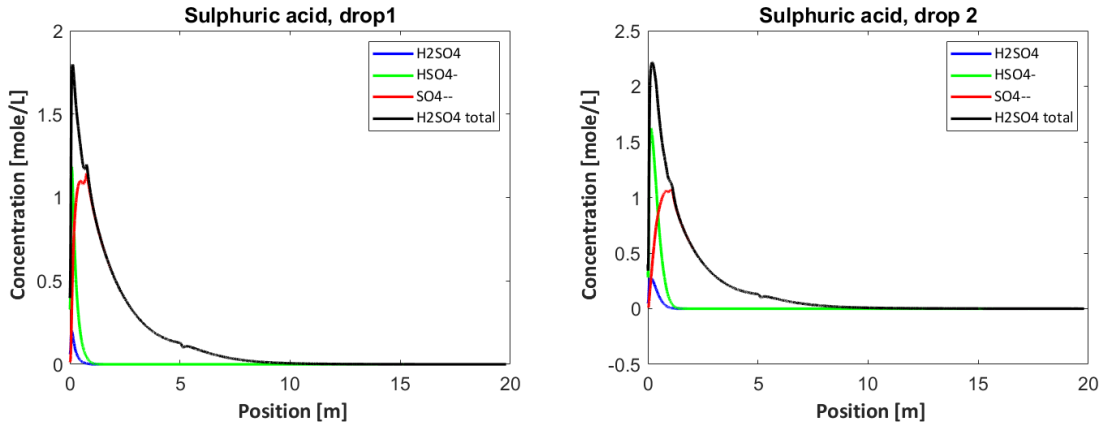

Figure (78) Sulphuric acid concentration as a function of position in the system for Droplet 1 (a) and Droplet 2 (b), for Case 4.

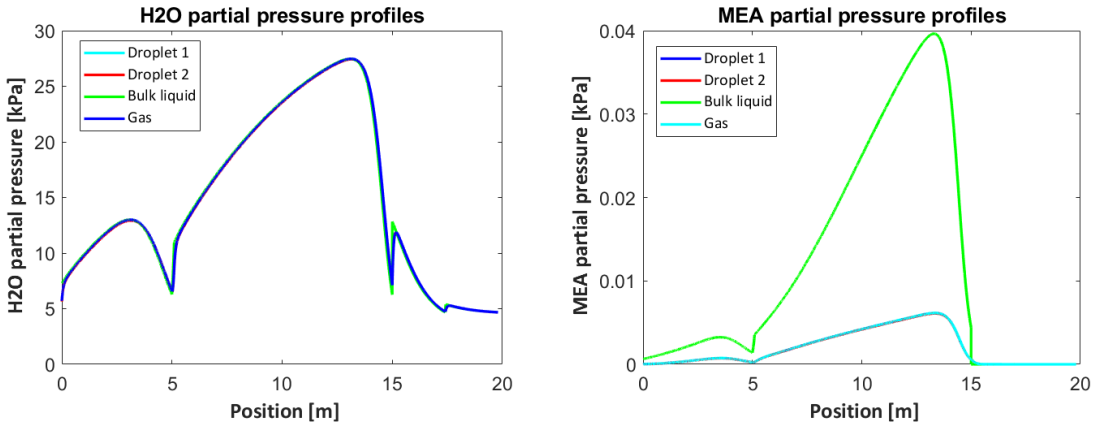

Figure (79) The partial pressure of H_2O (a) and the partial pressure of MEA (b) as a function of position in the system, for Case 4.

F.2.6 Case 5

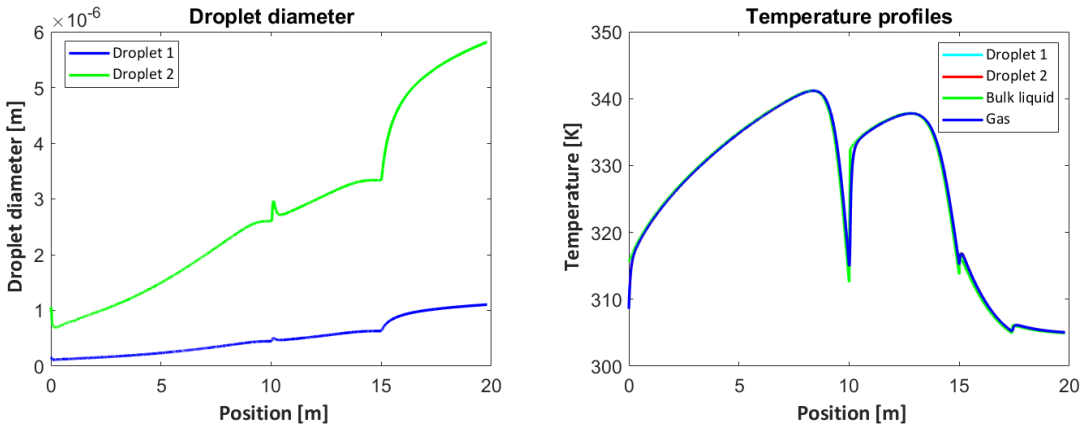

Figure (80) Droplet diameter for the two droplets (a) and the temperature profiles for the three phases (b) as a function of position in the sytem, for Case 5.

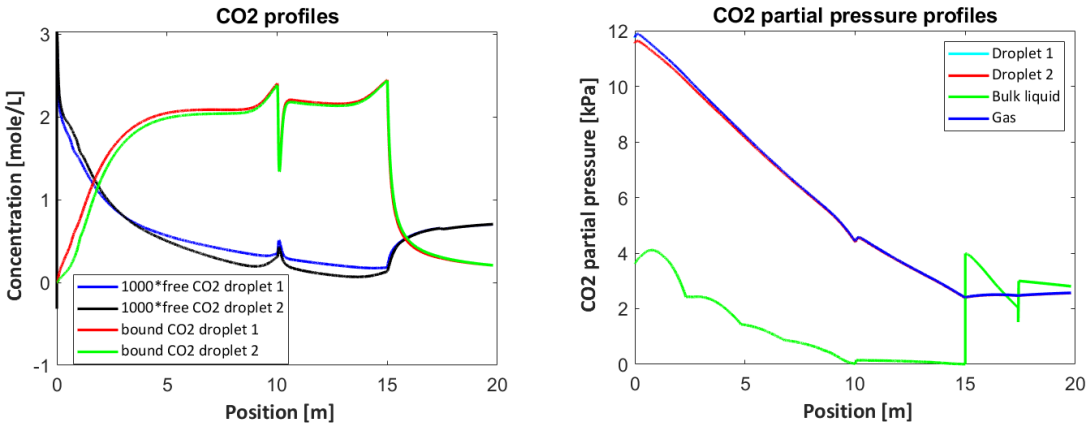

Figure (81) The concentration profile of CO_2 (a) and the partial pressure profile of CO_2 as a function of position (b), for Case 5.

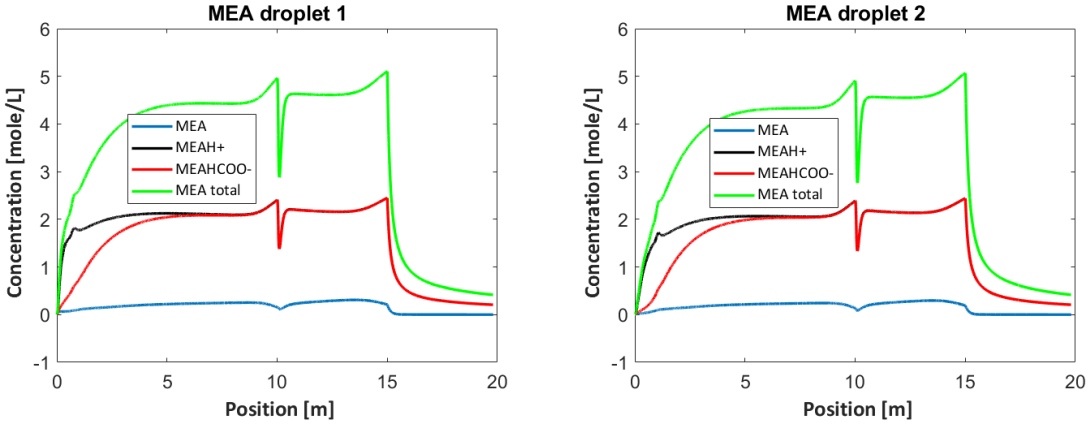

Figure (82) The concentration profile of MEA for Droplet 1 (a) and Droplet 2 (b) as a function of position in the system, for Case 5.

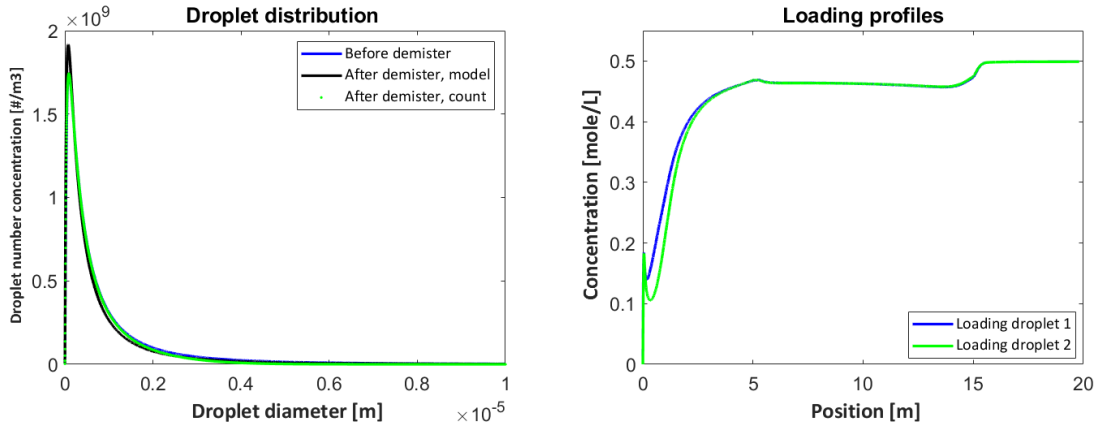

Figure (83) Droplet number concentration as a function of droplet diameter before and after the demister (a) and the loading as a function of position in the system (b), for Case 5.

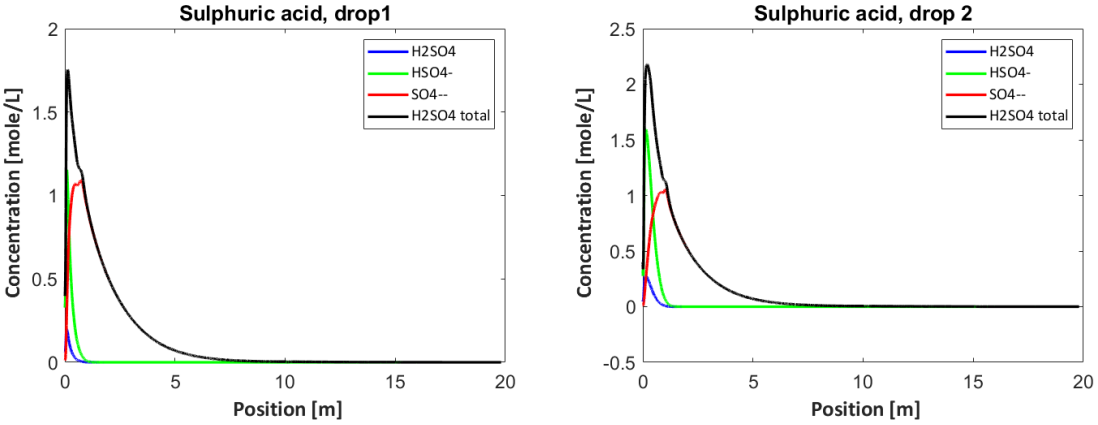

Figure (84) Sulphuric acid concentration as a function of position in the system for Droplet 1 (a) and Droplet 2 (b), for Case 5.

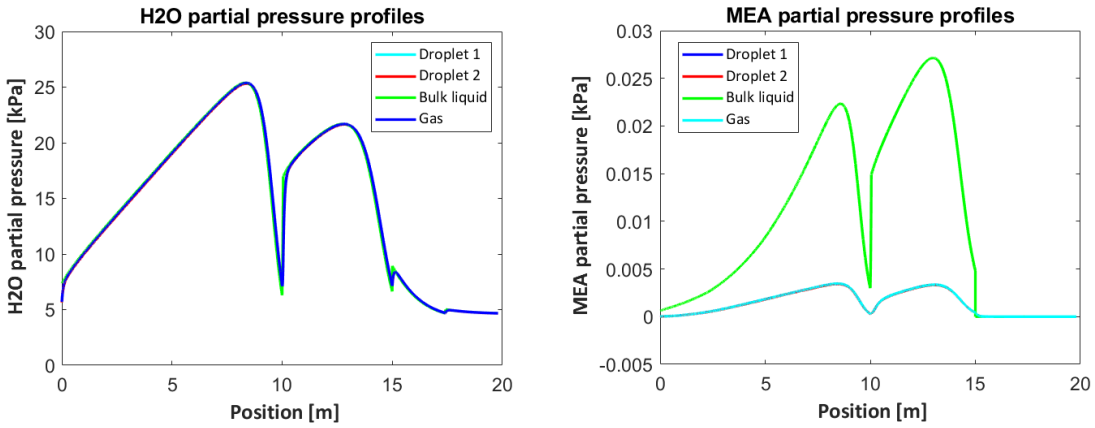

Figure (85) The partial pressure of H_2O (a) and the partial pressure of MEA (b) as a function of position in the system, for Case 5.

F.2.7 Case 6

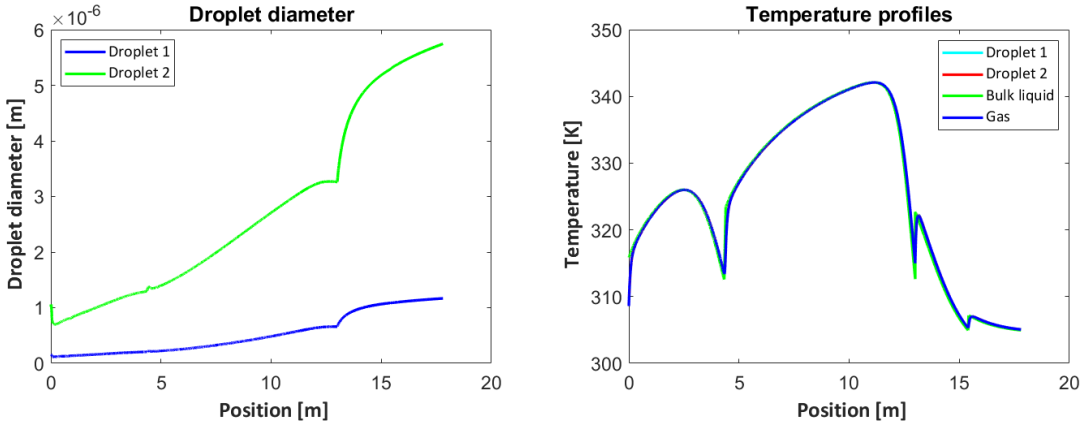

Figure (86) Droplet diameter for the two droplets (a) and the temperature profiles for the three phases (b) as a function of position in the system, for Case 6.

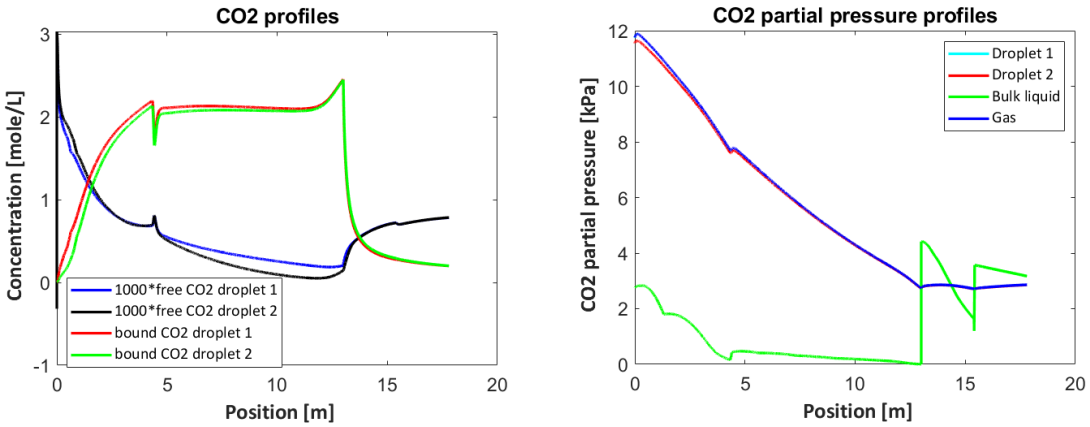

Figure (87) The concentration profile of CO_2 (a) and the partial pressure profile of CO_2 (b) as a function of position in the system, for Case 6.

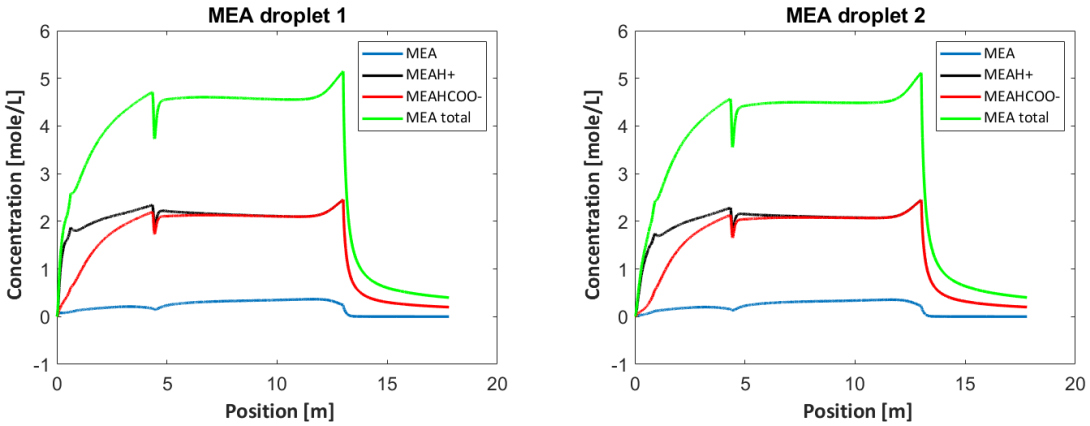

Figure (88) The concentration profile of MEA for Droplet 1 (a) and Droplet 2 (b) as a function of position in the system, for Case 6.

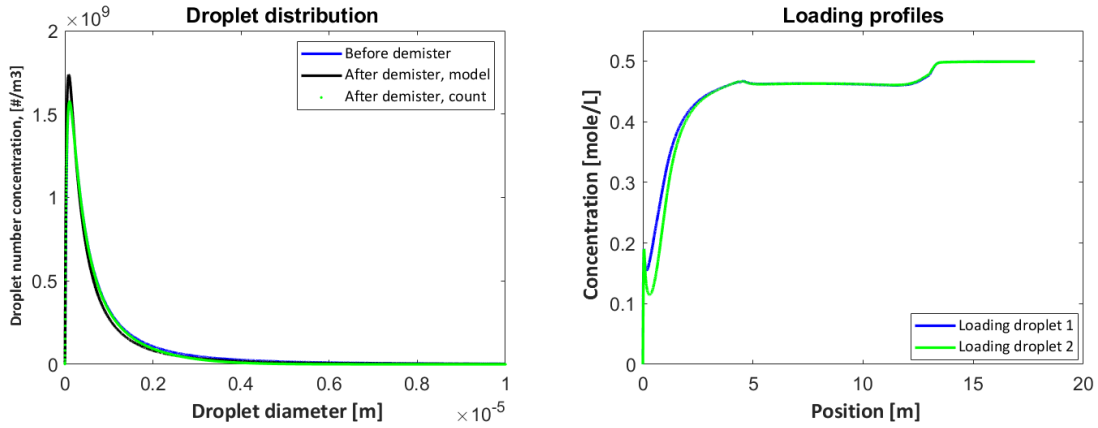

Figure (89) Droplet number concentration as a function of droplet diameter before and after the demister (a) and the loading as a function of position in the system (b), for Case 6.

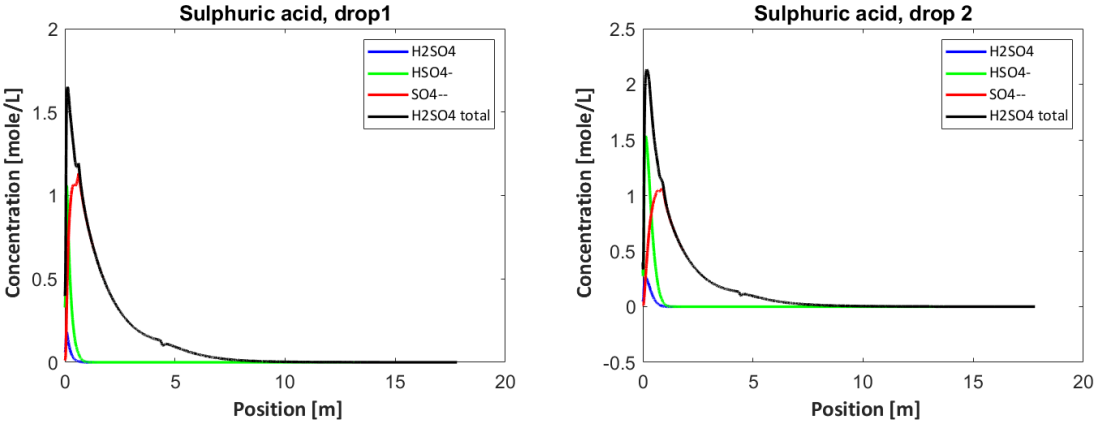

Figure (90) Sulphuric acid concentration as a function of position in the system for Droplet 1 (a) and Droplet 2 (b), for Case 6.

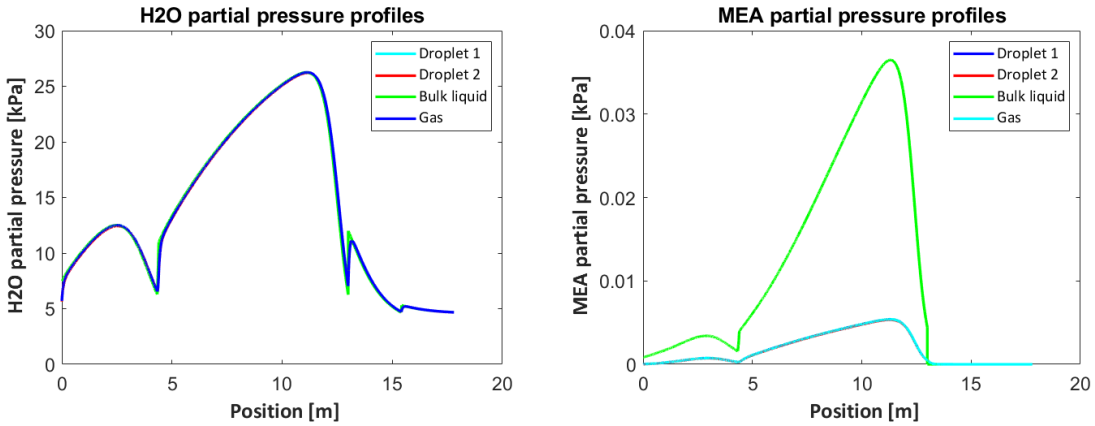

Figure (91) The partial pressure of H_2O (a) and the partial pressure of MEA (b) as a function of position in the system, for Case 6.

F.2.8 Case 7

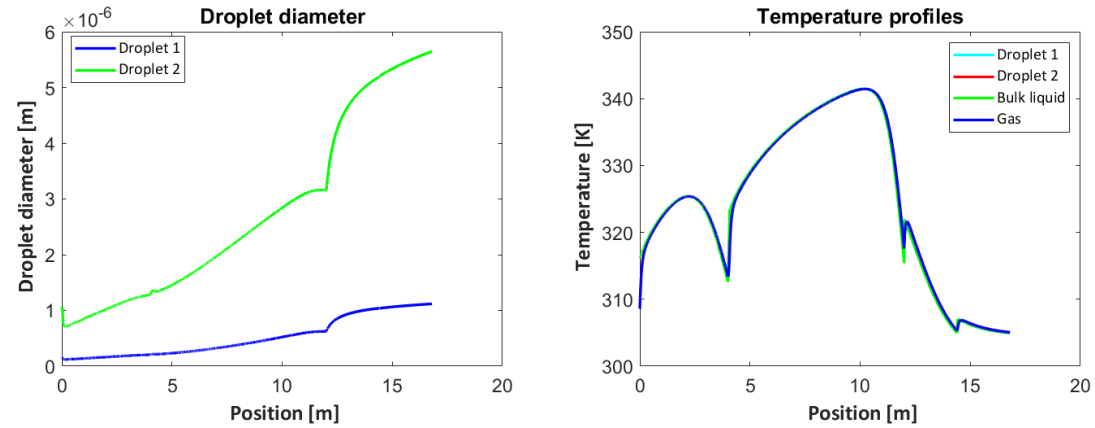

Figure (92) Droplet diameter for the two droplets (a) and the temperature profiles for the three phases (b) as a function of position in the system, for Case 7.

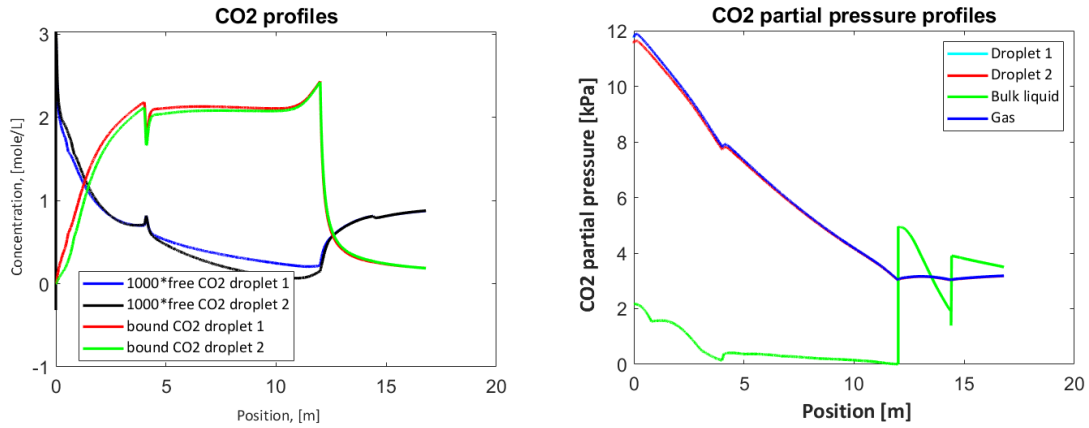

Figure (93) The concentration profile of CO_2 (a) and the partial pressure profile of CO_2 (b) as a function of position in the system, for Case 7.

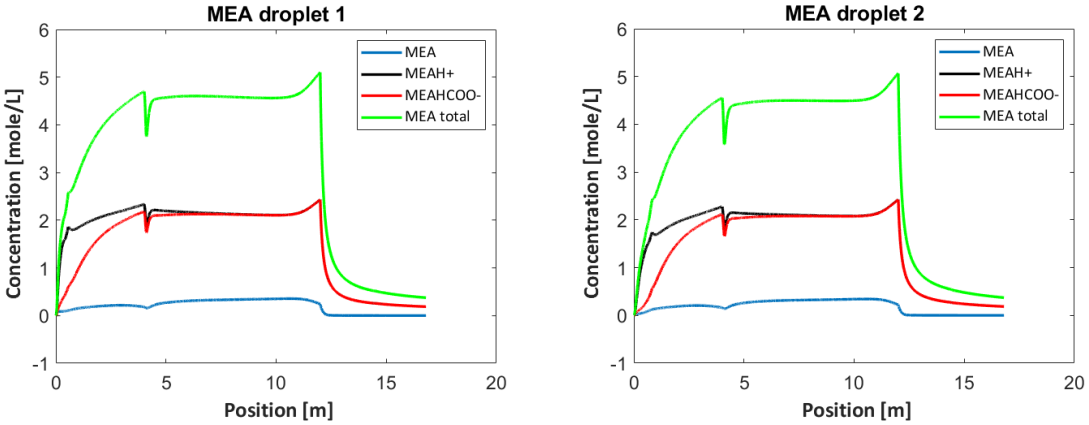

Figure (94) The concentration profile of MEA for Droplet 1 (a) and Droplet 2 (b) as a function of position in the system, for Case 7.

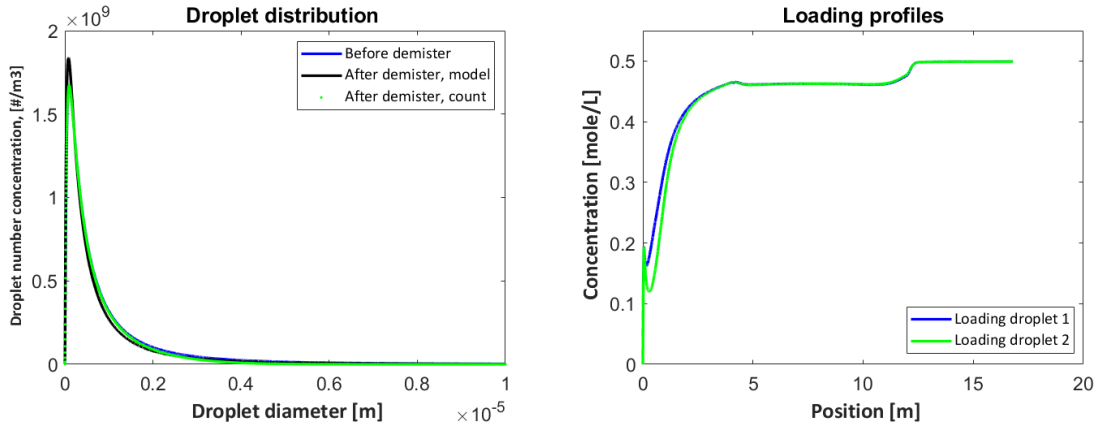

Figure (95) Droplet number concentration as a function of droplet diameter before and after the demister (a) and the loading as a function of position in the system (b), for Case 7.

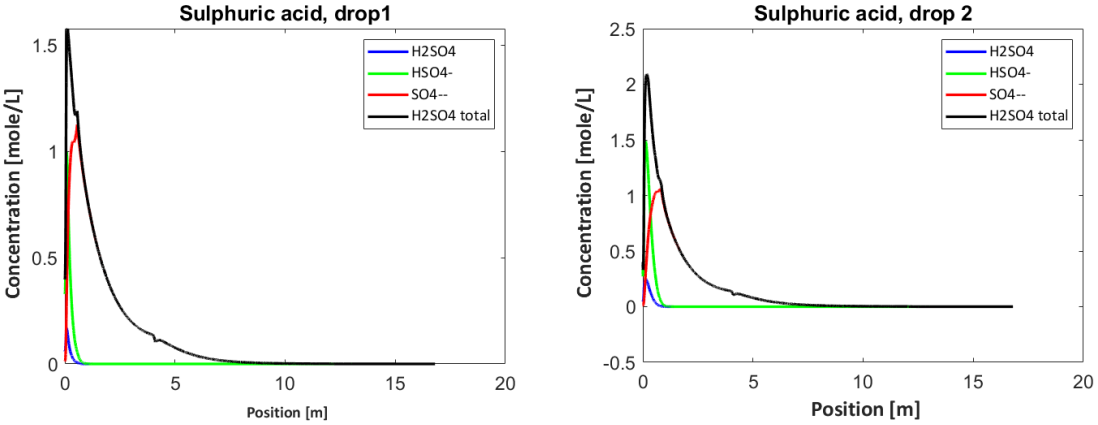

Figure (96) Sulphuric acid concentration as a function of position in the system for Droplet 1 (a) and Droplet 2 (b), for Case 7.

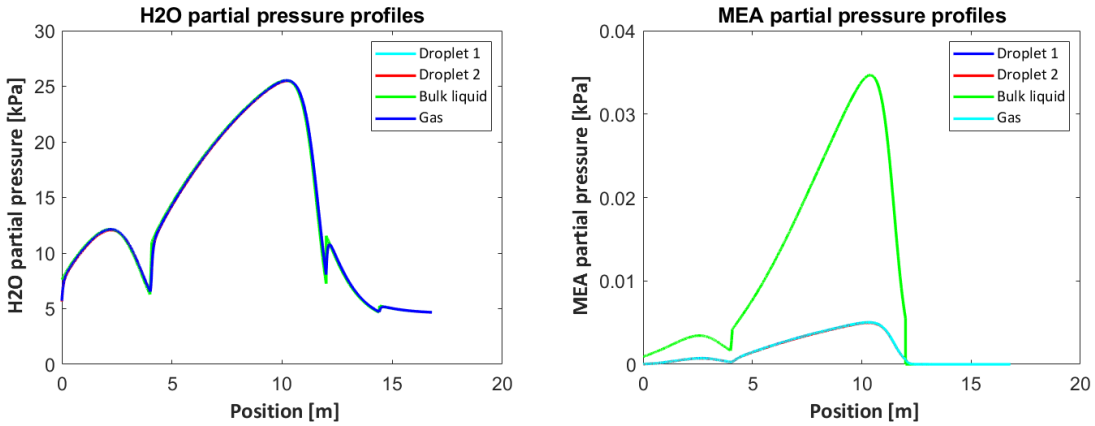

Figure (97) The partial pressure of H_2O (a) and the partial pressure of MEA (b) as a function of position in the system, for Case 7.

F.2.9 Case 8

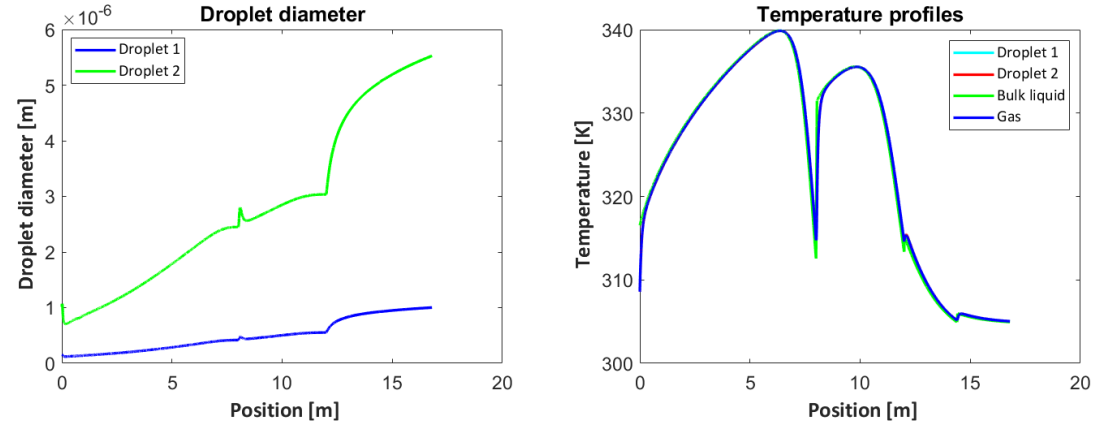

Figure (98) Droplet diameter for the two droplets (a) and the temperature profiles for the three phases (b) as a function of position in the system, for Case 8.

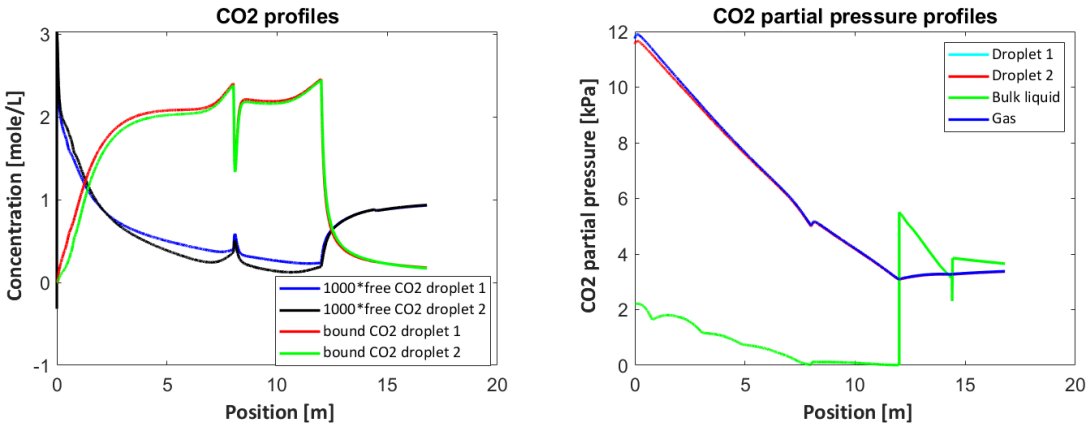

Figure (99) The concentration profile of CO_2 (a) and the partial pressure profile of CO_2 (b) as a function of position in the system, for Case 8.

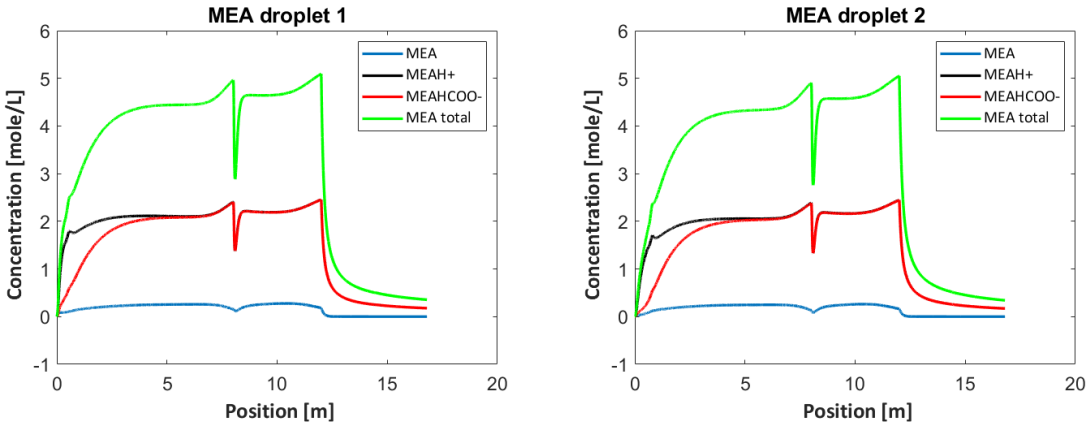

Figure (100) The concentration profile of MEA for Droplet 1 (a) and Droplet 2 (b) as a function of position in the system, for Case 8.

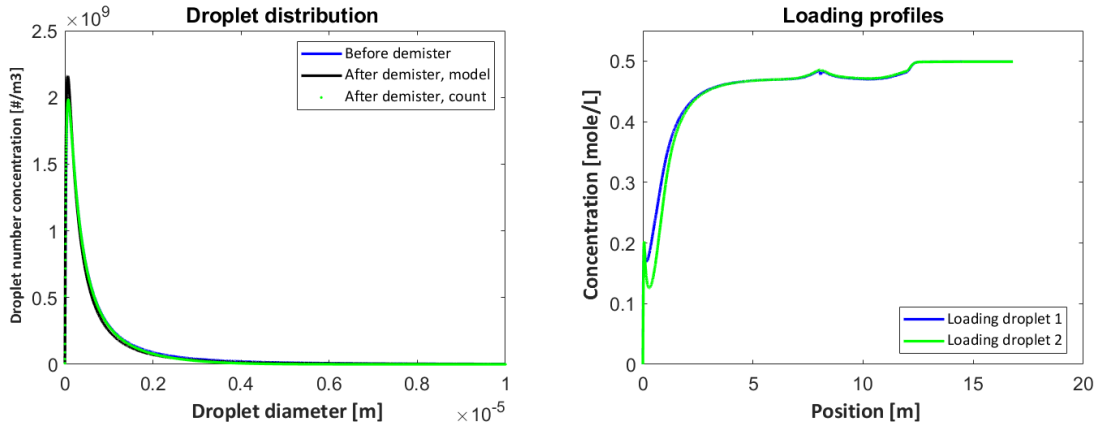

Figure (101) Droplet number concentration as a function of droplet diameter before and after the demister (a) and the loading as a function of position in the system (b), for Case 8.

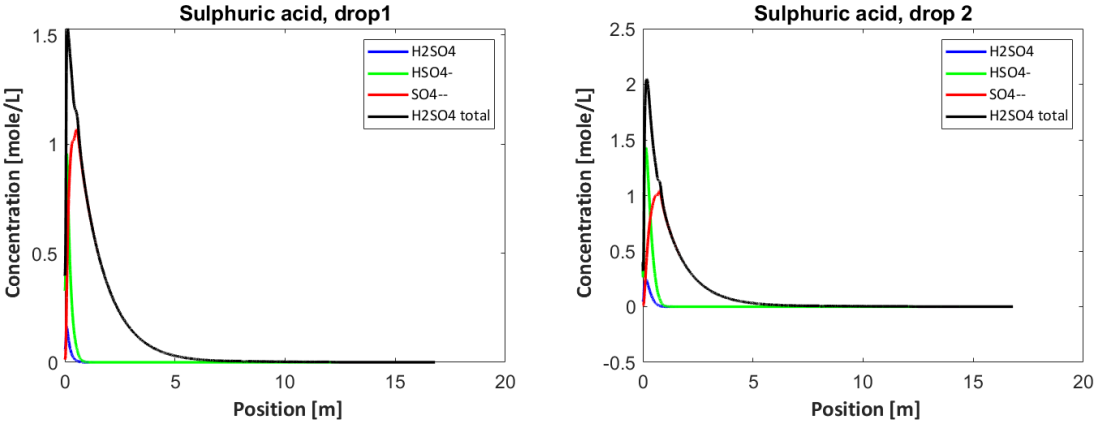

Figure (102) Sulphuric acid concentration as a function of position in the system for Droplet 1 (a) and Droplet 2 (b), for Case 8.

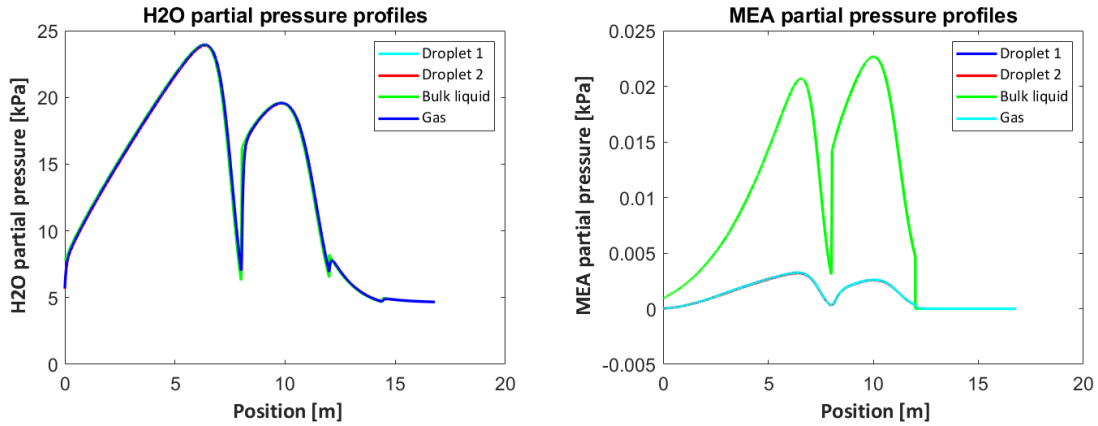

Figure (103) The partial pressure of H_2O (a) and the partial pressure of MEA (b) as a function of position in the system, for Case 8.

F.2.10 Case 9

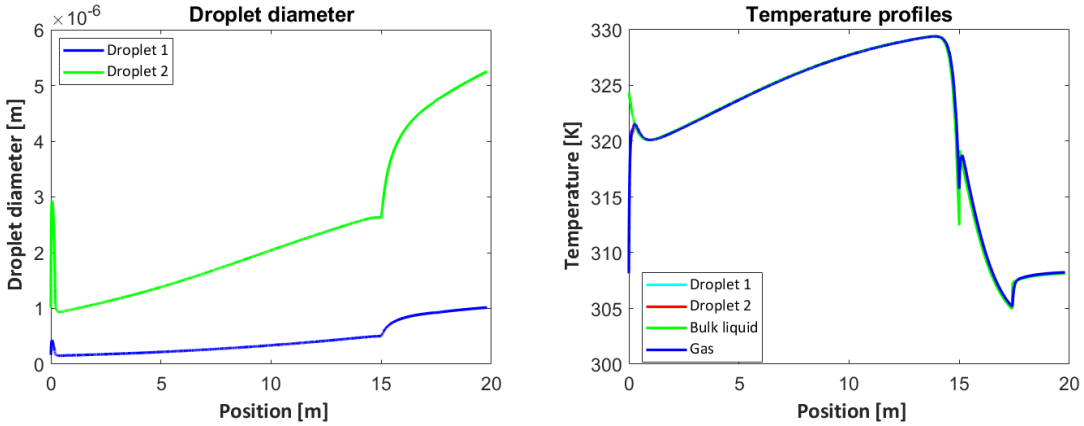

Figure (104) Droplet diameter for the two droplets (a) and the temperature profiles for the three phases (b) as a function of position in the system, for Case 9.

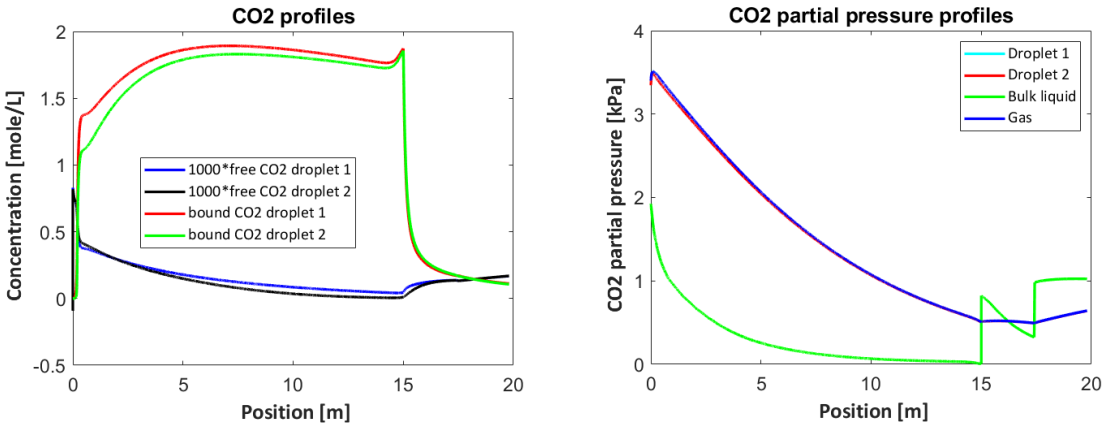

Figure (105) The concentration profile of CO_2 (a) and the partial pressure profile of CO_2 (b) as a function of position in the system, for Case 9.

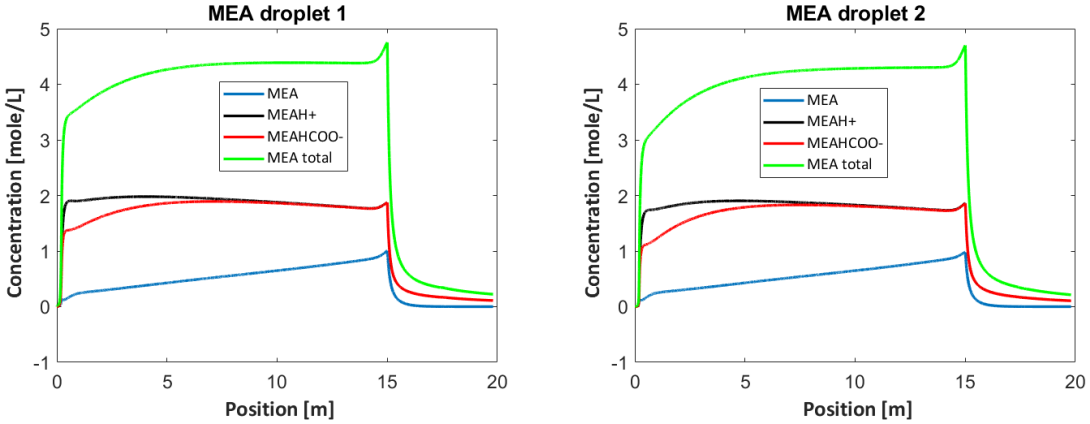

Figure (106) The concentration profile of MEA for Droplet 1 (a) and Droplet 2 (b) as a function of position in the system, for Case 9.

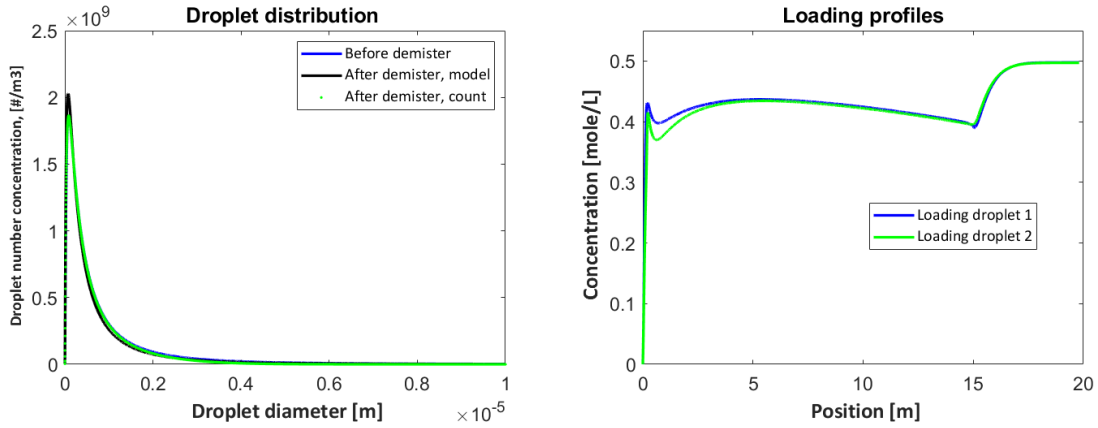

Figure (107) Droplet number concentration as a function of droplet diameter before and after the demister (a) and the loading as a function of position in the system (b), for Case 9.

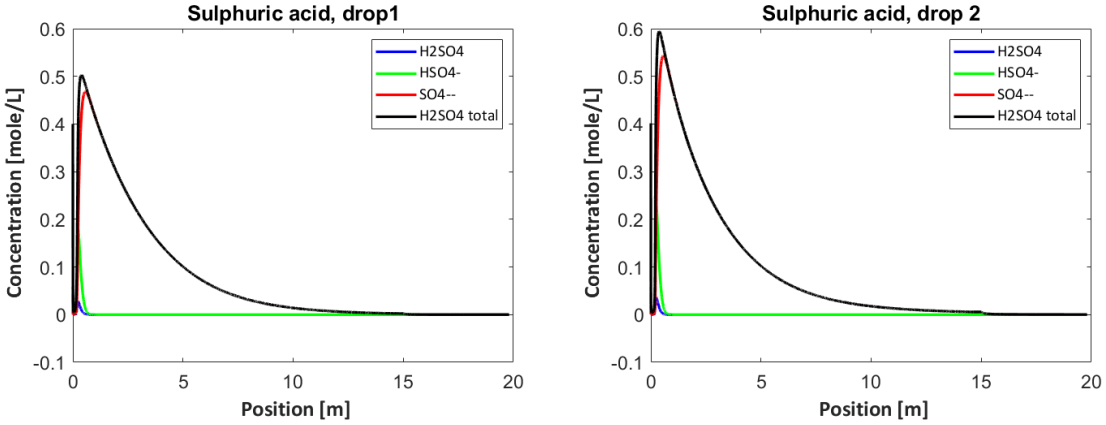

Figure (108) Sulphuric acid concentration as a function of position in the system for Droplet 1 (a) and Droplet 2 (b), for Case 9.

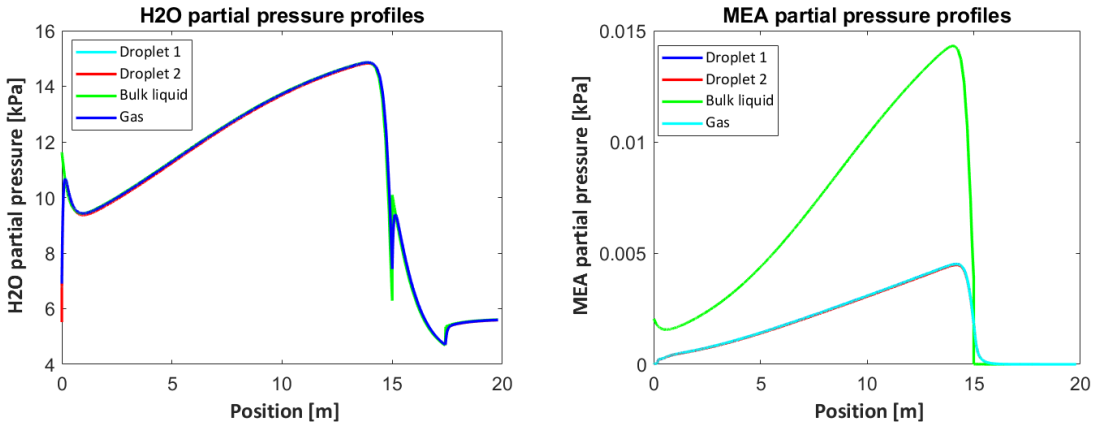

Figure (109) The partial pressure of H_2O (a) and the partial pressure of MEA (b) as a function of position in the system, for Case 9.

F.2.11 Case 10

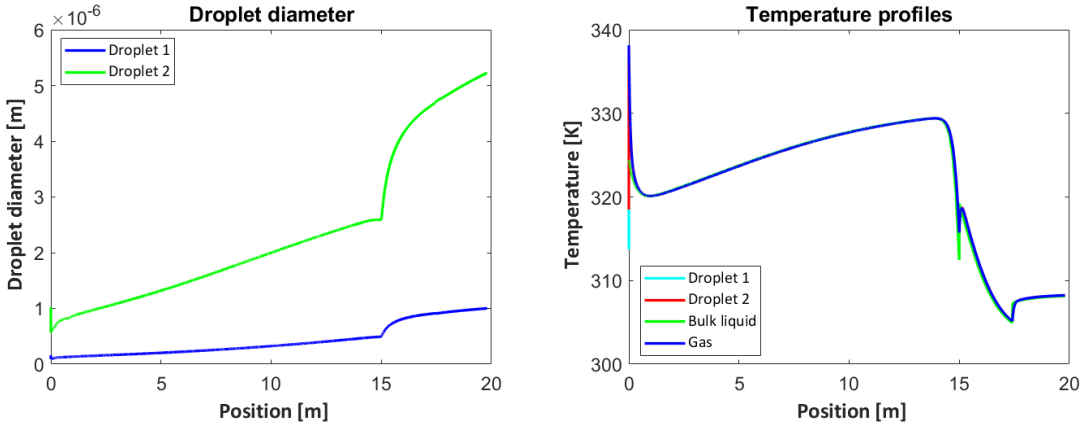

Figure (110) Droplet diameter for the two droplets (a) and the temperature profiles for the three phases (b) as a function of position in the system, for Case 10.

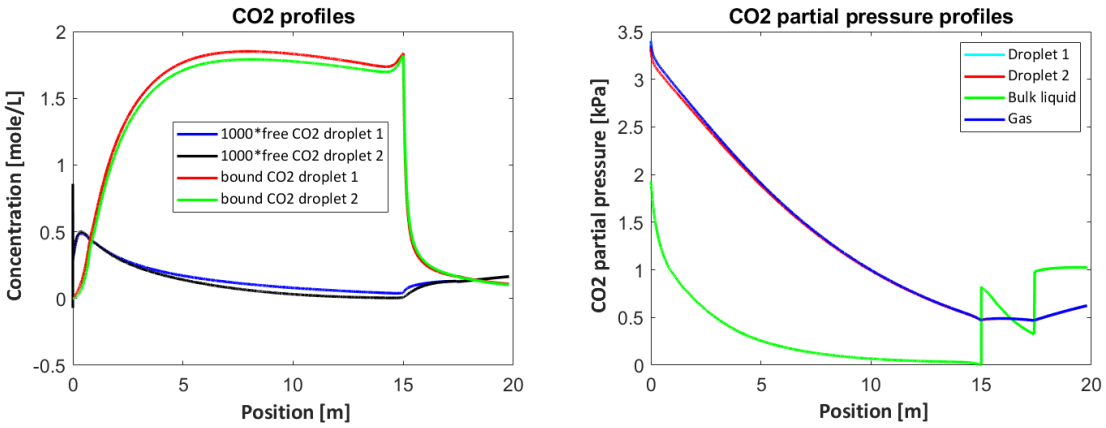

Figure (111) The concentration profile of CO_2 (a) and the partial pressure profile of CO_2 (b) as a function of position in the system, for Case 10.

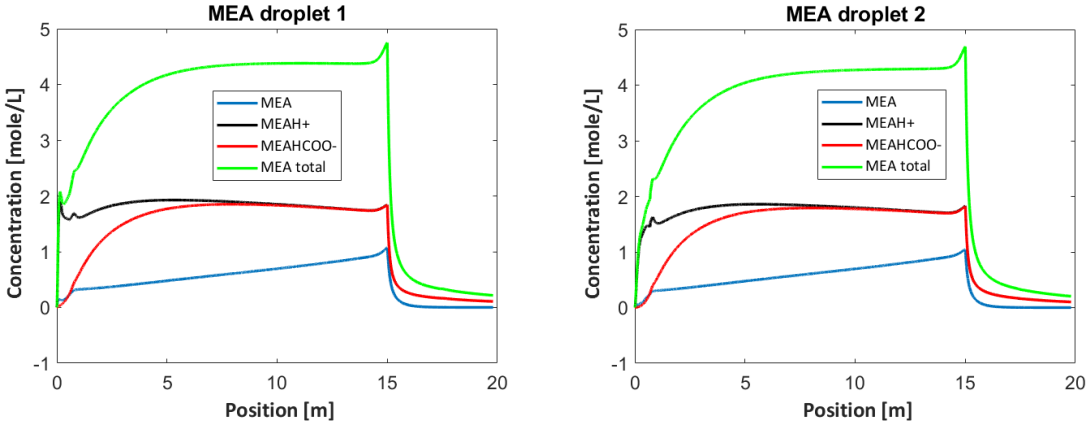

Figure (112) The concentration profile of MEA for Droplet 1 (a) and Droplet 2 (b) as a function of position in the system, for Case 10.

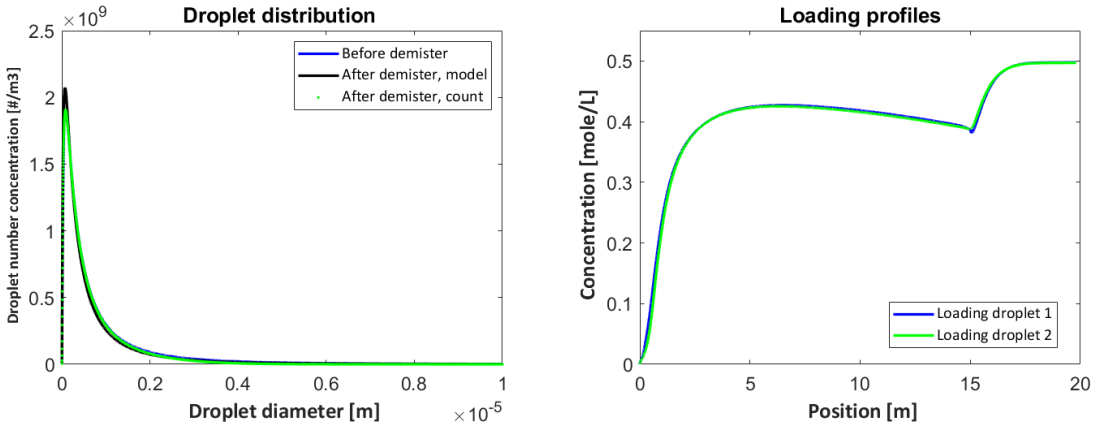

Figure (113) Droplet number concentration as a function of droplet diameter before and after the demister (a) and the loading as a function of position in the system (b), for Case 10.

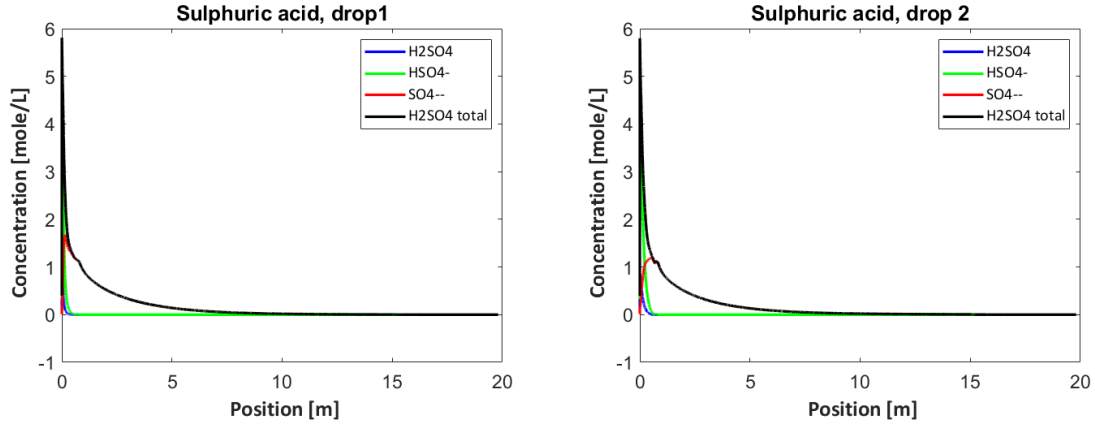

Figure (114) Sulphuric acid concentration as a function of position in the system for Droplet 1 (a) and Droplet 2 (b), for Case 10.

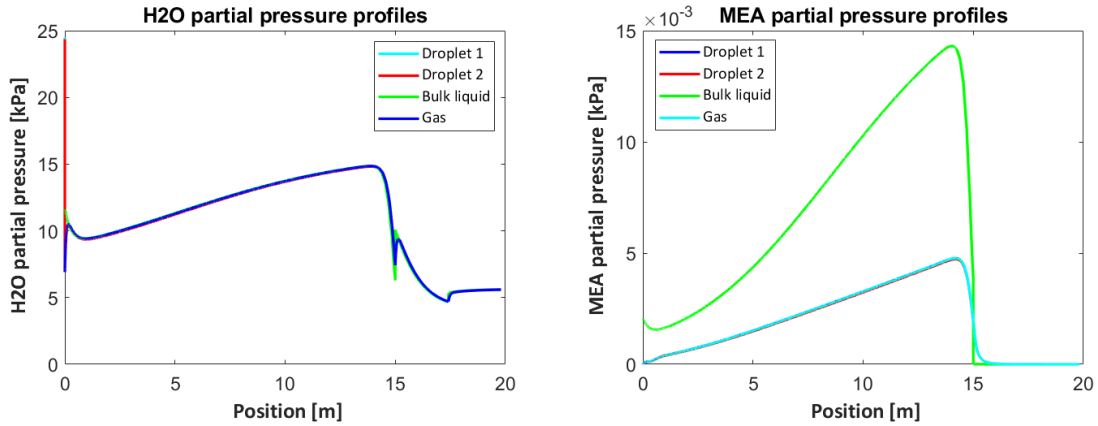

Figure (115) The partial pressure of H_2O (a) and the partial pressure of MEA (b) as a function of position in the system, for Case 10.

F.3 Diameter values

Table 24 shows the values at the end points in the diameter figures for all the cases. Figure 116 shows where the values are taken from.

Table (24) The values in the diameter profiles for cases after the absorber for Droplet 1 and 2, marked as "D1 abs" and "D2 abs", and at the end of the water washes, marked as "D1 WW" and "D2 WW".

Case	D1 abs [μm]	D1 WW [μm]	D2 abs [μm]	D2 WW [μm]
BC	3.86	6.31	0.88	1.45
1	3.86	6.76	0.88	1.55
2	3.86	6.15	0.88	1.41
3	3.86	5.61	0.88	1.29
4	3.47	5.92	0.74	1.27
5	3.33	5.81	0.63	1.10
6	3.26	5.75	0.67	1.17
7	3.17	5.65	0.62	1.12
8	3.05	5.53	0.55	1.00
9	2.03	4.47	0.38	0.71
10	2.63	5.25	0.50	1.02
11	2.59	5.23	0.49	1.00

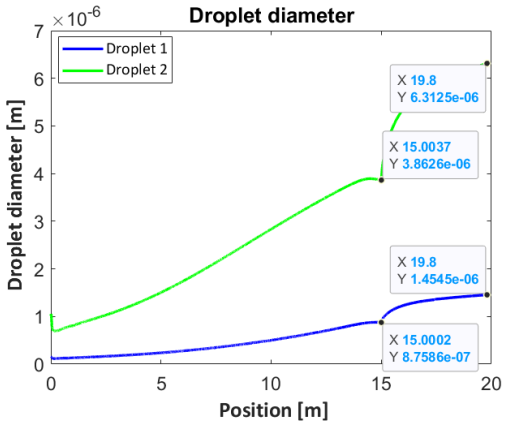

Figure (116) An example of a diameter profile that shows where the values in Table 24 are collected from.

Ingeborg Nesse

Researching the behaviour of aerosol emissions in an amine scrubbing system

NTNU
Kunnskap for en bedre verden